1978

Linear relationships in spectral parameters of some d6 and d8 isoelectronic and isostructural series of complexes

Linton Yarbrough II
Iowa State University

INFORMATION TO USERS

This was produced from a copy of a document sent to us for microfilming. While the most advanced technological means to photograph and reproduce this document have been used, the quality is heavily dependent upon the quality of the material submitted.

The following explanation of techniques is provided to help you understand markings or notations which may appear on this reproduction.

1. The sign or "target" for pages apparently lacking from the document photographed is "Missing Page(s)". If it was possible to obtain the missing page(s) or section, they are spliced into the film along with adjacent pages. This may have necessitated cutting through an image and duplicating adjacent pages to assure you of complete continuity.

2. When an image on the film is obliterated with a round black mark it is an indication that the film inspector noticed either blurred copy because of movement during exposure, or duplicate copy. Unless we meant to delete copyrighted materials that should not have been filmed, you will find a good image of the page in the adjacent frame.

3. When a map, drawing or chart, etc., is part of the material being photographed the photographer has followed a definite method in "sectioning" the material. It is customary to begin filming at the upper left hand corner of a large sheet and to continue from left to right in equal sections with small overlaps. If necessary, sectioning is continued again—beginning below the first row and continuing on until complete.

4. For any illustrations that cannot be reproduced satisfactorily by xerography, photographic prints can be purchased at additional cost and tipped into your xerographic copy. Requests can be made to our Dissertations Customer Services Department.

5. Some pages in any document may have indistinct print. In all cases we have filmed the best available copy.

University
Microfilms
International

300 N. ZEEB ROAD, ANN ARBOR, MI 48106
18 BEDFORD ROW, LONDON WC1R 4EJ, ENGLAND

Linear relationships in spectral parameters of some d^6 and d^8 isoelectronic and isostructural series of complexes

by

Linton Yarbrough, II

A Dissertation Submitted to the
Graduate Faculty in Partial Fulfillment of
The Requirements for the Degree of
DOCTOR OF PHILOSOPHY

Department: Chemistry
Major: Inorganic Chemistry

Approved:

Signature was redacted for privacy.

In Charge of Major Work

Signature was redacted for privacy.

For the Major Department

Signature was redacted for privacy.

For the Graduate College

Iowa State University
Ames, Iowa

1978

TABLE OF CONTENTS

LIST OF FIGURES

LIST OF TABLES

I. INTRODUCTION

The purpose of the studies described here was to investigate the ^{1}H nmr, ^{31}P nmr and uv/vis spectral characteristics of a series of isoelectronic and isostructural complexes of phosphite esters. The series studied were d^6[Cr(0), Fe(II), Co(III)] and d^8[Fe(0), Co(I), Ni(II)] complexes of trimethylphosphite, 4-R-2,6,7-trioxa-1-phosphabicyclo[2.2.2]octane and 1-phospha-2,8,9-trioxa-adamantane. The second and third row transition metal analogues of the trimethyl phosphite compounds were also prepared. In addition, analogous first row transition metal complexes of three other monocyclic phosphites and an additional bicyclic phosphite were prepared. It should be noted at this point that all five positions of the trigonal bipyramidal d^8 complexes were substituted with the ligand in question as were the six positions of the octahedral d^6 series. We, therefore, can make comparisons within a metal series of different ligands or comparisons of metal series (both across and down the periodic table) which are substituted with the same ligands.

There are a number of advantages in working with such series. The isostructural and isoelectronic nature of these complexes insures almost identical ligand-ligand interactions and molecular orbital characteristics, except

in the M-P bond. The high degree of symmetry of these complexes also facilitates the interpretation of the nmr and uv/visible spectroscopic results since the magnetic and electric fields are more isotropic, respectively. In short, these complexes present an excellent opportunity to study the affects of central metal charge on the ^{1}H, ^{31}P and uv/vis spectral characteristics with a minimum number of variable parameters.

Bodner (1, 2, 3, 4, 5) has recently published the ^{13}C nmr spectra of a number of transition metal carbonyls. In these papers he comments on the relationship between the ^{13}C chemical shifts and several structural and electronic parameters. He reports (1) a linear relationship between the ^{13}C chemical shift of the carbonyls and the metal formal charge in the series $(\pi\text{-}C_5H_5)M(CO)_3$ wherein M = Cr(-I), Mn(0) and Fe(I). Also reported (4) is a study of the Cr, Mo and W complexes of the form $L_nM(CO)_{6-n}$ where L is a wide variety of Group V ligands, mainly those of phosphorus. A monotonic shielding of the CO ^{13}C nmr resonance is observed in the Cr to Mo to W series which is "suggestive of a contribution to the chemical shift from neighboring diamagnetic shielding". However, in none of these cases is both nmr and uv/vis data presented nor are diamagnetic contributions to the chemical shifts considered quantitatively. Bodner's main conclusion is that increased

M-C π back-donation linearly follows an increase in the negative charge of the central metal.

Some additional work pertinent to this study has been reported by Beach and Gray (6, 7) concerning the uv/vis spectra of $M(CO)_6^x$ and $M'(CN)_6^y$ where M = Cr(0), Mo(0), W(0), V(-I), Re(I) and M' = Ti(III), V(III), Cr(III), Fe(III), Co(III), Fe(II), Ru(II), Os(II). However only pairs of complexes which are isoelectronic and isostructural are to be found among these compounds, rendering it impossible to determine whether or not spectral trends are monotonic with charge. The pairs of compounds studied by these workers which are of relevance here are $V(CO)_6^-$, $Cr(CO)_6$ and $Fe(CN)_6^{4-}$, $Co(CN)_6^{3-}$. In both of these pairs, the energy of the d-d transition was seen to fall with increasing metallic positive charge as in the case in the present study.

II. EXPERIMENTAL

A. Materials

All solvents were distilled from commonly accepted drying agents $(CH_3CH_2)_2O$ and THF from CaH_2 and $LiAlH_4$; CH_3OH from $Mg(OCH_3)_2$; CH_3CN and pentane from CaH_2; C_6H_6 from $LiAlH_4$; $(CH_3)_2CO$ and CH_2Cl_2 after shaking with Na and decantation. They were then sparged for at least 0.5 hr with N_2 and stored over 4A molecular sieves. The $P(OCH_3)_3$ used was dried by distilling off the benzene/H_2O azeotrope, distilling at atmospheric pressure (retaining the 112-113 °C fraction) and storing over 4A molecular sieves. The sources of organic reagents not commonly used are listed in the appropriate sections to follow. The commercial sources of inorganic compounds are listed below as well as sources which provided highly appreciated gifts of samples:

Alfa Products (Ventron); Beverly, Mass. - $Co(BF_4)_2 \cdot 6H_2O$, $Ni(BF_4)_2 \cdot 6H_2O$, $AgBF_4$, OsO_4, $RhCl_3 \cdot 3H_2O$, $IrCl_3 \cdot 3H_2O$, $RuCl_3 \cdot 3H_2O$.

Research Organic/Inorganic Chemicals; Belleville, N.J. - $FeCl_2$, $CrCl_2$, WCl_6, $W(CO)_6$, $MoCl_5$.

Aldrich Chemical Co., Inc.; Milwaukee, Wisc. - $(C_6H_5)_3CBF_4$, $NaB(C_6H_5)_4$.

Ames Laboratory, ERDA, Ames, Iowa - Fe, Cr (both metals were 99.9+% pure).

Dr. J. P. Jesson, Central Research and Development Department, E. I. du Pont de Nemours and Company; Wilmington, Del. - $PdCl_2$, $PtCl_2$, $[(C_2H_4)_2RhCl]_2$, $[(C_8H_{14})_2IrCl]_2$, $[(CH_3O)_3P]_4RuCl_2$.

Elemental analyses were carried out by Galbraith Laboratories, Inc.; Knoxville, Tenn.

B. Mass Spectra

Routine and low molecular weight mass spectra were obtained on an Atlas CH-4 instrument. An AEI MS-902 high resolution spectrometer was also used.

C. UV/Visible Spectra

Uv/visible spectra were recorded on a Cary Model 14 spectrometer in the double beam mode with pure solvent in the reference beam. A gas tight (septum sealed) cell was used for all solutions of M(0) compounds. The spectra were run at maximum chart speed (5 in/min) and minimum scan speed (5 nm/min) for maximum resolution (precision estimated at ± 0.3 nm). An average of three scans through the region of interest was used to report the wavelength of the maximum absorbance (λ_{max}) and the molar extinction coefficient (ε). The absorption curves were assumed to be Gaussian in shape; however, λ_{max} as determined by inspection differed slightly (maximum variation $\sim$ 2 nm) from the calculated value based

on this assumption. The variation was not enough to affect the generalizations discussed later, however. The solvents used and additional data are found in Section III. C.

D. NMR Spectra

All ^{1}H nmr spectra were obtained on a Varian Associates A-60 spectrometer or an Hitachi Perkin-Elmer R20-B spectrometer, both operating at 14.0 Kgauss. These instruments (and where appropriate the ^{31}P nmr spectrometer discussed later) were used to determine the purity of the solvents, ligands, intermediates and complexes in this study. Chemical shifts (δ) are reported in ppm relative to tetramethylsilane as an internal standard. Solvents and pertinent ^{1}H nmr data are found in Section III. D. 1.

^{31}P nmr spectra were obtained on a Bruker Model HX-90 instrument operating at a magnetic field strength of 21.3 Kgauss with a universal probe tuned to 36.434 MHz. A deuterium lock and external standard of 85% phosphoric acid were used with this spectrometer. All spectra were broadband proton decoupled with a Bruker B-SV3B broadband generator operating at 90 MHz with a white noise decoupling width of 1500 Hz. The Fourier transform was performed on a Nicolet Instruments Model 1089 Computer. Solvents and additional data concerning these spectra are found in Section III. D. 2, wherein chemical shifts (δ) are reported in ppm and a negative

shift indicates resonance at an applied magnetic field strength less than that of the standard. Coupling constants are reported in Hertz (Hz).

E. Gas/Liquid Chromatograms

The glc studies were done on a Varian Associates Aerograph Series 1700 chromatograph operating at a helium flow rate of 35.2 ml/min and a column temperature of 199 °C. The detector and injection port were held at 223 and 215 °C, respectively. A 5 ft by 3/16 in internal diameter stainless steel column packed with 10% Carbowax 20 M on acid washed Chromosorb G was used for the separations. Known samples of the compounds under study were used to standardize retention times for comparison with those reported earlier (8) under slightly different conditions.

F. Specialized Equipment

1. Rotating flask metal evaporation device

The rotating flask apparatus shown in Figure 1 was designed from the brief descriptions of Mackenzie and Timms (9) and Benfield et al. (10). Table 1 lists construction materials and notes which refer to the lettered arrows in Figure 1. A large spherical flask (1 or 2 l) equipped with 45/50 male standard taper fits into the female joint shown in the drawing. This flask was then rotated by the Buchi Rotavapor drive

around the metal evaporation portion of the mechanism. The solution of the ligand was kept cold by partially submerging the rotating flask in a large Dewar flask filled with liquid N_2 or other suitable coolant. Electrical insulation between the two small brass tubes (used to carry both cooling water and the current to heat the tungsten wire basket) was achieved through the use of the Stupakov fitting and the two Kovar seals bonded glass-to-glass. The tungsten wire baskets (made by winding 8-9 cm of 0.018 in wire around a wooden mandrel) were given a fused alumina coating by applying a water slurry of Al_2O_3, allowing it to air dry on the mechanism, evacuating the device and heating the basket to white heat for about one sec. This method produced a small cup which contained the molten metal while it evaporated. Vacuum was maintained during rotation by the use of two sets of three rubber "O" rings with intervening compression rings. These also acted as supports for the glass tube to maintain correct alignment. After lubricating the "O" rings with Dow Corning 550 Silicone pump oil, the rotating vacuum mechanism was assembled and the end caps tightened so that a vacuum seal was maintained between the glass and the "O" rings. Care was used in the adjustment so that the "O" rings were not compressed to the point where rotation was prevented. The threaded portions of the end caps and barrel were then treated with black wax

Fig. 1. Rotating Flask Metal Evaporation Device (Full scale)

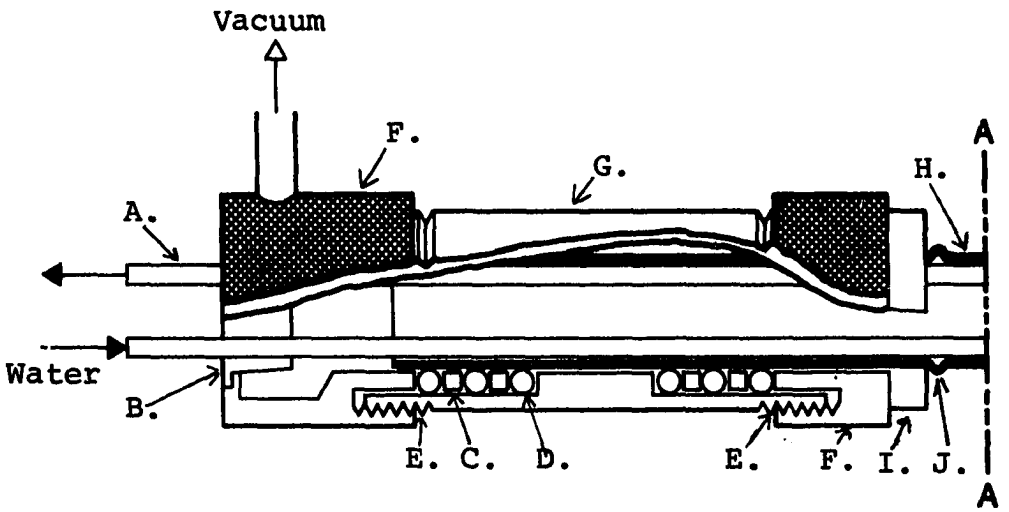
Vacuum
F.
G.
H.
A.
A
Water
B.
E. C. D.
E. F. I. J.
A

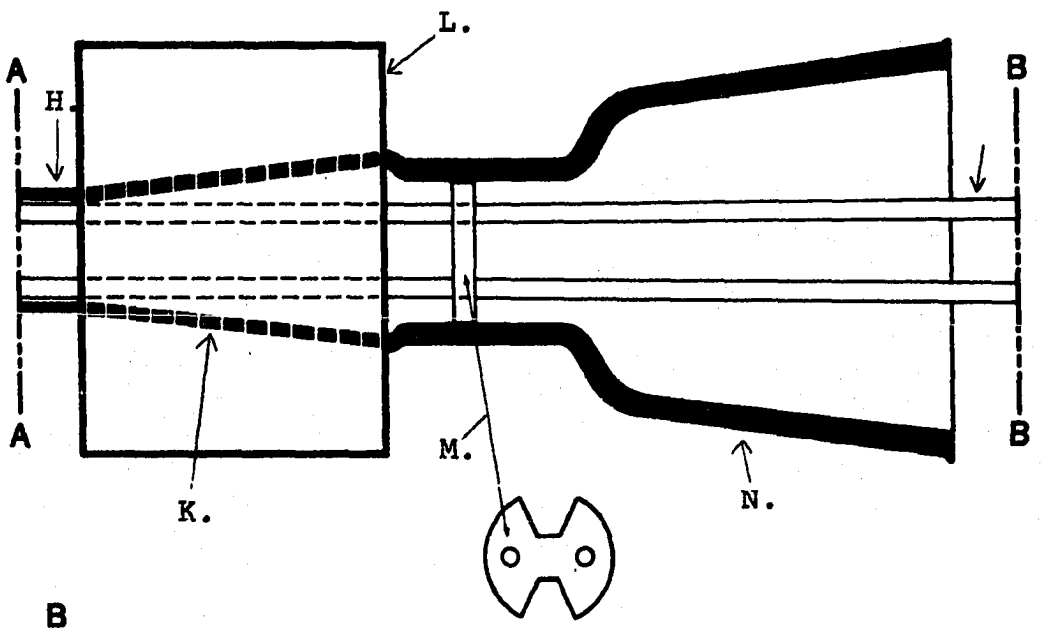
L.
A
H.
B
A
B
K.
M.
N.

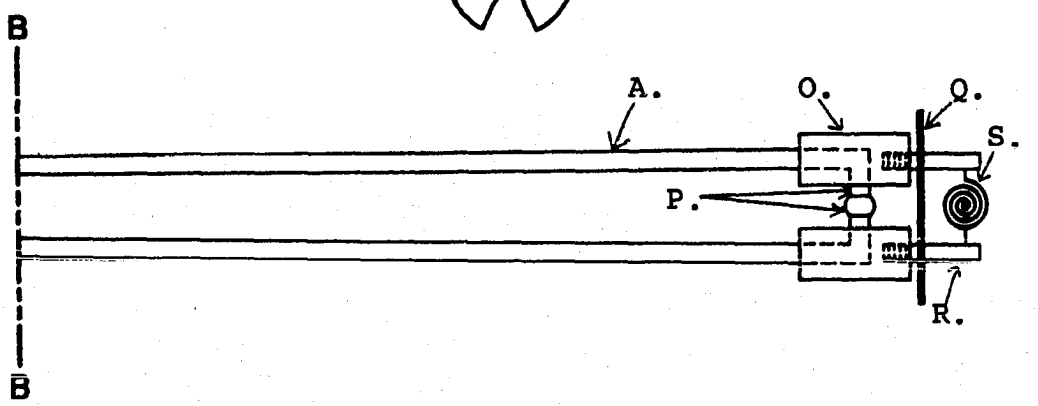
B
A.
O.
Q.
S.
P.
R.
B

Table 1. Construction materials and notes on construction for rotating flask metal evaporation device

(Contents of this table refer to the lettered arrows in Figure 1.)

A. Tube, 2.5 mm O.D., carries cooling water and electrical current: brass.

B. Stupakov fitting, tubing through ceramic center provides electrical insulation and vacuum seal.

C. Compression ring: brass.

D. "O" ring: rubber.

E. Threaded union between end caps and barrel; sealed with black wax.

F. End cap, knurled: brass.

G. Barrel: brass.

H. Glass tube: Pyrex.

I. Bearing; rides against ridge (J) to prevent atmospheric pressure forcing mechanism out of position: Teflon.

J. Raised ridge on glass tube.

K. Male 24/40 taper; black wax sealed to female joint in L.

L. Buchi Rotavapor drive.

M. Support; wedged inside glass tube to give support to and maintain alignment of brass tubes; side and front views: Nylon.

N. Female 45/50 joint; spherical flask fits into this joint.

O. Rectangular block; used for heat transfer and support for electrical leads (R): copper.

P. Kovar metal-to-glass seals; larger diameter portion is glass; provides electrical insulation while allowing passage of cooling water; Kovar glass and stainless steel.

Q. Heat shield to protect P: sheet mica.

Table 1. (Continued)

R.	Electrical leads; threaded for replacement: copper.
S.	Alumina coated tungsten wire basket.

sealant to prevent the end caps from working loose during operation and to provide a vacuum seal.

2. Static cylindrical metal evaporating device

This piece of equipment, shown in Figures 2 and 3, was based on a sketch by Timms (11). Table 2 lists construction materials and notes on the construction of this equipment and refers to the lettered arrows in Figures 2 and 3. Electrical insulation between the two semi-annular pieces (shown in Figures 2 and 3.a and b) was maintained by the Nylon lead-throughs in the lid, the Nylon support block and the two Kovar seals under the mechanism. The copper tubing carried both the current to heat the tungsten wire basket and the water to cool the evaporation mechanism. The circuit was completed by suspending the alumina coated basket in the cylindrical hole in the center of the mechanism. Further heat insulation was provided by fitting a small piece of fused alumina tubing inside this cylindrical opening and equipping the alumina tube with a disk of tantalum foil (0.007 in) wedged in place at the bottom. An additional heat shield of tantalum foil was attached to the bottom of the Nylon support ring. Correct alignment was maintained by the Nylon support attached to the semiannuli with countersunk machine screws. As with the rotating flask device, it was necessary to take rather elaborate precautions to protect the delicate glass union of

Fig. 2. Static Cylindrical Metal Evaporation Device (One half scale)

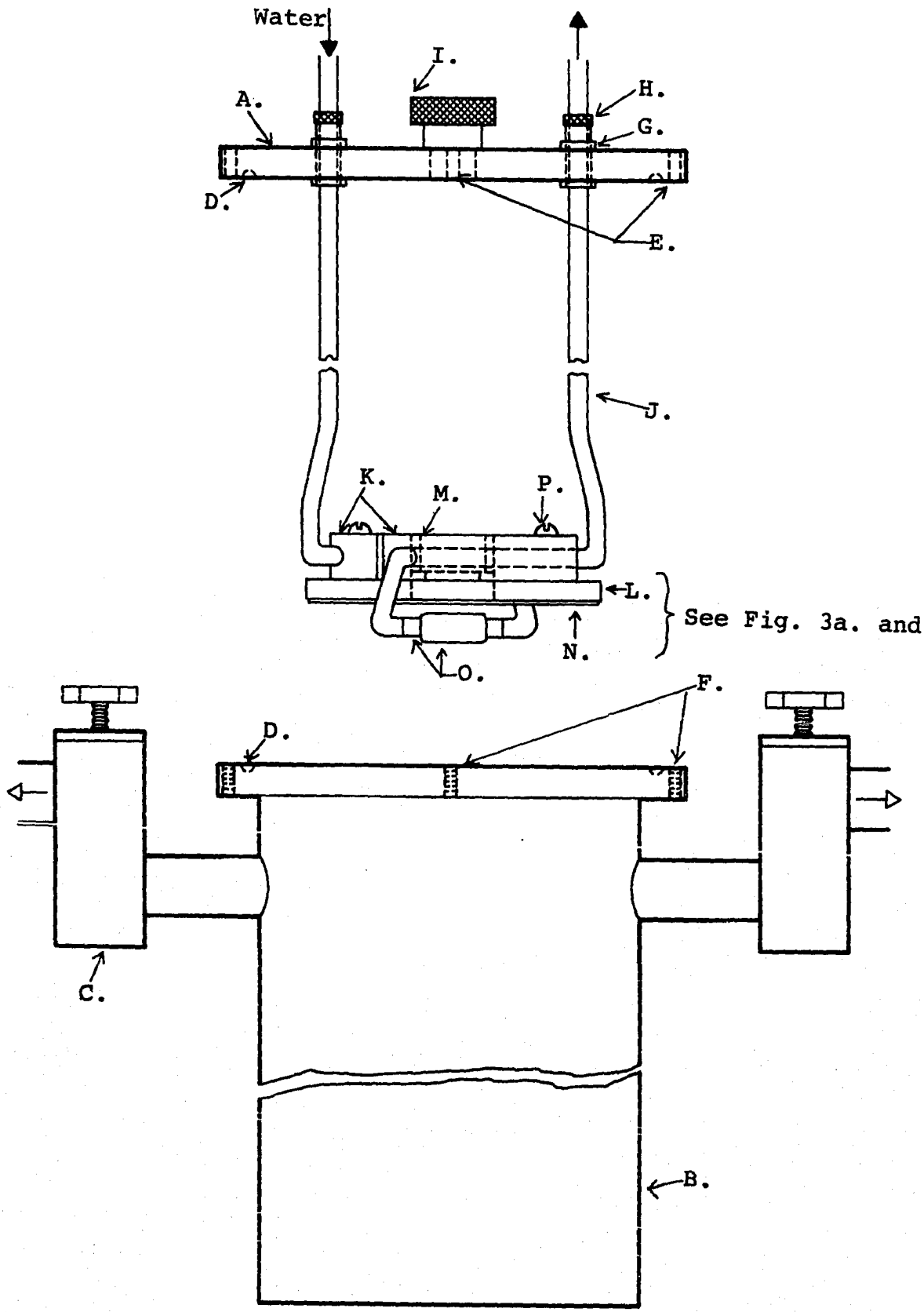
Water
I.
A.
H.
G.
D.
E.
J.
K.
M.
P.
L.
N.
O.
See Fig. 3a. and b
F.
D.
C.
B.

Fig. 3. Details of Static Cylindrical Metal Evaporation Device (a, b and c) and Solid Ligand Holder (d)

a. Top View

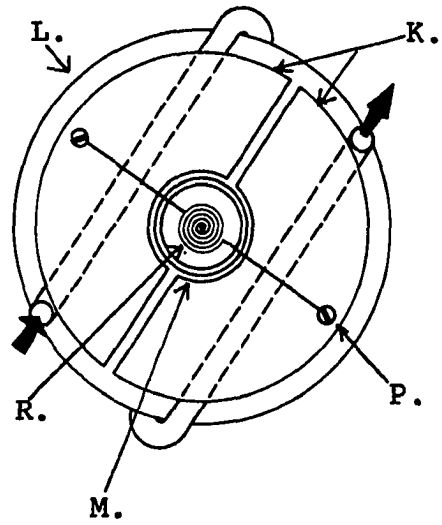

b. Bottom View

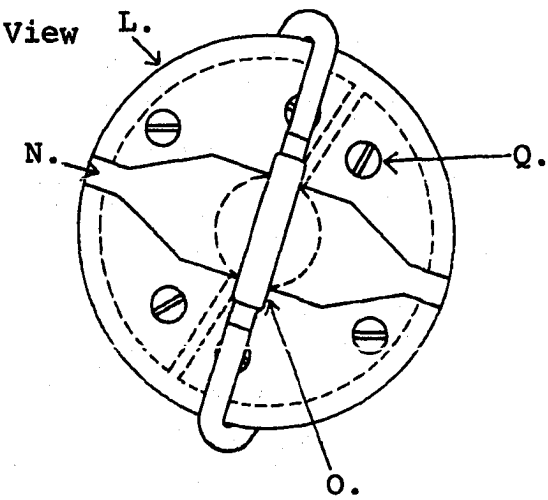

c. Wire Basket

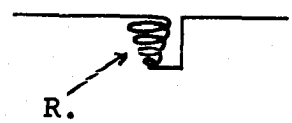

d. Holder

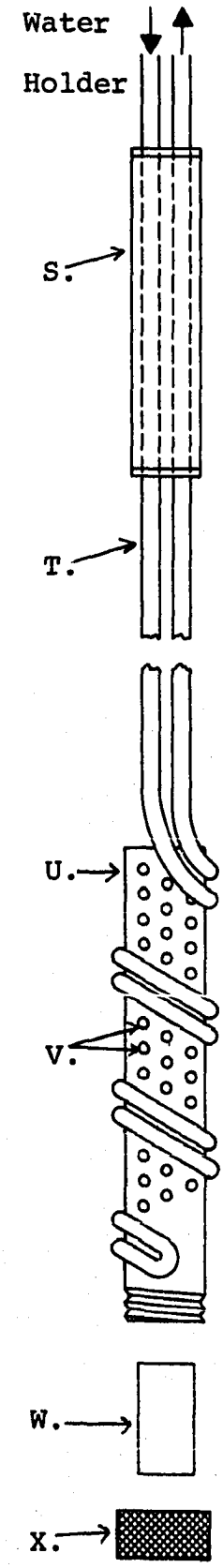

Table 2. Construction materials and notes on construction for static cylindrical metal evaporation device

(Contents of this table refer to the lettered arrows in Figures 2 and 3.)

A. Lid: stainless steel.

B. Main body; cylindrical, 0.060 in wall thickness, bottom piece and ring at top heliarc welded, copper tubing to valves (C) silver soldered: stainless steel.

C. Veeco bellows vacuum valves: brass.

D. "O" ring groove.

E. Holes to accept heat-treated machine screws to compress "O" ring in D.

F. Threaded holes to accept screws through E.

G. Seals; provide vacuum seal and electrical insulation: Nylon.

H. Seals; "O" ring compression type to seal copper tubing (J), knurled: brass.

I. Seal; "O" ring compression type to seal ligand disperser (see Figure 3.d, letter S), knurled: brass.

J. Tube; 6.25 mm O.D., carries cooling water and current: copper.

K. Semi-annuli; heat exchange and electrical contacts: brass.

L. Support; maintains correct alignment of K and provides electrical insulation: Nylon.

M. Heat shield; cylindrical tube, rests on two small semi-circular shelves on K, circular tantalum foil heat shield wedged in place at bottom of tube: fused alumina.

N. Heat shield; attached to L: tantalum foil.

O. Kovar metal-to-glass seals; larger diameter portion is glass; provides electrical insulation while allowing passage of cooling water: Kovar glass and stainless steel.

Table 2. (Continued)

P.	Small machine screw set into K to maintain correct alignment of and electrical contact for R: brass.
Q.	Flat head machine screws; countersunk into L, maintain correct alignment of K: brass.
R.	Tungsten wire basket before coating with alumina.
S.	Tube; fits into I, end pieces and T silver soldered, polished just before use each time: brass.
T.	Tubing; carries cooling/heating 2-propanol: copper.
U.	Tube: brass.
V.	Holes in U for escape of ligand.
W.	Cup; contains ligand, very close fit with U to provide good thermal contact: brass.
X.	End cap; knurled: brass.

the Kovar seals from excessive physical strain caused by thermal expansion and contraction. Due to the large amount of energy given off during the evaporation of the metal causing heating of the ligand and a concomitant rise in pressure, it was felt necessary to absorb as much of the excess heat as possible. It was this necessity which made the eventual design somewhat complex. Cooling water was passed through the body of one of the semi-annuli from one side, out the other side, down under the mechanism (where it passed through the Kovar seals), up to one side of the other semi-annulus, through the body and then back up to the exit.

The ligand was introduced into the reaction vessel by two methods: a simple glass tube with many holes to affect dispersion (used with volatile liquids) or the device used for volatile solid ligands shown in Figure 3.d. In both cases the device was held in place by the vacuum tight fitting in the center of the lid. The solid ligand was placed in the small cup, and after assembling the entire device, a vacuum of $\sim$ 1 torr was applied. 2-Propanol at -30 °C was circulated through the heat exchange coils of the ligand dispersing device (Figure 3.d), and further vacuum application reduced the system to 10^{-6} torr. At this time a liquid N_2 filled Dewar flask was placed around the entire apparatus, the 2-propanol was heated to reflux temperature (to sublime the ligand out through the small holes), cooling water was

circulated through the electrical leads, and current was applied to the tungsten basket to evaporate the metal. After evaporation for times varying up to 10 min the assembly was allowed to warm-up slowly to room temperature and transferred to an O_2-free, N_2-filled dry box while still evacuated. Interruptions in the evaporation were almost invariably caused by melting of the tungsten wire at the high resistance, tight turn at the bottom of the basket. The subsequent work-up of the runs is described in section II.G.2.

3. Additional equipment

A vacuum line of copper tubing (2.5 in O.D. for the manifold and main branches; 0.75 in O.D. for additional sections) was constructed using soft solder sweated joints. High vacuum, brass bellows valves were used throughout. Two fore pumps (one for initial pumping from atmospheric pressure and the second for final pumping through other traps and pumps), an oil diffusion pump and N_2(liq) cooled, stainless steel trap allowed pressures of 10^{-8} torr (determined by a calibrated cold cathode gauge) to be reached. This line was used in conjunction with the metal evaporation equipment discussed in the previous sections. A stainless steel dry box was re-conditioned and fitted with an hermetically sealed bellows pump (Model MB-21; Metbel Corp.,

Sharon Div., Sharon, Mass.) which circulated the N_2 atmosphere through a closed loop purification train consisting of three 10 cm (diameter) by 75 cm (length) columns. One of these was packed with 13A molecular sieves (solvent scavenger), one with an activated copper complex (O_2 scavenger; Catalyst R3-11; Chemical Dynamics Corp., S. Plainfield, N.J.) and one with 4A molecular sieves (H_2O scavenger). In addition, a N_2(liq) cooled solvent trap was placed between the box exit and the purification train to minimize contamination of the O_2 scavenger. The pressure drop and volume capacity of the bellows pump through the purification train was estimated and this allowed a turn-over of the box atmosphere at the rate of 2.5/hr.

G. Preparations

1. Ligands

The name, molecular formula, number symbol and preparative and/or purification procedure used in this paper are listed below for each ligand. For isomeric differences based on substituent orientation about phosphorus, α-β nomenclature is employed, wherein α refers to equatorial and β to axial orientation. The structural formulae for all but the first one are in Table 3.

Table 3. Structural formulae of ligands

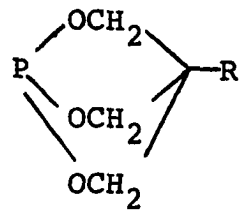

2--R

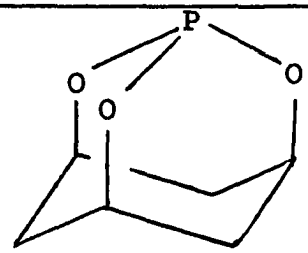

3

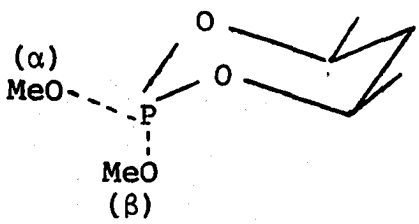

4-α and 4-β

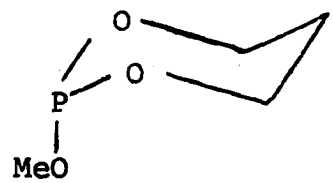

5-β

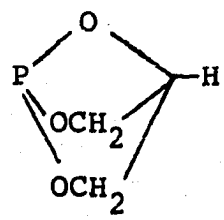

6

a. Trimethylphosphite $P(OCH_3)_3$; 1; distilled at atmospheric pressure, keeping the fraction boiling between 112-113 °C.

b. 4-Methyl-2,6,7-trioxa-1-phosphabicyclo[2.2.2]-octane $P(OCH_2)_3CCH_3$; 2-Me; prepared according to Verkade et al. (12).

c. 4-Ethyl-2,6,7-trioxa-1-phosphabicyclo[2.2.2]-octane $P(OCH_2)_3CCH_2CH_3$; 2-Et; prepared according to Verkade et al. (13).

d. 1-Phospha-2,8,9-trioxaadamantane $P(OCH)_3(CH_2)_3$; 3; prepared according to Verkade et al. (12).

e. 2-α-Methoxy-4,6-α,α-dimethyl-1,3-dioxa-2-phosphorinane $CH_3OP(OCHCH_3)_2CH_2$; 4-α; prepared according to White et al. (14).

f. 2-β-Methoxy-4,6-α,α-dimethyl-1,3-dioxa-2-phosphorinane $CH_3OP(OCHCH_3)_2CH_2$; 4-β; prepared according to Mosbo and Verkade (15).

g. 2-β-Methoxy-1,3-dioxa-2-phosphorinane $CH_3OP(OCH_2)_2CH_2$; 5-β; prepared according to White et al. (14) by a synthetic route originally discussed by Arbuzov and Zoroastrova (16).

h. 2,6,7-Trioxa-1-phosphabicyclo[2.2.1]heptane $\overline{P(OCH_2)_2CHO}$; 6; prepared according to Bertrand et al. (17), who used a slight modification of the original work of Denney and Varga (18).

2. Phosphite complexes of transition metals

The phosphite complexes of several series of d^6 and d^8 transition metal series are listed below by name, molecular formula and preparative method, using the number abbreviations from the previous section. Parts a-o concern the preparation of pentakis 1, 2-Me, 2-Et, 3, 4-α, 4-β, 5-β and 6 complexes of the first row d^8 transition metals Fe(0), Co(I) and Ni(II). The preparations of hexakis 1 d^6 complexes of the first, second and third row transition metals [Cr(0), Fe(II), Co(III); Mo(0), Ru(II), Rh(III); W(0), Os(II), Ir(III)] and some discussion concerning attempted preparations using other ligands are presented in parts p-x. The pentakis 1 complexes of the d^8 second and third row transition metals series Ru(0), Rh(I), Pd(II) and Os(0), Ir(I), Pt(II) are discussed in part y.

a. Pentakis(1)iron(0) The complex was prepared by the following three methods.

The static reactor shown in Figures 2 and 3 was used with the volatile ligand disperser discussed in section II.F.2. In a typical run, ∿ 0.5 g of Fe was evaporated and 8 ml of $P(OCH_3)_3$ co-condensed with the iron vapor onto the walls of the cylinder which was held at ∿ -196 °C by immersion in a N_2(liq) filled Dewar flask. The basket required a current of 18-20 amps at 12-15 volts in order to melt and evaporate the metal. The initial pressure was 10^{-5} torr,

and vacuum pumping was ceased during the run. At the end of the evaporation the vessel was allowed to warm to room temperature and all readily volatilized materials were removed by pumping and retained in a N_2(liq) cooled trap. No nmr or uv/visible spectral evidence for the desired product was seen in these materials. The vessel was then isolated from the atmosphere by the two Veeco valves and taken into a N_2-filled, O_2-free dry box. The dark brown-black oil was washed from the walls with three 10 ml portions of pentane and this suspension was filtered through a fine glass frit. Evaporation of the solvent and sublimation of the resulting black powder did notyield the expected product; however, the pentane filtrate from another run was concentrated to ∿ 3 ml and passed through a Millipore prefilter and filter (0.45 μ pore; Teflon) to produce a yellow solution which exhibited only absorbances in the ^{31}P nmr spectrum expected (see third method below) for the complex, the ligand and $(CH_3)_3PO$. The pentane solubility, solution color and ^{31}P nmr data are at present the only evidence available for the production of this compound in this manner.

The rotating flask assembly was used as a second method for preparing $Fe(\underline{1})_5$. In a typical run, a solution of 20 ml of $P(OCH_3)_3$ in 150 ml of methylcyclohexane was placed in a 1 liter flask equipped with a 45/50 male standard taper to fit the female joint shown in Figure 1. Several small pieces of iron weighing a total of ∿ 0.5 g were placed in the

tungsten wire basket. The flask was partially evacuated and the solution de-gassed by several freeze/pump/thaw cycles using N_2(liq) to solidify the solution. After warming the solution to its melting point, the flask was partially submerged in a pentane slush bath. The system was evacuated to 10^{-5} torr, and the flask rotated at $\sim$ 60 rpm. Heating the wire basket by passing a current of 18 amps at 12-13 volts caused a rapid rise in the pressure after a few seconds of evaporation. Upon cessation of the current for less than a minute, the vapor pressure in the system was again reduced to $\sim 10^{-5}$ torr, allowing the evaporation to continue. It was found that four to eight repetitions of this cycle were sufficient to evaporate $\sim$ 0.5 g of Fe. Unlike the case with the static cylindrical device, continuous vacuum pumping was maintained throughout the run with this apparatus. After allowing the black suspension produced by the evaporation to warm to room temperature, the apparatus was isolated from the stmosphere, detached from the vacuum pumping system and transferred to a N_2-filled, O_2-free dry box. The suspension was filtered through a fine glass frit and the resulting yellow filtrate evaporated to a dark yellow-brown oil. Extraction of this oil with two 40 ml portions of pentane and evaporation of the solvent produced 0.28 g of a pale yellow oily powder which was sublimed under vacuum (< 1.0 torr) at 80 °C. The ^{31}P nmr spectrum in D_6-acetone

showed the yellow sublimate to be contaminated with $(CH_3O)_3PO$. Addition of a known amount of $(CH_3O)_3PO$ and comparison of the changes in relative peak areas of the ^{31}P nmr spectra revealed that ∿ 0.21 g of the desired product had been formed. This amount represents a 4% yield based on evaporated iron.

The third process used for producing $Fe(\underline{1})_5$ is based on work by Muetterties and Rathke (19) published while this work was in progress. No experimental details were given in his paper, however. The following procedure was carried out in an N_2-filled, O_2-free dry box. In a 250 ml round bottom flask were placed 50 ml of THF, 50 ml of $P(OCH_3)_3$ and 2.63 g (20.0 millimole) of anhydrous $FeCl_2$; an amalgam consisting of 1.38 g Na (60.0 millimole) in 50 ml of Hg was added dropwise to this suspension. After three hr of vigorous stirring at room temperature, a black suspension resulted. This was decanted from the amalgam and vacuum pumped to dryness. The fine black powder remaining was washed with two 50 ml portions of pentane and filtered through a fine glass frit to yield a yellow solution. Vacuum evaporation of the solvent to dryness produced a dark yellow-brown powder. Sublimation of this powder at 80 °C and 0.5 torr gave clear yellow crystals (5.14 g) of the desired product in 38% yield based on $FeCl_2$. A recent reference (20) [also based on (19)] published after this part of these studies was

completed cites a yield of 40%. The mass spectrum consisted of a strong parent ion followed by stepwise loss of OCH_3 and $P(OCH_3)_3$ to $Fe[P(OCH_3)_3]_2$. The base peak corresponded to $P(OCH_3)_3$. This is a very air and/or water sensitive compound which should be stored cold and under an inert atmosphere. It is very soluble in solvents of widely varied polarity (pentane through CH_3OH) and appears to be more stable in storage as a solid than in solution; mp = 150-155 °C (decomp).

b. Pentakis(1)cobalt(I) tetrafluoroborate This compound was prepared according to Coskran et al. (21) except that the $Co(BF_4)_2$ solution was added to 10 ml neat $P(OCH_3)_3$.

c. Pentakis(1)nickel(II) tetrafluoroborate Reference 21 was followed for the preparation of this complex except that $Ni(BF_4)_2 \cdot 6H_2O$ was used instead of the analogous perchlorate salt.

d. Pentakis(2-Et)iron(0) The third method discussed in a. of this section was duplicated except that 39 g of the ligand in 30 ml of THF was used. After separation from the amalgam, the thick black suspension was diluted to twice its original volume with THF and rotated at 30,000 rpm for 30 min in a Beckman Model L-2 ultracentrifuge equipped with a Model 40 rotor of 26° fixed angle and 5.9 cm average radius. After careful decantation from the black sediment, the dark yellow solution was passed through a 0.45 μ Millipore

filter (Teflon) and used (with the addition of ∿ 15% by volume D_6-acetone as a deuterium lock source) for the ^{31}P nmr spectrum. The same solution after dilution with additional THF was used to obtain the uv/vis spectrum. The approximate yield of the reaction was calculated from the approximate molarity of the solution used for the uv/vis study. This molarity was roughly determined from the relative peak areas due to complex, ligand and $OP(OCH_2)_3CCH_2CH_3$ in the ^{31}P nmr spectrum and the weight of the residue remaining upon evaporation of the solvent from the uv/vis cell. For this experiment, equivalent nmr sensitivity of all chemically different P atoms was assumed and appropriate adjustment was made for the fact that the absorbance of the complex represented five P atoms whereas each of the other compounds represented one. Using the above values and assumptions and knowing that a 32-fold dilution was necessary to observe the lowest energy d-d transition band, an approximate yield of 2% was obtained.

The THF solution yielded the product (contaminated with ligand) as a pale yellow powder upon removal of the solvent. This material was very air and/or water sensitive, turning to a dark brown, oily solid upon exposure to air. The powder could be stored in a sealed glass vial in a Dry Ice chest for several days without noticeable change in appearance.

e. Pentakis(2-Me)cobalt(I) tetrafluoroborate The method described in part b. of this section for the

$P(OCH_3)_3$ analogue was used except that the saturated acetone solution of Co(II) was added to excess ligand (10 ml).

f. Pentakis(2-Me)nickel(II) tetrafluoroborate This compound was also prepared by the same technique used for its $P(OCH_3)_3$ counterpart (see part c.) except that the excess ligand was in an acetone solution saturated in metal salt.

g. Pentakis(3)iron(0) See the previous discussion in part d. of Fe(2-Et)$_5$ for a description of the method used to produce this complex. A yield of < 1% was estimated by the metal evaporation technique discussed earlier.

h. Pentakis(3)cobalt(I) tetrafluoroborate The references and discussions in parts b. and e. for analogous compounds are applicable for the preparative procedure followed for this complex and the yield was comparable.

i. Pentakis(3)nickel(II) tetrafluoroborate The preparation of the 2-Me counterpart of this compound was followed and the yield was comparable.

j. Pentakis(4-α or 4-β or 5-β)iron(0) The procedure described in part d. for the 2-Et analogue was used to produce these three previously unreported complexes and the yields were comparable. The only general difference being that $(CH_3CH_2)_2O$ was used as the solvent instead of THF.

k. Pentakis(4-α or 4-β or 5-β)cobalt(I) tetrafluoroborate These three previously unknown compounds were prepared according to methods discussed earlier for their

known analogues. The yields ranged between 4 and 6 percent. However, both the 4-α and 4-β preparations produced yellow oils which resisted all attempts to realize a crystalline product. The 5-β compound, however, was a solid like the 1, 2-Me and 3 complexes.

l. Pentakis(4-α or 4-β or 5-β)nickel(II) tetrafluoroborate The procedures discussed earlier for Ni(II) complexes were used to prepare these three previously unknown compounds as yellow solids in comparable yields.

m. Pentakis(6)iron(0) All of the attempts to prepare this compound by the methods used in this study produced only ambiguous ^{31}P, ^{1}H nmr and uv visible spectra.

n. Pentakis(6)cobalt(I) tetrafluoroborate A yellow solid was obtained with this ligand by procedures discussed earlier for Co(I) species. However, an immediate color change in the reaction mixture was not seen with this ligand as was the case with all of the other ligands. For reasons presented later in section III.D.2., some question has arisen as to the exact nature of this material. The preparation, however, is presented here for completeness.

o. Pentakis(6)nickel(II) tetrafluoroborate The same reservations and comments presented in part n. above apply to this compound whose preparation was attempted by methods discussed earlier for Ni(II) complexes.

p. Hexakis(1)chromium(0) The compound was made by the dropwise addition over a period of 30 min of 0.69 g

(30 millimole) of Na amalgamated with 40 ml of Hg to a cooled (-30 °C), vigorously stirred suspension of 1.23 g (10 millimole) of anhydrous $CrCl_2$ in 30 ml of pentane and 10 ml of $P(OCH_3)_3$ in a 125 ml round bottom flask. The equipment was charged, assembled and sealed in an inert atmosphere (O_2-free, N_2-filled dry box) but the addition was performed outside this environment. Stirring of the gray suspension with the amalgam was continued for an additional 1.5 hr, by the end of which the reaction had produced a very fine, deep black suspension. The cooling bath (Dry Ice/toluene) had been removed after one hr so that the reaction had time (∿ 30 min) to reach room temperature. The apparatus was then returned to the inert atmosphere box. After settling of the black solid and careful decantation, the colorless solution was filtered through a fine glass frit and reduced in volume by vacuum pumping to ∿ 5 ml. This solution was used (with the addition of a few drops of C_6D_6 as a deuterium lock source) for the ^{31}P nmr spectrum. The limitations of the sweep width on the ^{31}P nmr instrumentation prevented obtaining both the reference (85% H_3PO_4 = 0.0 ppm) and the observed absorbance on the same spectrum without any ambiguities arising as to the correct phasing and possible folding of both peaks. However, the excess ligand was observed at the correct chemical shift and thus, it was used as the reference point from which to measure the chemical shift of the complex. The uv/vis spectrum of this solution was

inconclusive regarding assignment of the d-d electronic transitions. Many attempts were made at making this compound by the two metal evaporation devices discussed earlier. Very tentative ^{31}P nmr evidence was produced from one run with the rotating flask. The yield of the $Na(Hg)/CrCl_2$ reaction could not be estimated but it is very low considering the high attenuation and large number of scans necessary to observe the ^{31}P nmr spectrum. Upon exposure to air or vacuum evaporation to dryness, the pentane solution produced a very small amount of gray-green solid. The oxide of Cr(III) and its hydrate are green and gray-green, respectively (22). Although not isolated, this compound was believed to have been produced because of the expected position of its ^{31}P chemical shift discussed later in Section III.A.

q. Hexakis(l)iron(II) tetrafluoroborate This compound was prepared by reacting 0.253 g (2.0 millimole) of anhydrous $FeCl_2$ with 0.779 g (4.0 millimole) of anhydrous $AgBF_4$ in 40 ml of THF in a 125 ml round bottom flask. The suspension, stirred at room temperature in an inert atmosphere for 30 hr, went through an initial white cloudiness to a fine black suspension after ∿ 6 hr to a final pink-purple suspension. It was found necessary to wait for this final condition before further reaction, otherwise $Ag(\underline{L})_4BF_4$ (as shown by ^{31}P and ^{1}H nmr spectra) was produced. The suspension was then filtered on a fine glass frit and the solid remaining weighed almost

exactly the combined weight of the two reactants. The filtrate contained a very small amount of unidentified pale yellow oil. Upon washing the precipitate with two 10 ml portions of CH_2Cl_2 the purple solid left on the frit was found to comprise (within 2.5%) the weight of AgCl expected to be produced. The pale pink CH_2Cl_2 solution was then added dropwise with stirring to 10 ml of $P(OCH_3)_3$ in a 50 ml Erlenmeyer flask and this produced a dark yellow solution. Addition of this solution to 50 ml of $(CH_3CH_2)_2O$ with stirring produced pale yellow crystals of the impure desired complex. Two or three repetitions of dissolving the complex in a minimum amount of CH_2Cl_2 followed by addition to $(CH_3CH_2)_2O$ finally produced white crystals of $Fe(\underline{L})_6(BF_4)_2$, and these were used for spectral studies and elemental analysis.

Analysis calculated for $C_{18}H_{54}B_2F_8FeO_{18}P_6$: C, 22.19; H, 5.60; F, 15.60; Fe, 5.73. Found: C, 21.87; H, 5.60; F, 15.48; Fe, 5.49.

r. Hexakis(1)cobalt(III) tetrafluoroborate The preparation of this complex followed Coskran et al. (21) except that the Co(II) solution was added to neat excess $P(OCH_3)_3$ (10 ml).

s. Hexakis(1)molybdenum(0) Attempts to prepare this compound by following the only other report of this compound (23) did not yield the desired product (see section III.A.2.j.). A rather air sensitive, pentane-soluble, white,

crystalline material exhibiting ^{1}H and ^{31}P nmr spectral characteristics consistent with the above formulation was prepared during this work by the following procedure. In a 125 ml round bottom flask was stirred a suspension of 30 ml of THF, 10 ml of $P(OCH_3)_3$ and 1.366 g (5.0 millimole) of $MoCl_5$ kept at -30 °C with a dry ice/toluene bath. To this was added dropwise over a period of 30 min an amalgam of 0.82 g (38 millimole) of Na in 40 ml of Hg. The reaction mixture was stirred for an additional hr while the cooling bath was allowed to warm to room temperature. The reaction progressed from an initial green to a final brown-black suspension and the reaction assembly was handled under inert conditions as discussed under section II.G.2.p. for the Cr analogue. After returning the reaction flask to the inert atmosphere box, the suspension was decanted from the amalgam and filtered through a fine glass frit. The filtrate was concentrated by vacuum pumping to a final volume of ∿ 10 ml and was then passed through a filtration/chromatography column of 12 mm I.D. and consisting of ∿ 3 cm of Cellulite filter aid (upper layer) and ∿ 7 cm neutral alumina (lower layer) with the two layers separated by packed glass wool. The column was prepared by pouring pentane slurries of each material into standing pentane. After lowering the pentane level to the top of the column material the pentane/MoL_6/L solution was carefully introduced to the column. The liquid

obtained upon lowering the level of this solution to the top of the column was discarded. Pentane was then added to the volume above the column and collection of the filtrate begun. The Cellulite layer rapidly became dark brown and a dark brown layer developed in the top ∿ 5 mm of the alumina section. Under this layer was a slowly moving yellow band which eventually diffused throughout the alumina. As soon as this yellow solution passed through the column, collection was stopped and the pentane solution collected was vacuum pumped to dryness to yield very pale brown crystals. Dissolution of the material in a minimum amount of pentane (∿ 10 ml) and passage through another short (∿ 1 cm) alumina column produced white crystals of what is believed to be the desired complex. The yield was 2.68 g (64% of theoretical based on $MoCl_5$). Instability of the product precluded a satisfactory elemental analysis.

t. Hexakis(1)ruthenium(II) tetraphenylborate This previously unreported compound was prepared by stirring 0.512 g (2.00 millimole) of $RhCl_3 \cdot 3H_2O$, 1.982 g (6.00 millimole) of $(C_6H_5)_3CBF_4$ and 60 ml CH_3CN in a 125 ml round bottom flask while simultaneously introducing 10 ml of $P(OCH_3)_3$ by rapid dropwise addition. The reaction became quite warm and started to bubble. The reaction flask was then heated by slowly refluxing the solvent for six hr. The resulting suspension was filtered through a fine glass frit to give a

pale yellow solution. The solvent and other readily volatilized products were removed by vacuum pumping to leave on oily yellow solid. This was washed with 200 ml each of pentane, $(CH_3CH_2)_2O$ and THF (in that order) by decantation to leave a small amount of yellow oil. When dissolved in 6 ml of CH_2Cl_2 followed by addition with stirring of the resulting solution to 50 ml of THF, this oil yielded 1.03 g (47% of theoretical based on $RhCl_3 \cdot 3H_2O$) of white crystals of $Rh(\underline{L})_6(BF_4)_3$. This material was used for the spectral work and elemental analysis.

Analysis calculated for $C_{18}H_{54}B_3F_{12}O_{18}P_6Rh$: C, 19.42; H, 4.87; B, 2.89; Rh, 9.19. Found: C, 20.16; H, 5.10; B, 2.26; Rh, 6.12.

u. Hexakis(1)tungsten(0) This previously unreported compound was prepared by a Na(Hg) reduction of WCl_4. The tetrachloride was prepared (24) by stirring a mixture of 8.01 g (20 millimole plus 1% excess) of WCl_6 and 3.52 g (10 millimole) of $W(CO)_6$ in 100 ml of chlorobenzene (previously dried over CaH_2 and sparged with N_2 for one hr) under slow reflux of the solvent and in an inert atmosphere. The course of the reaction was followed by watching for the cessation of CO passing through a mineral oil bubbler (after $\sim$ 2 hr). The reaction was continued for a total time of 3.4 hr at the end of which dark green-black crystals of WCl_4 had formed. These were filtered onto a fine glass frit, washed with two 20 ml

portions of C_6H_5Cl, ∿ 50 ml of pentane and finally ∿ 50 ml of $(CH_3CH_2)_2O$. The material was then dried by vacuum pumping overnight. The yield was 9.68 g (99% of theoretical).

The $W(\underline{1})_6$ was prepared by the dropwise addition over ∿ 30 min of 0.69 g (30 millimole) of Na (amalgamated in 30 ml of Hg) to a vigorously stirred, cooled (-30 °C) suspension of 30 ml of THF, 10 ml of $P(OCH_3)_3$ and 1.63 g (5.0 millimole) of WCl_4 in a 125 ml round bottom flask. The reaction was carried out under inert atmosphere conditions as described earlier for Cr(0) and Mo(0). After three hr (during the last of which the bath and vessel were allowed to warm to room temperature) a fine brown-black suspension had formed. A work up of decantation, filtration and column chromatography similar to that described for $Mo(\underline{1})_6$ produced white crystals of $W(\underline{1})_6$. The reaction yielded 2.69 g (58% of theoretical) of the moderately air sensitive compound. Of the two zero-valent d^6 compounds ($\overline{MoL}_6$, $\overline{WL}_6$) isolated, the tungsten complex is the more stable to storage. There was no visible change in appearance of the compound after two wk in a Dry Ice chest in contrast to MoL_6 which became noticeably brown after two days under the same conditions. Morever, the W compound can be exposed to air for short periods (< 5 sec) with no visible alteration of appearance while MoL_6 changes immediately to a dark brown oily solid under these conditions. Instability of the compound precluded obtaining a satisfactory elemental analysis.

v. Hexakis(1)osmium(II) tetraphenylborate Although the $P(OCH_2CH_3)_3$ analogue of this complex is mentioned in the literature (25, 26), there seems to be some mystery surrounding the precursor, $OsBr_2[P(C_6H_5)]_3$. This precursor is first mentioned by Vaska (28) and later by Couch and Robinson (24, 27), but the latter gives no references to the synthesis and the former provides no experimental details other than reactants to be used. For this work the similar starting material, $OsCl_2[P(C_6H_5)_3]_3$, was prepared (29) and used as follows. A suspension of 0.840 g (1.10 millimole) of $OsCl_2[P(C_6H_5)_3]_3$ in 10 ml of $P(OCH_3)_3$ and 30 ml of CH_3OH was stirred with heating at a slow reflux for 18 hr. At the end of this period the red-brown suspension was filtered through a fine glass frit and 1.0 g of $NaB(C_6H_5)_4$ in 5 ml of CH_3OH was added dropwise to the stirred yellow filtrate. This solution was then pumped to dryness and the resulting pale yellow solid washed repeatedly with THF. The yellow oil, which coated the flask after the reaction, was dissolved in 2 ml of CH_2Cl_2 and added dropwise to stirred THF (20 ml). A small amount of white solid precipitated in the above solution which was filtered onto a fine glass frit and washed with THF. This solid was then washed through the frit with 2 ml of CD_3CN and used for taking a ^{31}P nmr spectrum. Further discussion concerning the synthetic background and support for our assignment of the compound is found in section III.A.

w. Hexakis(1)iridium(III) tetrafluoroborate This compound was prepared in an analogous manner to its Rh(III) counterpart using 2.0 millimole of $IrCl_3 \cdot 3H_2O$. The reaction yielded 0.38 g (16% of theoretical) of the desired product as a very pale yellow oil. When dissolved in 2 ml of $(CD_3)_2CO$, this oil was used for obtaining the ^{31}P nmr spectrum. The spectral data presented later support the above formulation.

x. Pentakis(1)ruthenium(0), pentakis(1)rhodium(I) tetraphenylborate, pentakis(1)palladium(II) tetraphenylborate, pentakis(1)iridium(I) tetraphenylborate, pentakis(1)-platinum(II) tetraphenylborate These five complexes were prepared as part of a synthesis check for Inorg. Synth. (30). Most of the starting compounds were obtained from the authors. J. P. Jesson (see section II.A.) provided the following ^{31}P nmr data for the A_2B_3 pattern of the five P atoms in Os(1)$_5$: A_2 = -111 ppm, B_3 = -145 ppm, temp = -130 °C. From this data the chemical shift was obtained by taking the weighted average of the A_2 and B_3 chemical shifts. Information concerning the solvent used was not available. Further discussion concerning these synthetic routes and some difficulties encountered within them is found in section III.A.

3. N_2O_4 oxidation of phosphites and phosphite complexes of transition metals

Weighed amounts of 4-α (0.2160 g = 0.20 ml), 4-β (0.2167 g = 0.20 ml), $Co(4\text{-}\alpha)_5BF_4$ (0.1591 g), $Co(4\text{-}\beta)_5BF_4$ (0.1197 g), $Ni(4\text{-}\alpha)_5(BF_4)_2$ (0.2202 g) and $Ni(4\text{-}\beta)_5(BF_4)_2$ (0.2195 g) were placed in separate small vials each capped with a rubber septum. After flushing the vials with N_2 for a few minutes, 2.0 ml of $CHCl_2$ was injected into each vial to dissolve the complexes. A solution of N_2/N_2O_4 (∿ 30% by volume of N_2O_4) was then bubbled through the solutions for 2 hr. At the end of this period, N_2 only was bubbled through for an additional hr to produce clear, colorless solutions (in the case of ligands only) or purple-grey suspensions [in the case of the Co(I) complexes] or yellow-green suspensions [with the Ni(II) compounds]. These reactions were then placed in an inert atmosphere box, filtered through Cellulite and adjusted to a final volume of 1.0 ml by washing the filter with additional CH_2Cl_2. These final solutions were used for the gas/ chromatography described in section III.B.

III. RESULTS AND DISCUSSION

A. Synthetic Procedures

Pertinent background material, specific problems encountered during the syntheses and variation in the reported synthetic routes are the subject of this section. The order follows that of section II.G. However, only those reactions which offered substantial synthetic challenges, which produced new compounds or which differed from their published procedures are considered.

1. Ligands

The preparation of these compounds followed the literature cited earlier.

2. Phosphite Complexes of Transition Metals

a. $Fe(l)_5$ Several research groups [Muetterties and Rathke (19), Jesson et al. (30) and Tolman et al. (31)] were concurrently working on the synthesis of this compound or its PF_3 analogue [Timms (32)]. Except for Muetterties, these workers centered their investigations on metal evaporation techniques. Although metal evaporation methods have long been known (33), their application to metal complex synthesis is a fairly recent technique which has been reviewed (34). Publications from other laboratories (32, 34, 35, 36, 37, 38)

concerning a wide variety of transition metal compounds made by this method suggest that the devices described earlier in this dissertation do not produce sufficiently large quantities of metal vapor for reasonable yields to be obtained. Although the rotating flask apparatus is more efficient (34) for making compounds by metal evaporation the choice of solvents is seriously restricted. The solvent must be inert to reaction with the metal vapor. Thus halocarbons cannot be used because they have been shown (37, 38) to react with the evaporated metals. Alkenes are eliminated for the same reasons (37, 38), as are aromatics (39). Other functional groups (-OH, $-CO_2H$, -C≡C-, etc.) were not considered because of their possible high reactivity toward the metal or possible reaction with the complex (19). The solvent must have a freezing point substantially below the temperature at which the ligand has an appreciable vapor pressure (> 10^{-4} torr), and the solvent must be capable of dissolving a large excess of the phosphite ligand at very low temperatures. A high solvent polarity is particularly important in the case of the caged phosphites, but few polar solvents are available without the functional groups that have been eliminated from consideration. The solvent which was found to best meet these criteria was methylcyclohexane (mp = -126 °C).

The $Fe(\underline{l})_5$ complex was first mentioned in the literature by Muetterties and Rathke (19) but no details of the synthesis

were given. Other workers (30) cite a mp of 160 °C (decomp) which compares favorably with our value of 150-5 °C (decomp).

b. $Co(\underline{1})_5BF_4$ The original preparation of this compound (21) called for the addition of excess ligand to a solution of Co(II). This method, however, does not consistently reproduce the disproportionation of 2Co(II) to Co(I) and Co(III), but it will sometimes give a dark red-brown solution from which no Co(I) or Co(III) is obtained. Reversal of the order of addition and using neat ligand never failed,however, to give the desired compounds.

c. $Fe(\underline{2}\text{-Et})_5$ Numerous attempts to prepare this compound with the static reactor (using $\underline{2}$-Me because of its higher volatility) or the rotating flask (using the n-pentyl derivative, $\underline{2}\text{-}C_5H_{11}$, because of its higher solubility) were fruitless. Whereas both devices produced $Fe(\underline{1})_5$, neither produced $Fe(\underline{2}\text{-R})$, probably because in both cases the ligand concentration was much lower than with $P(OCH_3)_3$. This factor coupled with the inherently low yields of these methods (see section II.G.2.a.) apparently prevents the isolation of the desired product. A recent paper (31), however, describes the synthesis of a 1,5-cyclooctadiene intermediate, $Fe(COD)_2$, by metal evaporation techniques, and this was further reacted in situ with the ligand to produce $Fe(\underline{2}\text{-Et})_5$. This method overcomes the volatility and solubility problems of these caged ligands.

The main difficulty with this synthesis is removal of the extremely fine particles of elemental iron. This particulate matter rapidly plugs the pores of a fine glass frit or Millipore filter, and it passes through medium or coarse frits. The Fe/L/FeL_5 suspension also passes through a 10 cm long column of Cellulite filter aid as a dark brown-black, opaque suspension. The ultra centrifuge technique (see section II.G.2.d.) however, did produce clear solutions of the complexes and ligands.

Attempts to sublime excess ligand from the black solid remaining after pumping the original solution to dryness apparently resulted in the thermal decomposition of the product. The thermal instability of $Fe(\underline{1})_5$ has been noted (19, 30). There was no indication from the ^{31}P nmr spectrum that $Fe(\underline{2}\text{-Et})_5$ remained in the black powder produced by this sublimation. The high solubility of the compound in solvents of widely varied polarity prevented recrystallization of ligand-free FeL_5. Attempts to extract only the complex from the dried suspension also produced mixtures of L and FeL_5. It should be noted that the duPont workers (30) also were unable to separate this complex from the excess ligand.

d. $\underline{Co(2\text{-Me})_5BF_4}$ The discussion under b. above concerning the order of addition applies to this compound also.

e. $\underline{Fe(3)_5}$ This was the most poorly characterized of the FeL_5 (L = $\underline{1}$, $\underline{2}$-R, $\underline{3}$) series. The yield of this

complex was the lowest and the apparent instability the highest. The discussion concerning isolation of the $Fe(\underline{2}\text{-Et})_5$ compound presented earlier applies to this complex which also was not obtained free of the excess ligand.

f. $Fe(4\text{-}\alpha \text{ or } 4\text{-}\beta \text{ or } 5\text{-}\alpha)_5$ The purification techniques discussed earlier were applied to these compounds but they apparently thermally decomposed. Vacuum pumping to dryness of the original THF solution produced black powders from which no pure product was realized as shown by ^1H and ^{31}P nmr spectroscopy.

g. $Fe(6)_5$ The three methods discussed in section II.G.2.a. for the analogous $P(OCH_3)_3$ compound were used in several attempts to prepare this compound. However, no ^1H or ^{31}P nmr evidence for this complex was seen. A Na(Hg) reduction reaction did yield a pale yellow solution which was used to observe an uv/visible spectrum.

h. $Co(6)_5BF_4$ and $Ni(6)_5(BF_4)_2$ Unlike the reactions using other phosphite ligands, the preparation of these two compounds involved an apparent induction period before any color change was seen in the reaction mixture.

i. $Cr(1)_6$ All but one attempt to prepare this compound using either of the two metal evaporation devices were unsuccessful. Very tentative ^{31}P nmr evidence (a very small peak at -257 ppm) was realized from one run with the rotating flask. However, the low yield and thermal

instability of the complex coupled to limit this approach. Numerous Na(Hg) reductions, identical to the preparative method in section II.G.2.g. (except that THF or Et_2O was used as the solvent) produced only pale green solutions of extreme air sensitivity and posessing only ^{31}P nmr absorbances due to $P(OCH_3)_3$ and its oxide. In addition to these methods, an unsuccessful attempt was made to produce CrL_6 by the preparation of activated chromium metal in a manner used to synthesize $Cr(CO)_6$ (40). French workers (23) have attempted the preparation of this compound by the uv irradiation (Hg lamp) of a pentane and ligand solution of $Cr(CO)_6$. However, they produced only CrL_5CO and could not further substitute the metal with $P(OCH_2)_3$.

The solution of $Cr(\underline{1})_6$ produced as described in section II.G.2.g. using pentane as the solvent was very air, water and heat sensitive. Upon exposure to air a grey-green solid precipitated immediately while warming to room temperature produced a similar precipitate from the clear colorless pentane solution after ∿ 20 min. Although THF is known to coordinate to chromium halides (41a), it is somewhat surprising that this solvent as well as diethyl ether apparently interferes with the coordination of trimethyl phosphite.

j. $\underline{Fe(1)_6(BF_4)_2}$ Muetterties and Rathke (19) reports the preparation of the $B_{12}H_{12}^{2-}$ salt of this complex from excess ligand, FeI_2 and $Li_2B_{12}H_{12}$ but gives no details or spectral

data. Bancroft and Libbey (41b) have also recently discussed FeL_6^{2+} compounds. Our independent preparation of $FeL_6(BF_4)_2$ requires the use of $Fe(BF_4)_2$ solutions. Dichloromethane or CH_3OH or $(CH_3)_2CO$ solutions of $Fe(BF_4)_2$ are stable at room temperature in an inert atmosphere for less than 30 min; after which a dark purple-black precipitate begins to form. Evaporation of the CH_2Cl_2 solutions of $Fe(BF_4)_2$ discussed in section II.G.2.r. yields very soft, pale pink, clear crystals. These decompose to a dark purple, oily solid within a few minutes after removal of the solvent. Both as a solution and as a solid, $Fe(BF_4)_2$ decomposed overnight when stored in a Dry Ice chest.

A number of attempts to prepare other $FeL_6(BF_4)_2$ complexes (L = 2-R, 3, 5-α, 6) resulted in pale yellow solids. However, even after several re-precipitations, none of these compounds presented unambiguous ^1H and ^{31}P nmr spectra.

s. $Mo(1)_6$ Mathieu and Poilblanc (23) claim to have produced this complex by the uv irradiation (Hg lamp) of a pentane solution of $P(OCH_3)_3$ and $Mo(CO)_6$. They do not, however, give a detailed description of the synthesis. The ^1H nmr spectrum of $Mo(1)_5CO$ is reported by line shape and peak spacing but the chemical shift is not given. A chemical shift of 3.90 δ and line shape (apparent triplet) is reported in this paper for MoL_6. Upon repeating this experiment we were able to prepare MoL_5CO but further irradiation (up to

40 days total) did not produce a compound lacking a CO absorbance in the ir spectrum. The ^1H nmr spectrum of our MoL_5CO was a complicated mutiplet falling between 3.40 and 3.60 δ having identical peak spacings and relative peak heights similar to those reported by Poilblanc. The MoL_6 produced by the Na(Hg) reduction of $MoCl_5$ (see section II.G.2.s.) exhibited a ^1H nmr absorbance at 3.42 δ. If the center of the MoL_5CO absorbance (3.50 δ) is used as a basis, it seems unlikely to us that a chemical shift difference of 0.40 ppm (3.90-3.50) would arise as suggested by the French workers, when one $P(OCH_3)_3$ ligand is replaced by a CO. It seems more likely that the ^1H nmr chemical shifts of $Mo(\underline{1})_6$ and $Mo(\underline{1})_5CO$ would be quite similar as found in this work and by the similarity of the shifts in $Ni(\underline{3})_3CO$ and $Ni(\underline{3})_4$ (which exhibit a maximum difference between comparable protons of 0.04 ppm (42) and by the analogous 2-Me complexes which show a maximum difference of 0.06 ppm (43)).

1. $\underline{Rh(1)_6(BF_4)_3}$ The reaction between $(C_6H_5)_3CBF_4$ and $P(OCH_3)_3$ is known (45, 46) to produce $[(C_6H_5)_3C](CH_3O)_3P^+$-$BF_4^-$. Whether this phosphonium salt or $(C_6H_5)_3CBF_4$ acts as the electrophilic halogen abstractor in the reaction with $RhCl_3 \cdot 3H_2O$ is not known. In either case $(C_6H_5)_3CCl$ would be produced and this may react with the excess ligand by a Michaelis-Arbuzov process to produce $[(C_6H_5)_3C](CH_3O)_2PO$ and CH_3Cl. The latter product is known (47) to cause a rapid

Michaelis-Arbuzov rearrangement of $(CH_3O)_3P$ by an autocatalytic mechanism. This rearrangement and the concommitant production of gaseous product (CH_3Cl) could be the cause of the initial rise in temperature and bubbling of the reaction mixture. This side reaction as well as a reaction between $(C_6H_5)_3CBF_4$ and the water of hydration in $RhCl_3 \cdot 3H_2O$ may be the cause of the rather low yield (47%). Upon repeating the reaction with a 6:1 molar ratio of $(C_6H_5)_3CBF_4$ to $RhCl_3 \cdot 3H_2O$ (instead of 3:1 as in section II.G.2.u.), we were unable to isolate any $RhL_6(BF_4)_3$. The larger amount of $(C_6H_5)_3CBF_4$ may have induced a Micharlis-Arbuzov rearrangement of all the ligand before it could coordinate to the rhodium. A number of attempts to prepare $RhL_6(BF_4)_3$ by using $AgBF_4$ (as in the $FeL_6BF_4)_2$ preparation of section II.G.2.g.) or $(CH_3CH_2)_3OBF_4$ as the halogen abstractor, failed to produce the desired compound.

m. $\underline{W(1)_6}$ In the work of Poilblanc (23) cited earlier is described an attempt to prepare this compound by uv irradiation of $W(CO)_6$ in a pentane and $P(OCH_3)_3$ solution. Full phosphite substitution was not achieved however, and only WL_5CO was realized. The line shapes and chemical shifts of this complex in both the ^1H and ^{31}P nmr spectra as well as a comparison of the ^1H nmr data of ML_6 (M = Mo, W) and $ML_6(BF_4)_3$ (M = Rh, Ir) support the production of both the Mo and W compounds by our synthetic route.

n. $Os(1)_6[B(C_6H_5)_4]_2$ As stated earlier, the ethyl analogue is reported in the literature (24, 27) but very little is published concerning the $OsBr_2[P(C_6H_5)_3]_3$ precursor. In addition, the crystallization of $Os[P(OCH_2CH_3)_3]_6[B(C_6H_5)_4]_2$ is reported (24) to take five months. The use of the chloride compound, $OsCl_2[P(C_6H_5)_3]_3$ as the precursor was necessary in view of the lack of preparative information concerning the bromide compound. The solubility characteristics, preparative method and ^{31}P nmr spectral data are presently the only evidence to support this preparation.

o. $Ir(1)_6(BF_4)_3$ The discussion concerning the Rh(III) compound in part 1. above applies to this complex.

p. $Ru(1)_5$, $Rh(1)_5B(C_6H_5)_4$, $Pd(1)_5[B(C_6H_5)_4]_2$, $Ir(1)_5B(C_6H_5)_4$, $Pt(1)_5[B(C_6H_5)_4]_2$ A brief description of the reactions used to produce these compounds is included here because the work was done as part of a synthesis check of a paper submitted to Inorganic Syntheses by J. P. Jesson et al. (30) and is not as yet available to the literature. Most of the starting materials were provided by these authors and the references herein to these materials are those cited by them. Unless stated otherwise the reaction proceeded as described.

The Ru(0) compound was made by a Na(Hg) reduction of $RuCl_2[P(OCH_3)_3]_4$ (47) in the presence of excess ligand.

The Rh(I) complex is claimed by the authors to be produced by a reaction between $[(C_2H_4)_2RhCl]_2$ (48), $NaB(C_6H_5)_4$ and excess ligand. However, after following the preparation exactly as written we produced $Rh(\underline{1})_2B(C_6H_5)_4$ as shown by a comparison of its ^1H nmr spectrum with that published by Haines (49). However, this author does describe a method for regenerating the pentakis phosphite complex from the bis compound (49). After following this method, the desired Rh(I) compound was realized but with a somewhat lower yield than that reported by Jesson et al.

A reaction between $PdCl_2$, $NaB(C_6H_5)_4$ and excess $P(OCH_3)_3$ was used to prepare $Pd(\underline{1})_5[B(C_6H_5)_4]_2$.

A cyclooctene precursor, $[IrCl(C_8H_{14})_2]_2$ (50), was allowed to react with excess ligand and $NaB(C_6H_5)_4$ to prepare $Ir(\underline{1})_5B(C_6H_5)_4$.

The $Pt(\underline{1})_5[B(C_6H_5)_4]_2$ complex was prepared in a manner analogous to that of the Pd(II) compounds.

B. Gas/Liquid Chromatography Studies

It was felt that the somewhat ambiguous pattern of the uv/vis and ^{31}P nmr data (see later discussion and data tables) of the $\underline{4}$-α and $\underline{4}$-β complexes of Fe(0), Co(I) and Ni(II) could be clarified by determining whether or not the α or β orientation of the coordinate phosphite had been preserved. Since N_2O_4 is known to stereoretentively

oxidize phosphites to phosphates (15), it was felt that this oxidizing agent might also accomplish the same result with coordinated phosphites. Authentic samples of 4-α and 4-β were oxidized and used to verify the retention times for the phosphates reported earlier (8) under conditions which differed very slightly from those used here. The following data, showing the relative percentages of 4-α and 4-β found for each of the four compounds, reveal that the orientation about phosphorus was not always retained. The molecular formulas of the complexes below are based upon the orientation of the reactant phosphite ligand and may not truly reflect the orientation upon coordination.

$Co(4\text{-}\alpha)_5BF_4$: 16%α; 84%β.

$Co(4\text{-}\beta)_5BF_4$: 11%α; 89%β.

$Ni(4\text{-}\alpha)_5(BF_4)_2$: 100%α.

$Ni(4\text{-}\beta)_5(BF_4)_2$: 100%β.

The FeL_5 compounds were not included in this study since it was not possible to isolate them free of excess ligand. It is interesting to note that approximately the same relative percentages of α and β are seen for the two Co(I) compounds even though each was prepared from initially sterechemically pure ligand.

C. UV/Visible Spectroscopy Studies

The results of these studies are shown in Table 4 in which new compounds are underlined. The data obtained during this work agree well with those reported earlier for $Co(\underline{1})_5^+$, $Ni(\underline{1})_5^{2+}$, $Ni(\underline{3})_5^{2+}$ (21); $Co(\underline{2}\text{-Me})_5^+$, $Co(\underline{3})_5^+$ (14). Every effort was made to use identical solvents and anions within a series. In some cases, spectra were taken in different solvents, but the λ_{max} values were not found to vary substantially.

D. NMR Spectroscopy Studies

1. ^1H nmr spectroscopy

Table 5. lists the ^1H nmr data obtained. New compounds are underlined but only those which were isolated or those whose ^1H nmr absorbance was distinctly separated from the absorbances of known contaminants are included. The chemical shifts listed for $Co(\underline{1})_5^+$ are in good agreement with those reported earlier (51).

2. ^{31}P nmr spectroscopy

A compilation of the ^{31}P nmr data obtained is found in Table 6. Of the pentakis $\underline{1}$ complexes of the d^8 second and third row transition metals, only Rh(I) exhibits a room temperature spectrum. It was necessary to obtain the spectra

Table 4. Uv/visible spectra data

(The ligand abbreviations used in this table are from section II.G.1.)

Compound[a]	λ_{max} ($\bar{\nu}$)[b]	ε(molar extinct. coef.)	Solvent[c]
Fe(1)$_5$	359.5 (27,820)	9.7×10^2	CH_2Cl_2
Co(1)$_5BF_4$	379.5 (26,350)	8.4×10^2	CH_2Cl_2
Ni(1)$_5(BF_4)_2$	401.0 (24,940)	1.5×10^3	CH_2Cl_2
Fe(2-Et)$_5$	336.5 (29,720)	5×10^3	THF
Co(2-Me)$_5BF_4$	352.0 (28,410)	1.0×10^3	CH_2Cl_2
Ni(2-Me)$_5(BF_4)_2$	367.5 (27,210)	1.8×10^3	CH_2Cl_2
Fe(3)$_5$	336.2 (29,740)	2×10^3	THF
Co(3)$_5BF_4$	349.2 (28,640)	1.7×10^3	CH_3CN
Ni(3)$_5(BF_4)_2$	363.0 (27,760)	4.2×10^2	CH_3CN

[a]Previously unknown compounds are underlined. New compounds which differ from known analogs only in anion are not underlined. The spectra of this latter group and those of previously prepared complexes were retaken to standarize, where possible, solvent and anion and to measure λ_{max} more precisely.

[b]The wavelengths of the absorption maxima, λ_{max}, are expressed in nm; wave numbers, $\bar{\nu}$, are in cm^{-1}.

[c]THF = tetrahydrofuran; DMF = dimethylformamide.

Table 4. (Continued)

Compound[a]	λ_{max} ($\bar{\nu}$)[b]	ε (molar extinct. coef.)	Solvent[c]
$Fe(\underline{4}\text{-}\alpha)_5$	335.7 (29,790)[d]	8×10^3	$(CH_3CH_2)_2O$
$Co(\underline{4}\text{-}\alpha)_5BF_4$	369.5 (27,060)[d]	4.6×10^2	CH_2Cl_2
$Ni(\underline{4}\text{-}\alpha)_5(BF_4)_2$	391.5 (25,540)[d]	2.4×10^3	CH_2Cl_2
$Fe(\underline{4}\text{-}\beta)_5$	340.8 (29,340)[e]	4×10^3	$(CH_3CH_2)_2O$
$Co(\underline{4}\text{-}\beta)_5BF_4$	362.6 (27,580)[e]	4.7×10^2	CH_2Cl_2
$Ni(\underline{4}\text{-}\beta)_5(BF_4)_2$	392.4 (25,480)[e]	2.6×10^3	CH_2Cl_2
$Fe(\underline{5}\text{-}\beta)_5$	338.0 (29,590)[f]	5×10^3	$(CH_3CH_2)O$
$Co(\underline{5}\text{-}\beta)_5BF_4$	368.3 (27,150)[f]	2.7×10^3	CH_2Cl_2
$Ni(\underline{5}\text{-}\beta)_5(BF_4)_2$	388.0 (25,770)[f]	2.0×10^3	CH_2Cl_2

[d]Slope of λ_{max} vs metal charge as 27.90 (correl. coeff = 0.99).

[e]Slope of λ_{max} vs metal charge as 25.80 (correl. coeff = 0.99).

[f]Slope of λ_{max} vs metal charge as 25.00 (correl. coeff = 0.99).

Table 4. (Continued)

Compound[a]	λ_{max} ($\bar{\nu}$)[b]	ε(molar extinct. coef.)	Solvent[c]
Fe(6)$_5$ (?)[g]	352 (28,400)[h]		THF
Co(6)$_5$BF$_4$	358.1 (27,920)[h]	4.7×10^2	DMF
Ni(6)$_5$(BF$_4$)$_2$	367.0 (27,250)[h]	2.7×10^3	DMF

[g]Spectral data ambiguous for this compound.

[h]Slope of λ_{max} *vs* metal charge is 7.50 (correl. coeff. = 0.99).

Table 5. ^{1}H nmr data

(The ligand abbreviations used in this table are from section II.G.1.)

Compound[a]	$\delta^{1}H$[b]	Description of absorbance	Solvent[c]
$\underline{Fe(1)_5}$	3.50	broad singlet with ill defined, symmetrical shoulders	CD_3CN
$Co(1)_5BF_4$	3.64	2 sharp singlets (3.55, 3.73) with very broad but less intense absorbance between	Cd_3CN
$Ni(1)(BF_4)_2$	3.85	broad singlet	CD_3CN
$\underline{Fe(2\text{-Et})_5}$	3.49	very broad singlet with ill defined shoulder	THF
$Co(2\text{-Me})_5BF_3$	4.10	broad singlet with ill defined, symmetrical shoulder	CD_3CN
$Ni(2\text{-Me})_5(BF_4)_2$	4.50	broad singlet	CD_3CN

[a]Previously unknown compounds are underlined. New compounds which differ from known ones only in anion are not underlined. The spectra of this latter group plus those of previously prepared complexes were retaken to standardize, where possible, solvents and anions. However, in several instances spectra were taken in two different solvents with no significant change in δ.

[b]Chemical shifts are reported in ppm relative to TMS as an internal standard.

[c]THF = tetrahydrofuran.

Table 5. (Continued)

Compound[a]	δ^1H[b]	Description of absorbance	Solvent[c]
$Fe(\underline{1})_6(BF_4)_2$	3.80	broad singlet with symmetrical shoulder	CD_3CN
$Co(\underline{1})_6(BF_4)_3$	4.00	broad singlet with symmetrical shoulder	CD_3CN
$\underline{Mo(\underline{1})_6}$	3.42	broad singlet with ill defined, symmetrical shoulders	$(CD_3)_2CO$
$Ru(\underline{1})_6[B(C_6H_5)_4]_2$	3.78	broad singlet with symmetrical shoulders	CD_3CN
$\underline{Rh(\underline{1})_6(BF_4)_3}$	3.98	broad singlet with ill defined, symmetrical shoulders	CD_3CN
$\underline{W(\underline{1})_6}$	3.42	broad singlet with well defined, symmetrical shoulders	C_5H_{12}
$\underline{Ir(\underline{1})_6(BF_4)_3}$	3.98	broad singlet with ill defined, symmetrical shoulders	CD_3CN

Table 6. ^{31}P nmr data

(The ligand abbreviations used in this table are from section II.G.1.)

Compound[a]	^{31}P[b]	Description of absorbance	Solvent[c]	Temperature (°C)
Fe(1)$_5$	-179.2	sharp singlet	$(CD_3)_2CO$	22
Co(1)$_5BF_4$	-148.3	very broad singlet	$(CD_3)_2CO$	22
Ni(1)$_5(BF_4)_2$	-109.4	very sharp singlet	$(CD_3)_2CO$	22
Fe(2-Et)$_5$	-161.5	sharp singlet	THF/$(CD_3)_2CO$ (6:1)	22
Co(2-Me)$_5BF_4$	-136.2	broad singlet	$(CD_3)_2CO$	22
Ni(2-Me)$_5(BF_4)_2$	-106.5	sharp singlet	$(CD_3)_2CO$	22
Fe(3)$_5$	-185.4	broad singlet	THF/$(CD_3)_2CO$ (6:1)	22

[a] Previously unknown compounds are underlined. New compounds which differ from known ones only in anion are not underlined. The spectra of this latter group plus those of previously prepared complexes were retaken to use where possible, the same solvents and anions. However, in several instances spectra were taken in two different solvents with no significant change in δ.

[b] Chemical shifts are reported in ppm relative to 85% H_3PO_4 as an external standard.

[c] In multiple solvent systems, the ratio by volume is reported parenthetically. THF = tetrahydrofuran; DMF = dimethylformamide.

Table 6. (Continued)

Compound[a]	^{31}P[b]	Description of absorbance	Solvent[c]	Temperature (°C)
$Co(\underline{3})_5BF_4$	-155.3	very broad singlet	CD_3CN	22
$Ni(\underline{3})_5(BF_4)_2$	-125.7	very sharp singlet	CD_3CN	
$Ru(\underline{1})_5$	-169.3	very sharp singlet	$CH_2Cl_2/CDCl_3$ (1:1)	-20
$Rh(\underline{1})_5B(C_6H_5)_4$	-136.5	2 very sharp singlets (-132.2, -140.7); $J_{Rh-P} = 307 \pm 5$	$CH_2Cl_2/(CD_3)_2CO$ (4:1)	22
$Pd(\underline{1})_5[B(C_6H_5)_4]_2$	-101.3	2 ill defined multiplets (-99.8, -101.7)	$CH_2Cl_2/CDCl_3$ (1:1)	-50
$Os(\underline{1})_5$	-124.6	A_2 = -111, B_3 = -145; see section II.G.2.s		-130
$Ir(\underline{1})_5B(C_6H_5)_4$	- 98.9	very, very broad symmetrical singlet	$CH_2Cl_2/CDCl_3$ (1:1)	-50
$Pt(\underline{1})_5[B(C_6H_5)_4]_2$	- 74.0	singlet with 2 peaks due to J_{Pt-P} (=3590 ± 5)	$CH_2Cl_2/CDCl_3$ (1:1)	-50

Table 6. (Continued)

Compound[a]	^{31}P[b]	Description of absorbance	Solvent[c]	Temperature (°C)
$Fe(\underline{4}\text{-}\alpha)_5$	-177.8[d]	broad singlet with ill defined shoulders	$(CH_3CH_2)_2O/C_6D_6$ (9:1)	22
$Co(\underline{4}\text{-}\alpha)_5BF_4$	-149.3[d]	very, very broad singlet	$(CD_3)_2CO$	22
$Ni(\underline{4}\text{-}\alpha)_5(BF_4)_2$	-109.4[d]	singlet with sharp shoulders	$(CD_3)_2CO$	22
$Fe(\underline{4}\text{-}\beta)_5$	-177.3[e]	singlet with broad unsymmetrical shoulders near base of peak	$(CH_3CH_2)_2O/C_6D_6$ (9:1)	22
$Co(\underline{4}\text{-}\beta)_5BF_4$	-148.5[e]	very, very broad singlet	$(CD_3)_2CO$	22
$Ni(\underline{4}\text{-}\beta)_5(BF_4)_2$	-110.8[e]	sharp singlet	$(CD_3)_2CO$	22
$Fe(\underline{5}\text{-}\beta)_5$	-178.8[f]	broad singlet	$(CH_3CH_2)_2O/C_6D_6$ (9:1)	22

[d] Slope of $\delta^{31}P$ *vs* metal charge is 34.21 (correl. coeff. = 0.99).

[e] Slope of $\delta^{31}P$ *vs* metal charge is 33.28 (correl. coeff. = 0.99).

[f] Slope of $\delta^{31}P$ *vs* metal charge is 33.75 (correl. coeff. = 1.0).

Table 6. (Continued)

Compound[a]	^{31}P[b]	Description of absorbance	Solvent[c]	Temperature(°C)
$Co(\underline{5}\text{-}\beta)_5BF_4$	-148.8[f]	very, very broad unsymmetrical singlet	$(CD_3)CO$	22
$Ni(\underline{5}\text{-}\beta)_5(BF_4)_2$	-111.2[f]	sharp singlet	$(CD_3)CO$	22
$Co(\underline{6})_5BF_4$	-166.0	very, very broad singlet	DMF/$(CD_3)_2CO$ (3:1)	22
$Ni(\underline{6})_5(BF_4)_2$	-172.0	broad singlet	DMF/CD_3CN (3:1)	22
$Cr(\underline{1})_6$	-260.5	very sharp singlet	$\underline{n}\text{-}C_5H_{12}/C_6D_6$ (∿ 20:1)	22
$Fe(\underline{1})_6(BF_4)_2$	-150.5	very sharp singlet	$CH_2Cl_2/(CD_3)_2CO$ (6:1)	22
$Co(\underline{1})_6(BF_4)_3$	-103.8 J_{Co-P} = 430 ± 30 (?, see text)	very, very broad plateau (-51.6 to -152.8);	D_2O	22

Table 6. (Continued)

Compound[a]	^{31}P[b]	Description of absorbance	Solvent[c]	Temperature(°C)
$Mo(\underline{1})_6$	-172.1	very sharp singlet	C_5H_{12}/C_6D_6 (~ 20:1)	22
$Ru(\underline{1})_6(BF_4)_2$	-125.4	very sharp singlet	$(CD_3)_2CO$	22
$Rh(\underline{1})_6(BF_4)_3$	- 91.9	2 singlets, each with symmetrical shoulders; J_{Rh-P} = 138 ± 5	$(CD_3)_2CO$	22
$W(\underline{1})_6$	-143.9	sharp singlet, J_{W-P} = 500 ± 50	$n-C_5H_{12}/CDCl_3$	22
$Os(\underline{1})_6[B(C_6H_5)_4]_2$	- 84.0	sharp singlet	CD_3CN	22
$Ir(\underline{1})_6(BF_4)_3$	- 32.6	singlet	$(CD_3)_2CO$	22
$Co(\underline{2}\text{-Me})_6(BF_4)_3$	-111.6	very, very broad plateau (-67.6 to -153.3); J_{Co-P} = 390 ± 10 (?, see text)	D_2O	22
$Co(\underline{3})_6(BF_4)_3$	-124.5	very, very broad plateau (-78.8 to -167.7); J_{Co-P} = 360 ± 40 (?, see text)	D_2O	22

of the other five complexes at or near their respective coalescence temperatures. Although the ^{31}P chemical shifts of the A_2 and B_3 patterns of these compounds do have a temperature dependence, the chemical shift at coalescence is not a function of the temperature (52).

A description of the line shape of the absorbance is included in Table 6., however some additional points should be made concerning the complexes of 4-α, 4-β and 6. As stated earlier in section III.B., the pentakis (4-α and 4-β) cobalt(I) compounds very probably were each ligated with both the α and β ligand forms. This may be reflected in the ^{31}P nmr spectra of these two complexes in that the absorbances were much broader than any other Co(I) compound studied.

E. Theoretical Background

In the nmr experiment the magnetic dipole (a) of the nucleus precesses around the axis of the applied magnetic field (H_o) at the Larmor frequency (ω). If the frequency of an electric field (defined by $\nu=\omega/2\pi$) normal to H_o is equal to ω, then the precessing magnetic dipole can interact with the energy of the electric field. This interaction can be either absorption or emission, but since there are more nuclei in the lower energy state there will be a net absorption of energy. The energy exchange between the electric and magnetic dipoles can be expressed by

$$\Delta E(\mu, H_o) = -\vec{\mu} \cdot (I - \vec{\sigma}) \cdot \vec{H}_o \qquad \text{Eq. (1)}$$

wherein ΔE (as a function of μ and H_o) is the energy absorbed by the molecule when $\vec{\mu}$ and $\vec{H}_o$ couple; I is the identity matrix and $\vec{\sigma}$ is the shielding coefficient. Another way of expressing the relationship between the shielding coefficient and the magnetic field at the nucleus is

$$H_N = H_o(1-\sigma) \qquad \text{Eq. (2)}$$

where H_N is the magnetic field at the nucleus and H_o is the applied external field.

H_N is related to ν through the magnetogyric ratio (γ) by

$$\gamma = 2\pi\nu/H_N. \qquad \text{Eq. (3)}$$

In a series of papers Ramsey (53) developed an expression for the nmr shielding parameter, σ. His equations, however, are complex and beyond application to the larger molecules of chemical interest. This is mainly due to the lack of exactly (or nearly so) calculable molecular orbital functions for the ground and all the excited electronic states.

The Ramsey treatment has been greatly simplified by Saika and Slichter (54), who show that the Ramsey equation for σ is composed of a summation of these terms.

The first of these terms is the diamagnetic correction for the nmr active atom under investigation. The mathematical form of this part of the Ramsey equation is equivalent to

the Lamb expression (55) for the atomic diamagnetic susceptibility. The equation is dependent upon the isotropic distribution of the electronic charge and as such is limited to non-valence (closed shell) electrons because of their essentially spherical distribution. Diamagnetism is a positive contribution to σ and it is therefore a shielding parameter. To achieve resonance an increase in H_o is thus required.

The second term is the paramagnetic correction for the nmr active atom in question, and it represents the magnetic fields generated by the orbital motions of valence electrons. The paramagnetic phenomenon arises because of anisotropy in the bonding electrons caused by mixing of ground and excited electronic states and it leads to a negative contribution to the value of σ.

The third term of the Ramsey equation concerns the contributions (both diamagnetic and paramagnetic) to the magnetic field surrounding the atom in question stemming from the electrons of other atoms in the molecule.

In comparing the fluorine chemical shifts of F_2 and F^- Saika and Slichter in this same paper reasoned that the second term (paramagnetic) dominates σ for F_2. Their calculations of the diamagnetic term for a variety of fluorine compounds showed variation in this term of only 1% of the observed chemical shifts. The effects of neighboring atom electrons fall off rapidly with distance and were therefore discounted

for these calculations. Since the core electrons of the neighboring atoms are not easily polarized and their valence electrons are only partially within the atomic orbital system of the atom studied, the effect of both groups of electrons is minimized. Thus these workers concentrated on mathematically defining σ using only paramagnetic considerations. By assuming σ = 0 for F^- (because of its sphericity) they obtained the following equation for the difference in σ (and therefore in chemical shift also) between F_2 and F^-,

$$\Delta\sigma = -(2e^2\hbar^2/3m^2c^2)[(1/r^3)av]_p(1/\Delta E), \qquad \text{Eq. (4)}$$

where r is the average radius of a fluorine 2p orbital, ΔE is the average excitation energy between the ground and first excited electronic states and the remaining symbols have their usual meaning.

Within the ionic model for F_2 developed by Saika and Slichter, Δσ in Eq. 4 represents the effect of a single p electron. Muller et al. (56) accepted the assumptions developed by these authors, neglected the 3d orbital occupation "provisionally" and used this equation to discuss trends in ^{31}P chemical shifts differences among phosphines, halophosphines as well as phosphoryl and thiophosphoryl compounds. Two additional assumptions made were: $[(1/r^3)av]_p$ is essentially constant for a closely related series of molecules, as is ΔE. The discussion developed in this paper is based on a parameter proportional to the number of "unbalanced p electrons".

This parameter arises from the Saika and Slichter equation for the effect of a single p electron.

The first advance in quantitatively applying the Ramsey formulas was made by Karplus and Das (57). They devised a perturbation Hamiltonian to describe the paramagnetic effects of the external field. This Hamiltonian was itself composed of three Hamiltonians, only one of which describes the shielding interaction. These workers defined the expectation value of this Hamiltonian as the first order σ. The second order σ (made by application of the Hamiltonian to both the ground and excited states) was then developed in terms of the atomic orbitals and their coefficients. They then used this calculated σ with Eqn. 1 to discuss ^{19}F chemical shifts of polyfluorobenzenes in terms of s and p orbital populations and their effects on ionic character, hybridization and double bonding.

Letcher and Van Wazer (58, 59) in a series of papers discussed ^{31}P chemical shifts using a modification of the Karplus and Das formulation. Letcher and Van Wazer classified the molecular orbitals (MO's) of a PR_3 molecule in four types: a σ orbital containing the phosphorus lone pair, three σ orbitals between phosphorus and its substituents, a set of PR π orbitals within nodal planes containing the C_{3v} axis and a second set of PR π orbitals containing nodal planes normal to the planes of the first set. Following some work

of Jameson and Gutowsky (60) for d orbital inclusion and using the above classification of the MO's in PR_3, Letcher and Van Wazer derived the following formula for the chemical shift relative to a particular standard,

$$\sigma = -(2e^2\hbar^2/3m^2c^2)[(1/r^3_{av})_p\zeta_1 + (1/r^3_{av})_d\zeta_2](1/\Delta E) \quad \text{Eq. (5)}$$

where the radii (r) of the p and d orbitals are the average values for trivalent phosphorus, ΔE is the "mean excitation potential" (this is approximated by the molecular ionization potential) and ζ_1 and ζ_2 are the electron occupation parameters of the phosphorus p and d orbital, respectively. These last two terms are derived from the atomic orbital coefficients used in generating the molecular orbitals. By theoretically determining the effects of the R-P-R angle and the electronegativity of R on ζ_1 and ζ_2 and by assuming constant values for r_p, r_d and ΔE among similar phosphorus compounds, these workers were able to rationalize the chemical shifts of a number of phosphorus compounds on the basis of σ and π bonding arguments. As can be seen by referring to Eqs. 4 and 5, both Muller (through a valence bond approach) and Letcher and Van Wazer (through a molecular orbital approach) derived expressions for σ of essentially the same form.

F. Discussion

1. Implications of the experimentally determined linear relationships

In this section implications of the linear relationships between δ ^{31}P and the lowest d-d transition as a function of charge in a series of complexes is discussed and a comparison of the results of other work which bears upon these observations is presented. Included is a discussion of the relationship between the theoretical considerations presented in the previous section and the ^{31}P nmr results obtained in the present study.

The trends shown in Figs. 4-6 support the contention that the paramagnetic term dominates the shielding parameter. Thus the ^{31}P chemical chift progresses linearly to higher applied field with increasing formal charge in these isoelectronic, isostructural series of complexes. However, trends in ^{1}H chemical shifts are generally dominated by diamagnetic influences because the exicitation energy from the ground state to empty higher energy hydrogen orbitals is large compared to larger atoms, and hydrogen uses an isotropic orbital (1s) to form molecular orbitals. For the first of these reasons hydrogen MO's do not readily mix with higher energy MO's under the influence of the magnetic field. Thus the local paramagnetic effects are minimal and the ^{1}H nmr

Fig. 4. ^{31}P Chemical Shift vs. Metal Charge for 1st, 2nd and 3rd Row d^8 Complexes of 1

Row	Slope	Correlation Coefficient
1st	34.90	1.0
2nd	34.00	1.0
3rd	25.30	1.0

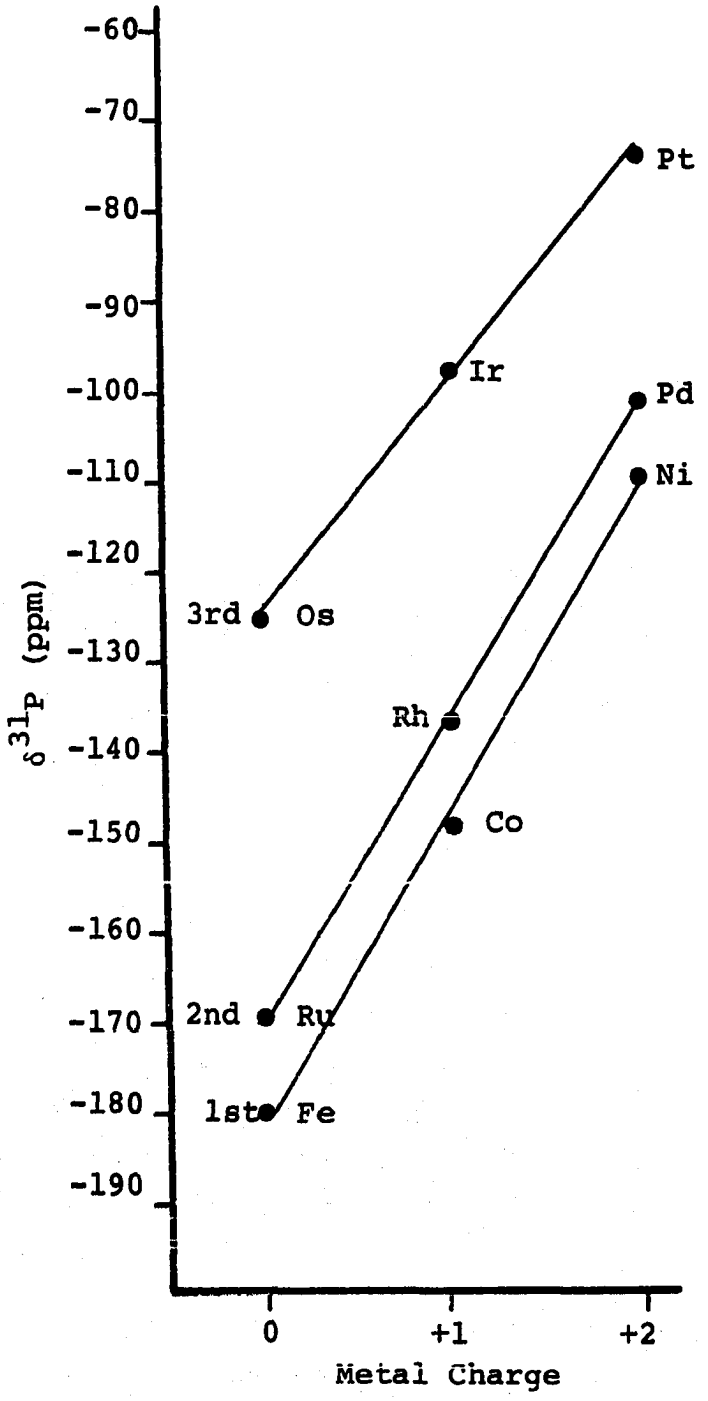
-60
-70
-80
-90
-100
-110
-120
-130
-140
-150
-160
-170
-180
-190
$\delta^{31}P$ (ppm)
Pt
Ir
Pd
Ni
3rd
Os
Rh
Co
2nd
Ru
1st
Fe
0
+1
+2
Metal Charge

Fig. 5. ^{31}P Chemical Shift vs. Metal Charge for 1st, 2nd and 3rd Row d^6 Complexes of 1.

Row	Slope	Correlation Coefficient
1st	52.63	1.0
2nd	26.25	1.0
3rd	36.08	1.0

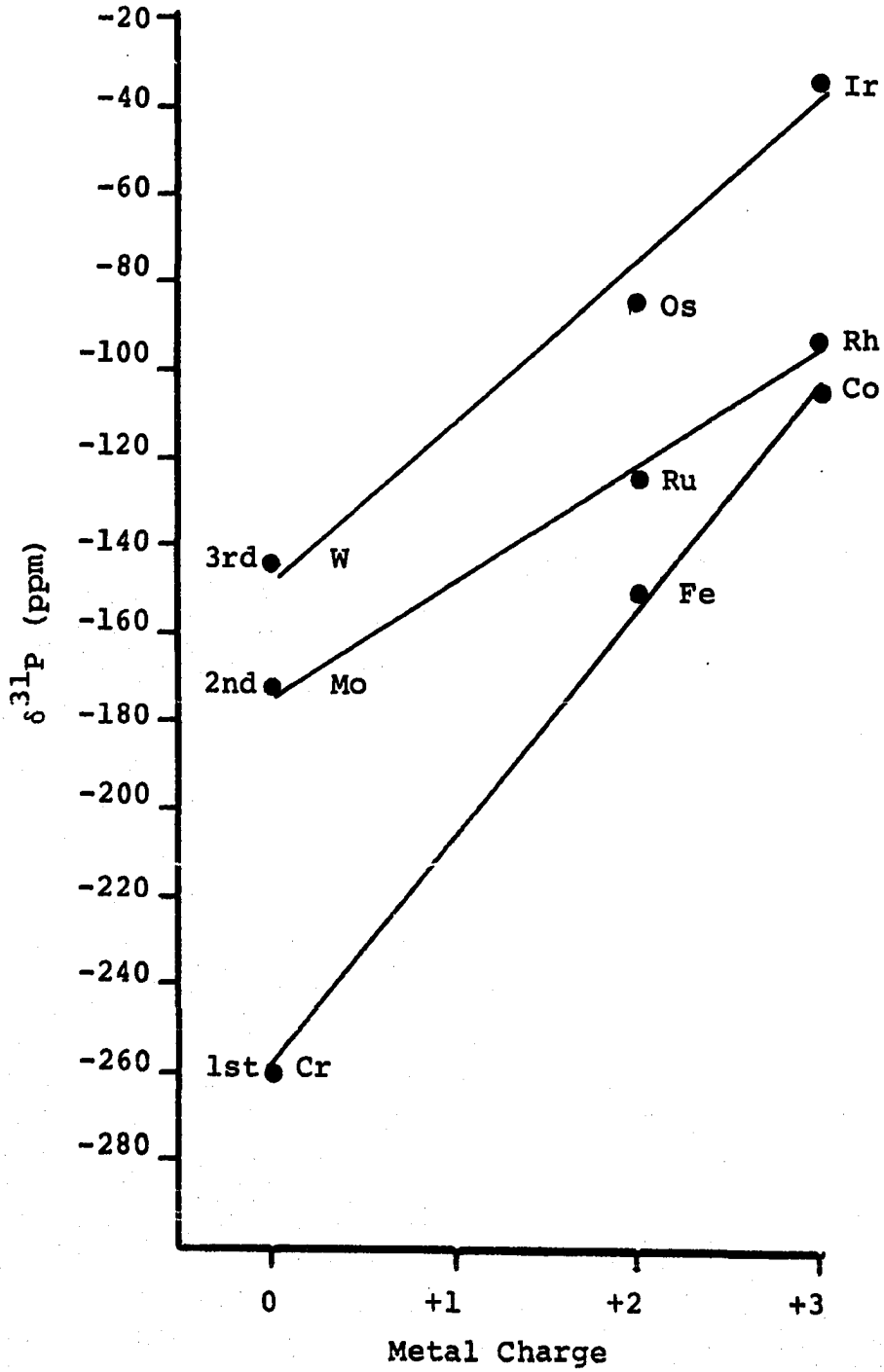
-20
-40
-60
-80
-100
-120
-140
-160
-180
-200
-220
-240
-260
-280
$\delta^{31}P$ (ppm)
Ir
Os
Rh
Co
Ru
Fe
3rd
W
2nd
Mo
1st
Cr
0
+1
+2
+3
Metal Charge

Fig. 6. ^{31}P Chemical Shift vs. Metal Charge for 1st Row d^8 Complexes of 1, 2-R and 3.

L	Slope	Correlation Coefficient
1	34.90	1.0
2-R	27.50	1.0
3	29.85	1.0

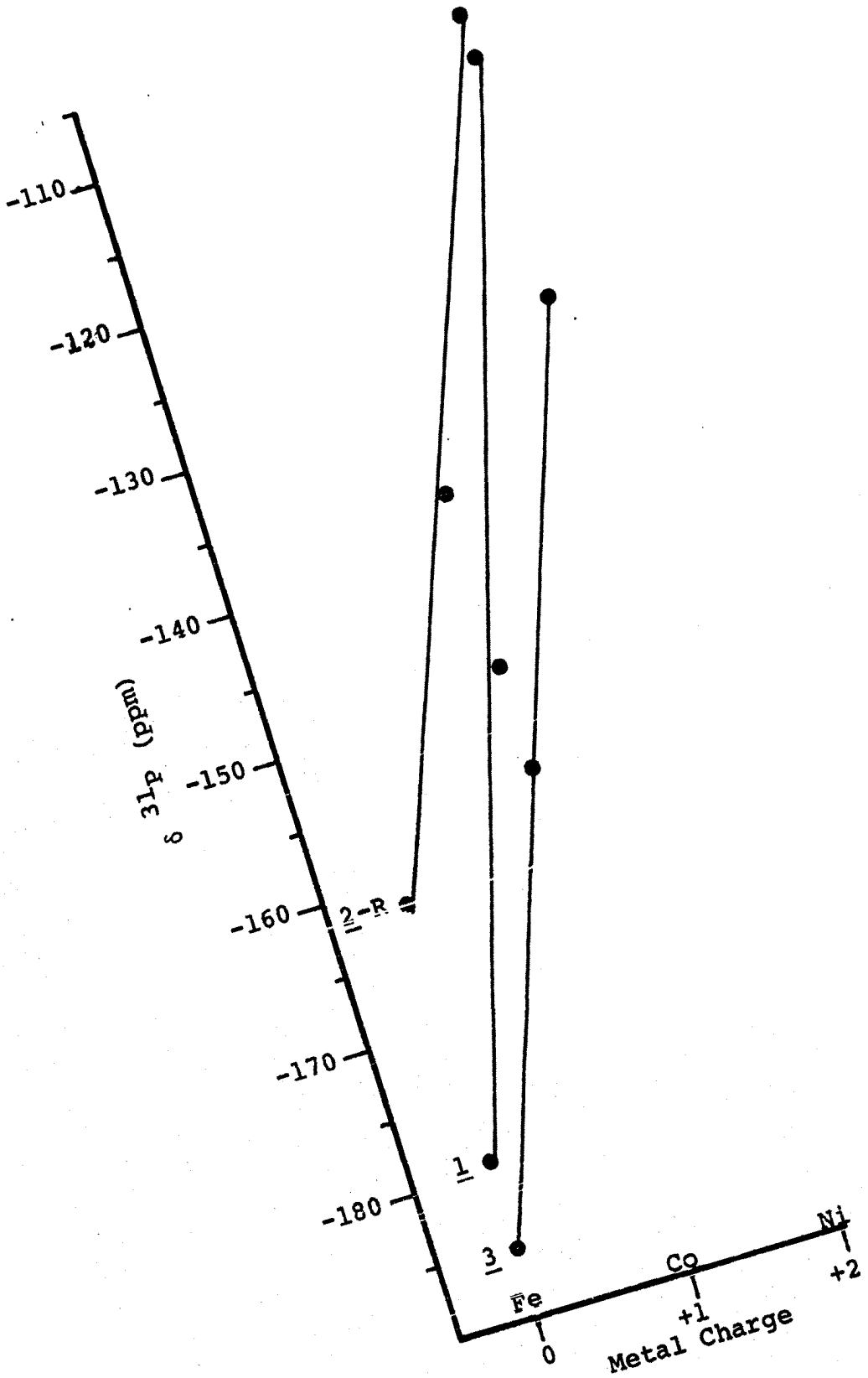
-110
-120
-130
-140
-150
-160
-170
-180
δ 31P (ppm)
2-R
1
3
Fe
Co
Ni
0
+1
+2
Metal Charge

chemical shifts arise primarily from diamagnetic effects. Since diamagnetic effects vary very little (see later) the range of chemical shifts for protons is much smaller than that of other nmr active nuclei. ^{59}Co chemical shifts range over 10,000 ppm, for example, whereas ^{1}H shifts rarely fall without the +10 to -2ppm range. ^{1}H chemical shifts progress to lower applied fields with increasingly electronegative substituents. However, in Figs. 4-6 the ^{31}P chemical shifts progress to higher applied field with increasingly electronegative substituents (increasing metal formal positive charge) which is consistent with the dominance of paramagnetic effects. The question of whether either the Muller or Letcher and Van Wazer expression for the paramagnetic factor might be shown to be more appropriate in interpreting the present data now arises.

In the Muller expression (Eqn. 4) the $[1/r^3)av]_p$ term would be expected to be the dominant factor in producing the trends shown in Figs. 4-6 by the following reasoning. In hydrogenic orbitals, r and ΔE are proportional to $1/Z^*$ and $(Z^*)^2$, respectively, where Z^* is the effective nuclear charge. An increase in the positive charge of the central metal would be analogous in effect to decreasing the Z^* on phosphorus as sensed by its electrons. If Z^* decreases then 1/r must decrease and $1/\Delta E$ must increase. The $\delta^{31}P$ values show a linear decrease in σ with increasing metallic charge and so the term containing 1/r must dominate the value

of σ. This dominance is further emphasized by raising 1/r to the third power.

Letcher and Van Wazer (58, 59) assumed constant values for $[(1/r^3)av]_p$ and, $[(1/r^3)av]_d$ and $1/\Delta E$ for a series of related phosphous compounds. Using this assumption, it is seen from Eqn. 5 that one of the following three possibilities must obtain with increasing metal positive charge: (a) both ζ_1 and ζ_2 decrease, (b) ζ_1 decreases and ζ_2 increases but with differing rates to produce a net decrease, (c) vice versa of (b). It should be noted that since $r_d > r_p$ the effects of changes in ζ_1 and ζ_2 upon σ are modified by the r^{-3} terms in such a manner that changes would have to be much greater in ζ_2 to dominate opposing variations in ζ_1 than in ζ_1 to oppose ζ_2.

Either the dominant dependence of the shielding factor on r in Eqn. 4 or on $\zeta_1 + \zeta_2$ in Eq. 5 would, therefore, reflect the linear relation of the ^{31}P chemical shift and metal formal charge. Only one of these effects can dominate since a combination of two such influences would lead to a quadratic relation as shown by Eq. 5. The Muller expression places emphasis on the basicity (σ donor ability) of the phosphorus through the p orbital contribution to the lone pair orbital while the Letcher and Van Wazer equation stresses both the σ basicity (ζ_1) and π acidity (ζ_2) of phosphorus in the M-P bond.

The uv/vis data graphed in Fig. 7 can be shown to support the Letcher and Van Wazer approach. This plot shows a monotonic decrease in the energy of the lowest energy uv/vis band with increasing metal formal positive charge. Arguments presented in the literature (61) assign this band to the e' → a' d-d transition in the $Co(\underline{1})_5^+$ and $Ni(\underline{1})_5^{2+}$ complexes. Although this transition in d^8 trigonal bipyraimdal molecules of D_{3h} symetry is not a direct measure of the ligand field splitting, it should reflect relative values of the ligand field strength (61) especially among compounds of great structural and electronic similarity. That the Co ($\underline{1}$ or $\underline{2}$-Me)$_5$ and $Ni(\underline{1}$ or $\underline{2}$-Me$)_5^{2+}$ ions are both trigonal bipyramidal has been shown (61) and by the same reasoning Fe ($\underline{1}$ or $\underline{2}$-Et)$_5$ should have the same structure. Likewise, this series of d^8 complexes of $\underline{3}$ should also have D_{3h} symmetry. These assertions are confirmed by the x-ray crystallographic determinations of $Ni(\underline{3})_5^{2+}$ (62) and $Co(\underline{2}\text{-Me})_5^+$ (63).

The ligand field splitting induced by these phosphites is felt (61) to be dominated by their π bonding acidity. From purely σ bonding arguments the ligand field splitting is expected to rise with increasing metallic charge due to increased attraction for the ligand electrons. However, since the energy of the lowest energy d-d transition falls in the series Fe(0), Co(I), Ni(II), π bonding

Fig. 7. UV/Visible Absorbtion vs. Metal Charge for 1st Row d^8 of 1, 2-R and 3

L	Slope	Correlation Coefficient
1	20.75	1.0
2-R	15.50	1.0
3	13.40	1.0

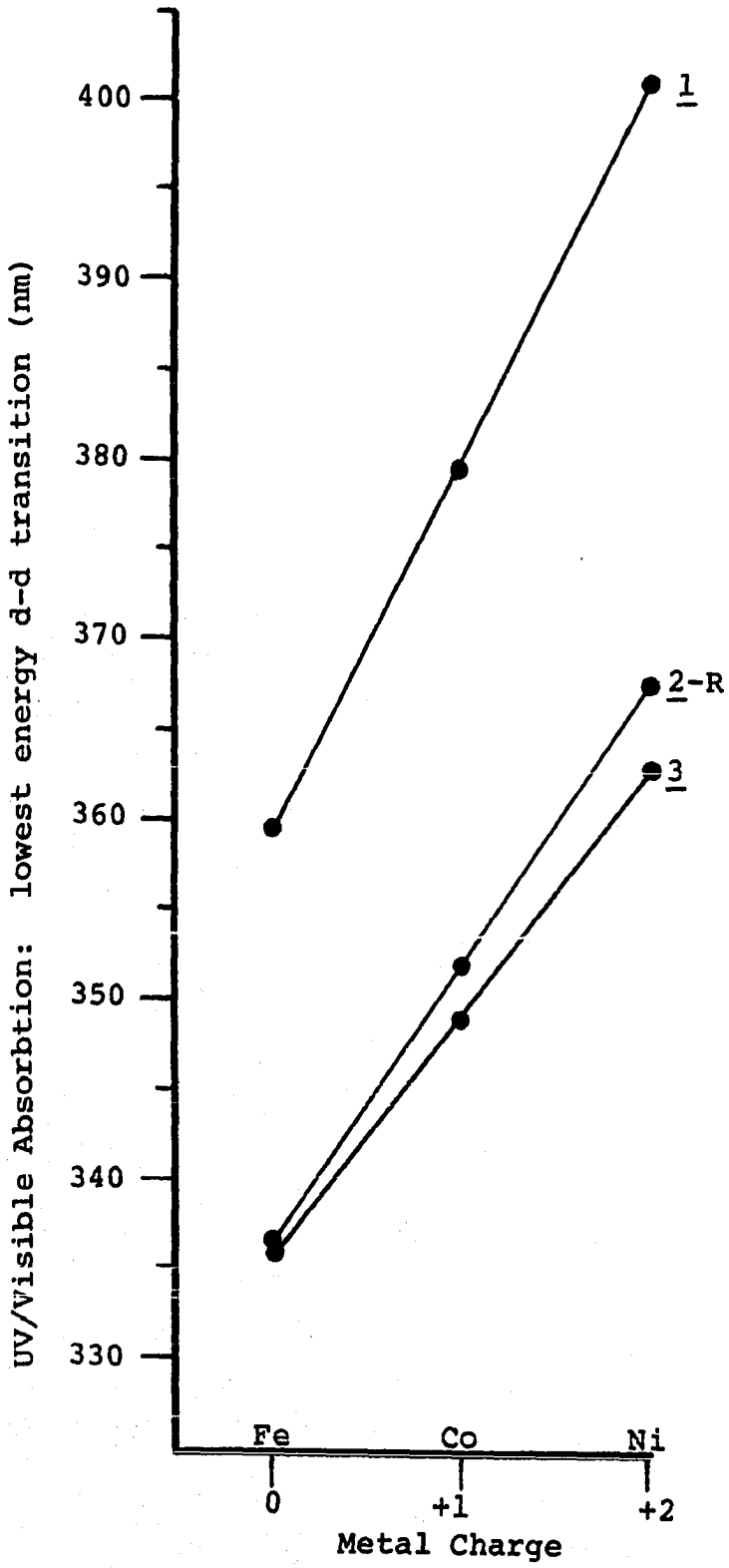
UV/Visible Absorbtion: lowest energy d-d transition (nm)
400
390
380
370
360
350
340
330
1
2-R
3
Fe
Co
Ni
0
+1
+2
Metal Charge

effects (which could involve phosphorus 3d orbitals) very probably dominate the trend (31). Therefore the effects of these orbitals may also be important in determining the ^{31}P nmr spectral properties of these complexes. The Letcher and Van Wazer equation, due to its inclusion of 3d orbital effects through ζ_2, will therefore be considered the formulation of choice to describe the shielding parameter.

The lack of pure samples of $Rh(\underline{1})_6^{3+}$ and $Ir(\underline{1})_6^{3+}$ prevented any meaningful study of the uv/vis spectra of the second and third row transition metal d^6 series. As stated earlier, no d-d transition assignments could be made from the uv/vis spectrum of $Cr(\underline{1})_6$. However, the two low energy absorptions of both $Fe(\underline{1})_6^{2+}$ and $Co(\underline{1})_6^{3+}$ were measured in CH_3CN and found to be 349.9 nm ($\varepsilon = 3.4 \times 10^3$) and 296.2 nm ($\varepsilon = 2.6 \times 10^3$) for the former and 339.8 nm ($\varepsilon = 1.4 \times 10^3$) and 306.4 nm ($\varepsilon = 1.9 \times 10^3$) for the latter. The values for Co(III) agree well with those reported previously (21). Following earlier work by Verkade (61), the ratio of the Slater-Condon integrals, F_2/F_4 was assigned a value of 10 and the ligand field splitting Dq was calculated using the above data for the iron(II) and cobalt(III) complexes to be 3380 cm^{-1} and 3080 cm^{-1} respectively. Although data are available for only two members of the series, it is seen that the ligand field splitting falls with increasing metallic charge in the d^6 systems as it did in the d^8 complexes.

Because extensive use of the Letcher and Van Wazer approach (58, 59) will be made later, a brief outline of its development will now be given. The four types of molecular orbitals mentioned earlier were defined by these authors in terms of the symmetrically appropriate atomic orbitals of phosphorus and the bonding MO's of the substituents. The squared projections of the four MO's were used to define two parameters, s and t. The values of s and t were then used to define ζ_1 and ζ_2. The reasoning of Coulson (64) in assigning orbital electron density based on electronegativity (χ) differences was then used by these authors to define two additional parameters, h_R and h_M, where R and M refer to the phosphorus substituent and metal, respectively:

$$h_R = 1.00-0.16(\chi_R-\chi_P) + 0.0035(\chi_R-\chi_P)^2 \qquad \text{Eq. (6)}$$

$$h_M = 1.00-0.16(\chi_M-\chi_P) + 0.0035(\chi_M-\chi_P)^2 \qquad \text{Eq. (7)}$$

Further simplification was achieved by using only s and p orbitals for σ bonding and limiting π bonding to d orbitals. Using the above definitions and simplifications along with normalization and orthogonality consideration, ζ_1 was defined by

$$\zeta_1 = 3[(h_R^2/2) + h_M-h_Mh_R] + 3\mu(h_R-h_R^2 + h_Mh_R-h_M), \qquad \text{Eq. (8)}$$

where μ is dependent upon the R-P-R angle (θ) by

$$\mu = 1/(1-\cos\theta). \qquad \text{Eq. (9)}$$

By correlating the chemical shift data of a number of PR_3 compounds where π bonding effects could be discounted, these authors defined ζ_2 by

$$\zeta_2 = 16.80\ (\gamma_6^2 + 0.33\ \gamma_{10}^2), \qquad \text{Eq. (10)}$$

where γ_6 and γ_{10} are the AO coefficients of the phosphorus d orbitals used in forming P-R and P-M π bonds, respectively.

The above formulations of Letcher and Van Wazer were used to calculate h_M, h_R, ζ_1, ζ_2 and $n\pi$ (the number of π electrons within the phosphorus d orbital system) for the first row d^6 and d^8 complexes of trimethylphosphite and the remaining members of the M(0) triads. These values are collected in Table 7. A recent compilation (65) of electronegativities based on the Allred and Rochow method was the source for M(0) values and χ's for most of the charged metals were obtained from the original paper (66) and another publication by Allred (67). However, the electronegativities of Co(I) and Co(III) were not available and so χ for Co(III) was assigned the value of Fe(III) on the basis of equivalent electronegativities for Cr(III) and Mn(III) (=1.50). χ for Co(I) was assinged the average value between Co(0) and Co(II). The values of $\chi(P)$ and $\chi(OCH_3)$ were those used by Letcher and Van Wazer as were the values of B, f and δ_o. These electronegativities were used to determine h_M and h_R and thus ζ_1. The values for ζ_2 were obtained from Eq. 11 below.

Table 7. Data used in Letcher and Van Wazer equation

M	$\delta\ ^{31}P$	χ_M	h_M	ζ_1	ζ_2	n_π
Cr(0)	-260.5	1.56	1.1066	1.4845	5.6445	2.02
Fe(II)	-150.5	1.83	1.0548	1.4804	4.1974	1.50
Co(III)	-103.8	1.96	1.0317	1.4786	3.5918	1.28
Mo(0)	-172.1	1.30	1.1613	1.4888	3.3547	1.20
W(0)	-143.9	1.40	1.1397	1.4871	3.0800	1.10
Fe(0)	-179.2	1.64	1.0907	1.4833	4.3034	1.54
Co(I)	-148.3	1.79	1.0621	1.4810	4.0672	1.45
Ni(II)	-109.4	1.91	1.040	1.4793	3.5926	1.28
Ru(0)	-169.3	1.42	1.1355	1.4868	3.5991	1.29
Os(0)	-124.6	1.52	1.1147	1.4852	3.0012	1.07

$\chi_P = 2.15$	$\chi_R = 3.55$
$\theta = 101.8°$	$\mu = 0.8302$
$\beta = -7940$ ppm	$f = 6.74 \times 10^{-3}$
$\delta_o = 11828.5$ ppm	$h_R = 0.8446$

and the calculated ζ_1 value. In this equation

$$\delta-\delta_o = B\zeta_1 + Bf\zeta_2, \qquad \text{Eq. (11)}$$

$B = (-2e^2h^2/3m^2c^2\Delta E)(r_{av}^{-3})_p$ and $f = (r_{av}^{-3})_d/(r_{av}^{-3})_p$. It should be noted that Eqs. 5 and 11 are identical.

The number of π electrons in the phosphorus d orbital system, n_π, was defined (58, 59) in terms of ζ_2:

$$n_{\pi} = \zeta_2/2.80. \qquad \text{Eq. (12)}$$

This relationship, determined by Letcher and Van Wazer is based upon correlations of chemical shift data among structurally similar compounds which differ in that some [e.g., PH_3, $P(CH_3)_3$] have no possibility of π bonding while in others [e.g., $P(OCH_3)_3$, PX_3] π bonding is an important consideration.

The n_{π} column in Table 7. is confirmatory of the conclusions drawn earlier in this section from the uv/vis data, namely, that a decrease in M-P π bonding occurs with increasing metal positive charge (increasing electronegativity) within both the d^6 and d^8 first row series. However, amongst the M(0) triads increasing electronegativity (Mo < W < Cr and Ru < Os < Fe) does not induce an analogous decrease in n_{π}. It should be pointed out here that although ζ_2, and thus n_{π}, consists of π electron densities from both the M-P and P-R bonds, the former should be much more affected by changes in χ_M than the latter. It is felt therefore that changes in n_{π} will reflect changes in the metal to phosphorus back donation more than changes in the P-R system. Before discussing this point further, however, some additional discussion of the Ramsey equation is necessary.

In the Saika and Slichter degradation of the Ramsey equation discussed in section III.E., the shielding parameter was defined by three terms:

$$\sigma = \sigma^P + \sigma^D + \sigma^M, \qquad \text{Eq. (13)}$$

where σ^P and σ^D are, respectively, the paramagnetic and diamagnetic contributions of the nmr active atom and σ^M is the sum of the paramagnetic and diamagnetic contributions of the rest of the molecule. The expression for the shielding coefficient can then be expanded to

$$\sigma = \sigma^P + \sigma^D + \sigma^{DM} + \sigma^{PM}. \qquad \text{Eq. (14)}$$

The workers mentioned earlier (Saika and Slichter, Muller, Letcher and Van Wazer) have discounted variations in the last three terms. Changes in the fourth term were shown to be particularly small (54) because σ^{PM} falls off by $1/r^3$, where r is the distance from the nmr active nucleus to the valence electrons inducing the paramagnetism. However, the second and third terms have been discussed by Flygare and Goodisman (68). They defined this total diamagnetic shielding of atom k in a molecule by

$$\sigma^{TD} = \sigma_k^D + \frac{e^2}{3mc^2} \sum_{\alpha \neq k} \frac{Z_\alpha}{r_\alpha}, \qquad \text{Eq. (15)}$$

where σ_k^D is the diamagnetic susceptibility of k (= σ^D of previous equation), Z_α is the atomic number of atom α, r_α is the distance between atoms k and α, and the summation is carried out over all atoms in the molecule except k. The last term in Eq. 15 is equivalent to σ^{DM} of the previous equation.

Using the data from the axially coordinated trimethyl phosphite in a published X-ray crystal structure (69a) the following values were obtained directly or from simple geometric considerations: P-O = 1.574Å, O-C = 1.410Å, OPM = 116.3°, OPO = 101.8°, POC = 129.1°. The hydrogen atoms were assigned a tetrahedral arrangement about carbon using the C-H bond length in methanol, e.g. 1.096Å (22, pg. F-129). Since dihedral angles were not reported, and insufficient data were given by these workers to calculate them, a geometry search for the minimum in calculated total molecular energy was carried out. An arbitrary point on the C_{3v} axis of the PO_3 moiety was chosen and used to define the MP/OC dihedral angle. Three PO/CH dihedral angles (180, 220 and 260°) at four MP/OC dihedral angle values (90, 120, 150 and 180°) gave twelve sets of coordinates for all of the atoms in the $P(OCH_3)_3$ molecule. Fenske-Hall MO calculations (69b) were carried out on each set and the results are shown in Figure 8. An energy minimum was found at an MP/OC dihedral angle of 150° and a PO/CH angle of 180°. In addition to the open chain phosphite, 1, the two cage ligands, 2-Me and 3 were studied. A recent X-ray crystal structure determination of $Co(2\text{-Me})_5^+$ (63), a structure determination of $Ni(3)_5^{2+}$ (62) and assignment of the values in methanol to the unreported carbon-hydrogen distances in the complexes allowed the

Fig. 8. Calculated Total Energy as a Function of PO/CH and MP/PO Dihedral Angles (0.000 = -691.13110 Hartrees)

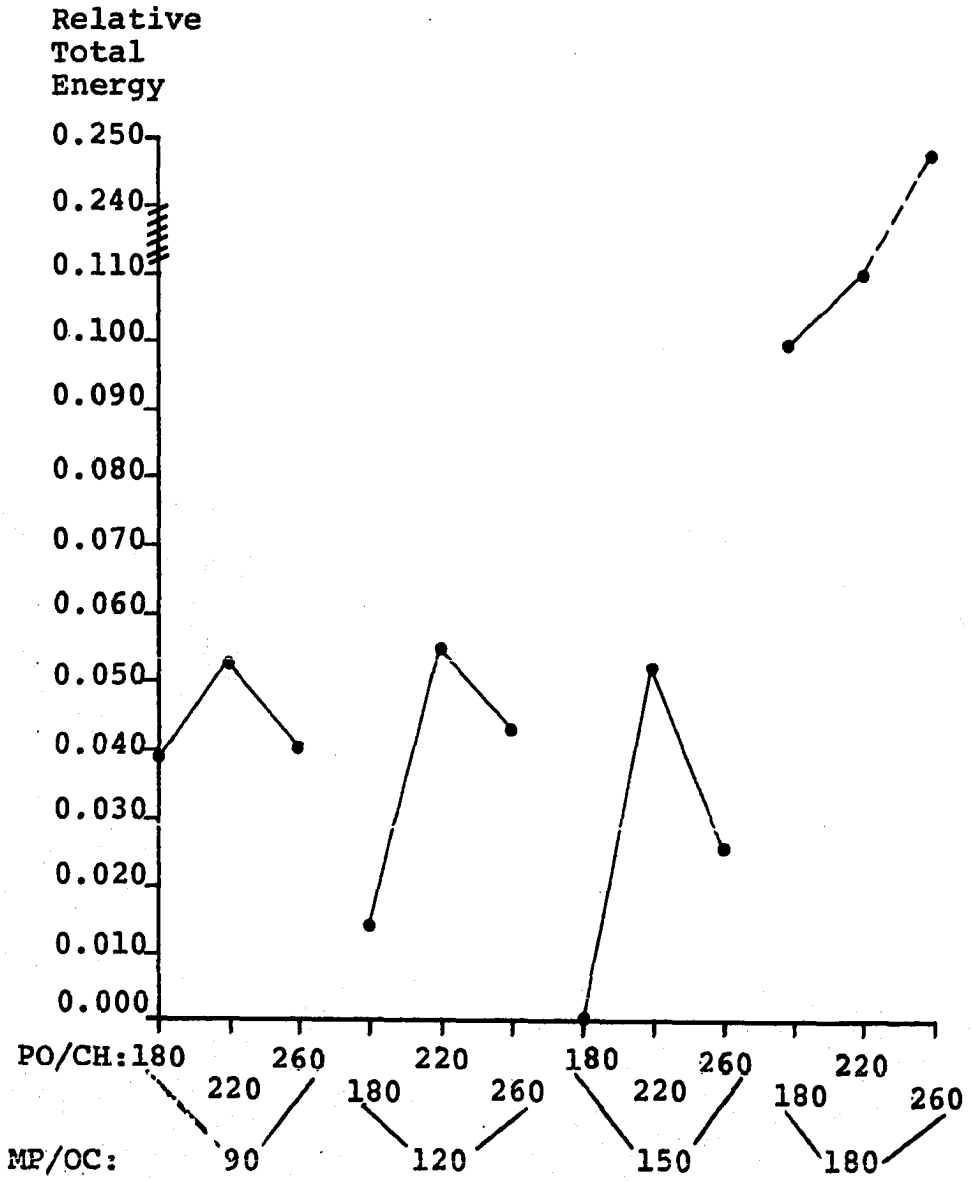
Relative
Total
Energy
0.250
0.240
0.110
0.100
0.090
0.080
0.070
0.060
0.050
0.040
0.030
0.020
0.010
0.000
PO/CH:180
220
260
180
220
260
180
220
260
180
220
260
MP/OC:
90
120
150
180

determination of the coordinates of all the atoms in these molecules also. All equivalent bond lengths and angles were averaged and used as input for standard coordinate generating computer programs. The data used for 2-Me are: MPO = 116.8°, POC = 117.1°, OPO = 101.2°, OCC* = 109.0°, CC*C = 109.4°, CC^*C_T = 109.6°, C^*C_TH = 109.6°, P-O = 1.593Å, O-C = 1.470Å, C-C* = 1.521Å, C^*-C_T = 1.560Å and C_T-H = 1.096Å. For the adamantoid caged ligand, 3, the data were as follows: MPO = 115°, POC* = 116°, OPO = 104°, $C^*C_RC^*$ = 112°, OC^*H = C^*C_RH = 109.6°, P-O = 1.58Å, O-C* = 1.49Å, C*-C = 1.56Å, C*-H = C_R-H = 1.096Å. In the above data, the asterisk stands for the bridgehead carbon, T stands for tail carbon and R stands for ring carbon. Scale drawings of these ligands are found in Appendix A.

Having established coordinates for the atoms of the ligands, the question of M-P bond length arises. Surprisingly few X-ray crystal structure determinations of transition metals coordinated with 1, 2-R or 3 have been reported. This is especially true of Fe, Co and Ni in the oxidation states studied here. However, the axial and equatorial bond lengths in $Co(2\text{-}R)_5^+$ are reported (63) as are those in $Ni(3)_5^{2+}$ (62). If the M-P bond length in the phsophite coordinated ligand in $Fe(CO)_3[P(OCH_2)_3P][P(CH_2O)_3P]$ (70) is assinged to that of $Fe(2\text{-}R)_5$ then two members [Fe(0) and Co(I)] of this ligand series are known. Published tables of atomic radii (71) show an increase of 0.04 Å from

Co(III) to Co(II). If the same increase is allowed on going from Co(II) to Co(I) (= 0.69Å) and this is compared to Ni(II) (= 0.70Å), then the Ni-P bond length can be said to be 0.01Å longer than the Co-P length, although the difference is admittedly small. Having now a complete series of bond lengths, the same differences were applied to the other ligand series wherein the Ni(II) bond length was known in each case: $Ni(\underline{3})_5^{2+}$ = 2.167Å (64) and $Ni(\underline{1})_2I_2$ = 2.175Å (69). In all cases where both axial and equatorial bond lengths were reported, an average of the two was used. This difference was usually quite small, e.g. 0.004Å in $Co(\underline{2}\text{-Me})_5^+$. The value from $Cr(CO)_5P(OC_6H_5)_3$ (72) was used for $Cr(\underline{1})_6$ and the values for Fe(II) and Co(III) were obtained during this work (see Section IV). Values for the M-P bond lengths within the M(0) triads were obtained by applying the difference in radii between metals to a known bond length. For example, the radius of Fe(0), Ru(0) and Os(0) are reported (71) to be, respectively, 1.30Å, 1.40Å, 1.40Å. The difference was applied to the M-P calculated for $Fe(\underline{1})_5$ to give the values shown in Table 8. The same method was used for the d^6 triads which also appear in Table 8 where published values are underlined.

Using these bond lengths and the positional data from each of the ligands, the intramolecular distances between an axial phosphorus and all the remaining atoms in the molecule

Table 8. Metal-phosphorus bond lengths

M(O)	M(I)	M(II)
Fe: 1 = 2.153	Co: 1 = 2.165	Ni: 1 = 2.175
2-R=2.116	2-R=2.128	2-R=2.138
3 = 2.145	3 = 2.157	3 = 2.167
Ru: 1 = 2.163		
Os: 1 = 2.163		

M(O)	M(II)	M(III)
Cr: 2.31	Fe: 2.28	Co: 2.26
Mo: 2.36		
W: 2.36		

were determined for each d^8 complex. The same calculation was done for an equatorial phosphorus atom. Identical calculations were also completed for distances between a P atom and the cis and trans ligand in the d^6 systems. These values were then divided into the appropriate atomic number for use in Eq. 15. The sums for these Z_α/r_α terms are collected in Table 9, wherein L is the sum of the interactions between P and the atoms of the organic moiety which contains that P atom, E is the sum of the interaction between an equatorial P and all the other ligands, but not its own organic moiety, A is the axial sum as for E, M is the metal interaction, Cis is the interaction between P and the

Table 9. Data used in Flygare and Goodisman equation[a]

Complex	L	E or Cis	A or Trans	ST	M	T
$Fe(\underline{1})_5$	24.768	62.444	63.550	87.654	12.076	99.730
$Co(\underline{1})_5^{+}$	"	62.177	63.341	87.411	12.471	99.882
$Ni(\underline{1})_5^{2+}$	"	61.956	63.159	87.205	12.874	100.079
$Ru(\underline{1})_5$	"	62.223	63.326	87.432	20.342	107.774
$Os(\underline{1})_5$	"	"	"	"	35.136	122.568
$Fe(\underline{2}\text{-Me})$	28.027	68.817	69.875	97.267	12.287	109.554
$Co(\underline{2}\text{-Me})_5^{+}$	"	68.526	69.583	96.976	12.688	109.664
$Ni(\underline{2}\text{-Me})_5^{2+}$	"	68.293	69.347	96.742	13.096	109.838
$Fe(\underline{3})_5$	30.464	73.368	74.496	104.283	12.121	116.404
$Co(\underline{3})_5^{+}$	"	73.070	74.195	103.984	12.517	116.501
$Ni(\underline{3})_5^{2+}$	"	72.823	73.947	103.737	12.921	116.658
$Cr(\underline{1})_6$	24.768	64.758	11.649	101.175	10.390	111.565
$Fe(\underline{1})_6^{2+}$	"	65.414	11.772	101.954	11.404	113.358
$Co(\underline{1})_6^{3+}$	"	65.859	11.856	102.483	11.947	114.430
$Mo(\underline{1})_6$	"	63.687	11.449	99.904	17.797	117.701
$W(\underline{1})_6$	"	"	"	"	31.356	131.260

[a]Values given in $(\text{Å})^{-1}$.

cis ligands in O_h complexes, Trans is the analogous calculation for the trans ligands, ST is the subtotal for all ligand interactions and T is the total including the metal interaction. Since there are three equatorial and two axial P atoms in the d^8 complexes, the total ligand interaction (T) was weighted by adding 0.4A plus 0.6E. A sample calculation of values obtained for $Fe(\underline{1})_5$ is found in the Appendix.

Using published values for the constants (22, pg. F-138) and the literature values for σ_k^D (73), Eq. 15 can now be written as

$$\sigma^{TD} = 966.6 \times 10^{-6} +$$

$$\left[\frac{(4.8033 \times 10^{-10}\text{esu})^2}{3(9.1090 \times 10^{-28}\text{g})(2.9979 \times 10^{10}\ \text{cm/sec})^2}\right]\sum_{\alpha\neq k} Z_\alpha/r_\alpha$$

from which we see that

$$\sigma^{TD} = 966.6\ \text{ppm} + \left[(9.393 \times 10^{-14}\ \text{cm}\ \frac{\text{Å}}{10^{-8}\text{cm}})\sum_{\alpha\neq k} Z_\alpha/r_\alpha(\text{Å})\right]$$

The final form of this equation used for calculational purposes is

$$\sigma^{TD} = 966.6\ \text{ppm} + \left[9.393\text{Å}\sum_{\alpha\neq k} Z_\alpha/r_\alpha(\text{Å})\right]\text{ppm}$$

This last form of Eq. 15 and the ^{31}P chemical shifts were then used to calculate the paramagnetic contribution to the chemical shift, σ^P, for each complex. The values of σ^{TD} and σ^P

determined by this method are listed in Table 10. It should be noted that changes in σ^{TD} are relatively small compared to changes in σ^{P} although the absolute values of both parameters are approximately equivalent. The concept of paramagnetic dominance of the ^{31}P chemical shift is thus supported.

We return now to the question of a relationship between the metal electronegativity and n_π. Although σ^P is not definable in terms of ζ_1 and ζ_2, changes in σ^P should be by the following reasoning. Following Eq. 11, the definition below can be made:

$$\Delta\sigma^P = B\Delta\zeta_1 + Bf\Delta\zeta_2. \qquad \text{Eq. (16)}$$

Using the above equation and the values of ζ_1 determined experimentally, one should be able to calculate ζ_2. However a reference ζ_2 value cannot be determined experimentally so an arbitrary value must be assigned. The calculated values of n_π are probably meaningless but the trends expressed by them within a series should reflect the validity of this theoretical approach. A reference parameter is therefore defined, ζ_2', which is the value of ζ_2 of Fe(0) for the d^8 series and Cr(0) for the d^6. This definition has the advantage of allowing a comparison of n_π and n_π' (which will be derived from ζ_2') both of which are based upon the same reference point. An example calculation of the Fe(0)/Ru(0) pair will clarify the above arguments.

Table 10. Diamagnetic and paramagnetic parameters

Complex	n_π [a]	σ^{TD} [b]	σ^{P} [b]	ζ_2' [a]	n_π' [a]	χ_m
$Fe(\underline{1})_5$	1.54	1903.3	-2082.5	≡4.3034	≡1.54	1.64
$Co(\underline{1})_5^+$	1.45	1904.7	-2053.0	4.0934	1.46	1.79
$Ni(\underline{1})_5^{2+}$	1.28	1906.5	-20.5.9	3.6524	1.30	1.91
$Ru(\underline{1})_5$	1.29	1978.8	-2148.1	5.0099	1.79	1.42
$Os(\underline{1})_5$	1.07	2117.8	-2242.4	7.0094	2.50	1.52
$Fe(2\text{-}Me)_5$	N.A.	1995.5	-2157.0	N.A.	N.A.	
$Co(\underline{2}\text{-}Me)_5^+$	N.A.	1996.6	-2132.8	N.A.	N.A.	
$Ni(\underline{2}\text{-}Me)_5^{2+}$	N.A.	1998.2	-2104.7	N.A.	N.A.	
$Fe(\underline{3})_5$	N.A.	2059.9	-2245.3	N.A.	N.A.	
$Co(\underline{3})_5^+$	N.A.	2060.8	-2216.1	N.A.	N.A.	
$Ni(\underline{3})_5^{2+}$	N.A.	2062.3	-2188.0	N.A.	N.A.	
$Cr(\underline{1})_6$	2.01	2014.4	-2274.9	≡5.6445	≡2.01	1.56
$Fe(\underline{1})_6^{2+}$	1.50	2031.3	-2181.8	4.5131	1.61	1.83
$Co(\underline{1})_6^{3+}$	1.28	2041.3	-2145.1	4.0944	1.46	1.96
$Mo(\underline{1})_6$	1.20	2072.0	-2284.1	5.7784	2.06	1.30
$W(\underline{1})_6$	1.10	2199.4	-2343.3	6.5369	2.33	1.40

[a] The lack of electronegativity data for the OR groups in caged phosphites prevented the calculation of these values for these ligands.

[b] Unit is ppm.

$$\Delta\sigma^{P}(Fe/Ru) = -2082.5-(-2148.1) = 65.6 \text{ ppm}$$

$$65.6 \text{ ppm} = -7940 \text{ ppm } (1.4868-1.4833) + (-7940 \text{ ppm})(6.74 \times 10^{-3})(4.3034-\zeta_2')$$

$$\zeta_2' = 5.0099$$

$$n_\pi' = \zeta_2'/2.80 = 1.79$$

This method was used to calculate ζ_2' for the first row series and M(O) triads of the d^6 and d^8 series. By comparing the n_π and n_π' columns in Table 10 it can be seen that this calculation made very little difference in the values for the first row series since the diamagnetic correction is rather constant. Thus the n_π' values still follow the trends expected from the electronegativities. However, the n_π' values now indicate that the second and third row metals in both series are greater than the corresponding first row metals as would be expected on electronegativity grounds. The failure of the n_π' values of the M(O) triads to exactly parallel the electronegativity variations may be a result of incorrect bond lengths. An increase in the W-P or Os-P bond length of 0.15Å above the value used would have made the n_π' values fall between those of their respective first and second rows counterparts, as expected. However, the main conclusion is that with diamagnetic considerations the π electron density trend is more in line with the electronegativities of the metals. Similar comparisons of n_π'

values for other complexes was prevented by a lack of metal electronegativity data.

The effect of different overlap abilities among the metals in each triad is probably minimal. Letcher and Van Wazer (59) have shown that the overlap integral makes only a small contribution to the electron population functions. Furthermore, the variations in overlap between the metals of a triad should not be particularly large owing to their similar size and electronegativity. Thus, when comparing orbital populations among triad members, overlap considerations would presumably give rise to changes in a term whose effect is small.

The values of σ^P for 1, 2-Me and 3 are listed in Table 10 for the d^8 series. What can be said concerning these ligands, in the light of these data, which are plotted in Fig. 9? Let us assume that the term

$$\frac{(1/r^3)_p - (1/r^3)_d}{\Delta E}$$

is essentially constant for all three ligands (as did Letcher and Van Wazer for compounds of far less structural and chemical similarity). Let us also assume that the sum of ζ_1 and ζ_2 is a constant, normalizable to 1.00,

$$\zeta_1 + \zeta_2 = 1.00 \qquad \text{Eq. (17)}$$

Fig. 9. σ^P vs. Metal Charge for 1, 2-Me and 3 d^8 Complexes

L	Slope	Correlation Coefficient
1	34.90	1.0
2-Me	27.50	1.0
3	29.85	1.0

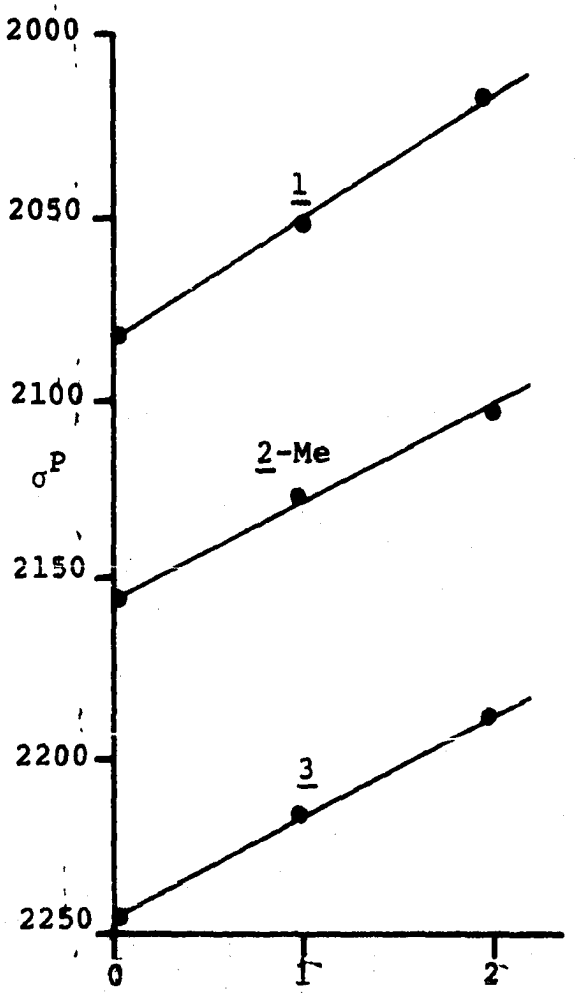
2000
2050
2100
2150
2200
2250
σ^P
1
2-Me
3
0
1
2
Metal Charge

If we define

$$\zeta_1 = \alpha - \beta C, \qquad \text{Eq. (18)}$$

where C is the metallic charge, then Eq. 5 can be rewritten as

$$\begin{aligned} \sigma^P \propto S &= \zeta_1 (1/r^3)_p + \zeta_2 (1/r^3)_d \\ &= \zeta_1 (1/r^3)_p + (1-\zeta_1)(1/r^3)_d \\ &= (1/r^3)_d + \alpha[(1/r^3)_p - (1/r^3)_d] - \beta C[(1/r^3)_p - (1/r^3)_d] \end{aligned} \qquad \text{Eq. (19)}$$

Note that since the phosphorus p orbital density is expected to decrease with increasing metal charge, β must be inherently positive. Since σ^P is proportional to S, the relative absolute values of the slopes in Fig. 9 (1, 33.44; 3, 28.65; 2-Me, 26.18) will show the same relationship as if S were plotted versus metal charge. This implies that $\beta_1 > \beta_3 \geq \beta_{2\text{-Me}}$, which in turn shows that loss of p orbital density and gain of d orbital density is more facile with 1 than with 2-Me or 3 with increasing metal charge. It is interesting to note that the plots of the lowest d-d band frequency (in cm^{-1}) in these complexes versus their charge (Fig. 7) also yield slopes whose absolute values are in order 1(1440) > 2(1255) > 3(1095). Thus the ligand fields also apparently change with increasing metal charge more rapidly for 1 than for the

caged ligands. Both results suggest a greater electronic flexibility for the acyclic ligand than the caged ligands which is not unexpected in view of the greater conformational flexibility of 1.

At zero charge, Equation 18 yields

$$\zeta_1 = \alpha \qquad \text{Eq. (20)}$$

Since the amount of shielding of phosphorus depends upon the p orbital density (ζ_1) and since the shielding expressed by σ^P of the three FeL_5 complexes is in the order 1 > 2-Me > 3, it follows that $\alpha_3 < \alpha_{2\text{-Me}} < \alpha_1$. Therefore, at zero charge, the p electron density follows the order 3 < 2-Me < 1 and the d orbital density is the opposite. This implies that the σ basicity is in the order 3 < 2-Me < 1 and that the π acidity is in the opposite order 3 > 2-Me > 1. Two points should be made concerning the ordering of σ basicities and π acidities: a) The basicity order does not agree with that of Verkade (61) determined from BH_3 displacement studies (2-Me < 3 < 1). However, this adduct is incapable of strong π back donation to the phosphorus. The synergistic effect of the M-P π bond upon the M-P σ bond could be responsible for the change in order seen here. b) Without taking into consideration the diamagnetic contributions the order would have been 3 < 1 < 2-Me for σ basicity, by applying the above arguments to Fig. 6. While the relative basicities of the

bicyclic systems are not firmly established, the acyclic compounds are less ambiguously known to be more basic than the caged compounds (61). Thus, consistency with other experiments demonstrating the greater σ basicity of 1 than caged phosphites strongly suggests that diamagnetic effects be considered in the interpretation of the ^{31}P data.

Using the above definitions and equations of Letcher and Van Wazer the polarizability of phosphorus (an experimentally determined parameter) can be calculated to test the validity of this approach. The following derivation was developed with the greatly appreciated assistance of Dr. D. K. Hoffman. If χ_p is assumed to be constant with increasing metal charge, then the earlier definition of ζ_1 can be expressed as

$$\zeta_1 = C(1) + C(2)h_M \qquad \text{Eq. (21)}$$

$$C(1) = 3[(1/2)h_R^2 + \mu h_R - \mu h_R^2] = 1.397 \qquad \text{Eq. (22)}$$

$$C(2) = 3(1-h_R + \mu h_R - \mu) \qquad \text{Eq. (23)}$$

$$= 0.0792$$

and expansion of $\zeta_2 = 16.8[\gamma_6^2 + (1/3)\gamma_{10}^2]$ yields:

$$\zeta_2 = U + C(3)\gamma_{10}^2 \qquad \text{Eq. (24)}$$

$$U = 16.80\gamma_6^2 = \text{unknown constant} \qquad \text{Eq. (26)}$$

$$C(3) = 5.60 \qquad \text{Eq. (26)}$$

The following definitions are now made.

ρ = metal formal charge

τ = charge induced on phosphorus by the metal

ℓ = M-P bond length

α = polarizability of phosphorus

Following basic electrostatic laws (for which any one of a number of elementary physical chemistry texts can be consulted), the definition below can be made,

$$\frac{\alpha\rho}{\ell^2} = \tau\ell \qquad \text{Eq. (27)}$$

$$\tau = \frac{\alpha\rho}{\ell^3} \qquad \text{Eq. (28)}$$

If τ at ρ=0 is defined as zero then the induced charge on phosphorus within the metal series is a simple linear function of the metal formal charge, ρ. The total electron occupation of phosphorus O_T as determined by the P-M bond can be expressed in terms of the appropriate AO coefficients β, γ_3, γ_{10} and γ_{12} of the phosphorus s, pz, dxz and dyz orbitals, respectively. Since the two pi orbitals are symmetrically equivalent, $\gamma_{10} = \gamma_{12}$ and

$$O_T = \beta^2 + \gamma_3^2 + 2\gamma_{10}^2, \qquad \text{Eq. (29)}$$

when it is recalled that d orbitals are restricted to pi bonding. The above equation reduces to

$$O_T = h_M + 2\gamma_{10}^2 \qquad \text{Eq. (30)}$$

since h_M is a measure of the electron density residing on phosphorus in the M-P σ bonding system. When expressed in terms of the charge induced on phosphorus by the metal, the last equation becomes

$$O_T - \tau = h_M + 2\gamma_{10}^2, \qquad \text{Eq. (31)}$$

from which one obtains

$$\gamma_{10}^2 = (O_T - \tau - h_M)/2 \qquad \text{Eq. (32)}$$

Substitution of this into the earlier definition of ζ_2 yields

$$\zeta_2 = U + \frac{C(3)}{2}(O_T - \tau - h_M) \qquad \text{Eq. (33)}$$

$$= C(4) - \frac{C(3)}{2}(\tau + h_M), \qquad \text{Eq. (34)}$$

where

$$C(4) = U + \frac{C(3)O_T}{2} \qquad \text{Eq. (35)}$$

= unknown constant

From the earlier definition of ζ_1, the following is obtained,

$$\zeta_2 = C(4) - \frac{C(3)}{2}[\tau + \frac{\zeta_1 - C(1)}{C(2)}] \qquad \text{Eq. (36)}$$

$$= C(5) - \frac{C(3)}{2}[\tau + \frac{\zeta_1}{C(2)}] \qquad \text{Eq. (37)}$$

where

$$C(5) = C(4) + C(3)C(1)/2C(2) \qquad \text{Eq. (38)}$$

$$= \text{unknown constant}$$

Plots of ζ_1 vs. metal charge (which is proportional to the formal charge ρ) for both of the first row d^6 and d^8 complexes of $P(OCH_3)_3$ were made and found to be linear (Fig. 10). Therefore ζ_1 can be expressed as

$$\zeta_1 = a + a(1)\rho \qquad \text{Eq. (39)}$$

Substitution of this expression for ζ_1 into Eq. 37 gives

$$\zeta_2 = C(5) - \frac{C(3)}{2}(\tau + \frac{a + a(1)\rho}{C(2)}), \qquad \text{Eq. (40)}$$

which can be expressed as

$$\zeta_2 = C(6) - \frac{C(3)}{2}(\frac{\tau}{\rho} + \frac{a(1)}{C(2)})\rho, \qquad \text{Eq. (41)}$$

where

$$C(6) = C(5) - \frac{C(3)a}{2C(2)} \qquad \text{Eq. (42)}$$

$$= \text{unknown constant.}$$

Fig. 10. ζ_1 vs. Metal Charge for d^6 and d^8 Complexes of 1

	Slope	Correlation Coefficient
d^6	505.4	1.0
d^8	500.0	0.99

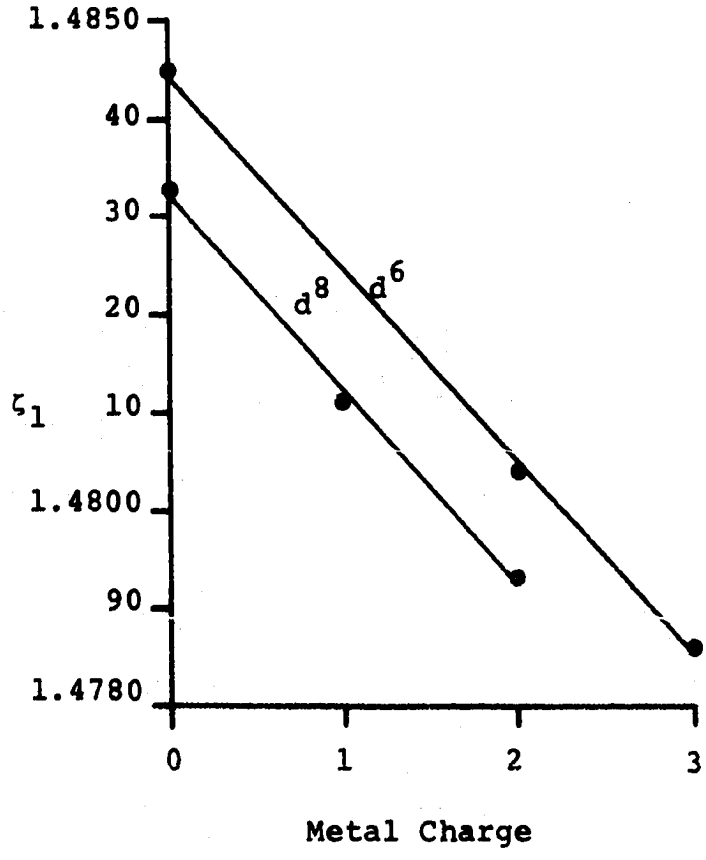
1.4850
40
30
20
10
1.4800
90
1.4780
ζ_1
d^8
d^6
0
1
2
3
Metal Charge

From the earlier definition of τ we can define the term M as

$$\frac{\tau}{\rho} = \frac{\alpha}{\ell^2} = M. \qquad \text{Eq. (43)}$$

Substitution for M into the definition derived for ζ_2 in Eq. 41 yields

$$\zeta_2 = C(6) - \frac{C(3)}{2}(M + \frac{a(1)}{c(2)})\rho \qquad \text{Eq. (44)}$$

Equation 11 is now expressed as

$$\delta - \delta_o = B[\zeta_1 + f(\zeta_2)], \qquad \text{Eq. (45)}$$

where

$$B = \frac{-2c^2\hbar^2}{3m^2e^2\Delta E}(1/r^3_{av})_p \qquad \text{Eq. (46)}$$

and

$$f = (1/r^3_{av})_d/(1/r^3_{av})_p. \qquad \text{Eq. (47)}$$

Substitution of ζ_1 and ζ_2 into the above equation for the chemical shift (δ) relative to that of a particular standard produces

$$\delta - \delta_o = B[(a + a(1)\rho) + f\{C(6) - \frac{C(3)}{2}(M + \frac{a(1)}{c(2)})\rho\}] \qquad \text{Eq. (48)}$$

which on expansion and collection of terms becomes

$$\delta-\delta_o = C(7) + B[a(1)-\frac{fC(3)}{2}\{\frac{a(1)}{C(2)} + M\}]\rho, \qquad \text{Eq. (49)}$$

where

$$C(7) = B(a + fC(6)). \qquad \text{Eq. (50)}$$

Equation 49 is of the form

$$\delta-\delta_o = C(7) + Q\rho, \qquad \text{Eq. (51)}$$

where C(7) is an unknown constant and Q is composed of all known or determinable terms except one, α, the polarizability. The slope of the chemical shift (or here the paramagnetic contribution to the chemical shift) versus metal charge should, therefore be a function of M ($=\alpha/\ell^3$) and a number of determinable constants and values.

The plots of σ^P vs. ρ (Fig. 11) produced the following values for the slope:

$$Q(d^6) = 43.7357$$

$$Q(d^8) = 33.3000$$

The values of a(1) were determined from the slope of ζ_1 vs. ρ (Fig. 10) for each set of complexes as described earlier:

$$d^6a(1) = -1.9786 \times 10^{-3}$$

$$d^8a(1) = -2.0000 \times 10^{-3}$$

Fig. 11. σ^P vs. Metal Charge for d^6 and d^8 Complexes of 1

	Slope	Correlation Coefficient
d^8	33.30	1.0
d^6	43.74	1.0

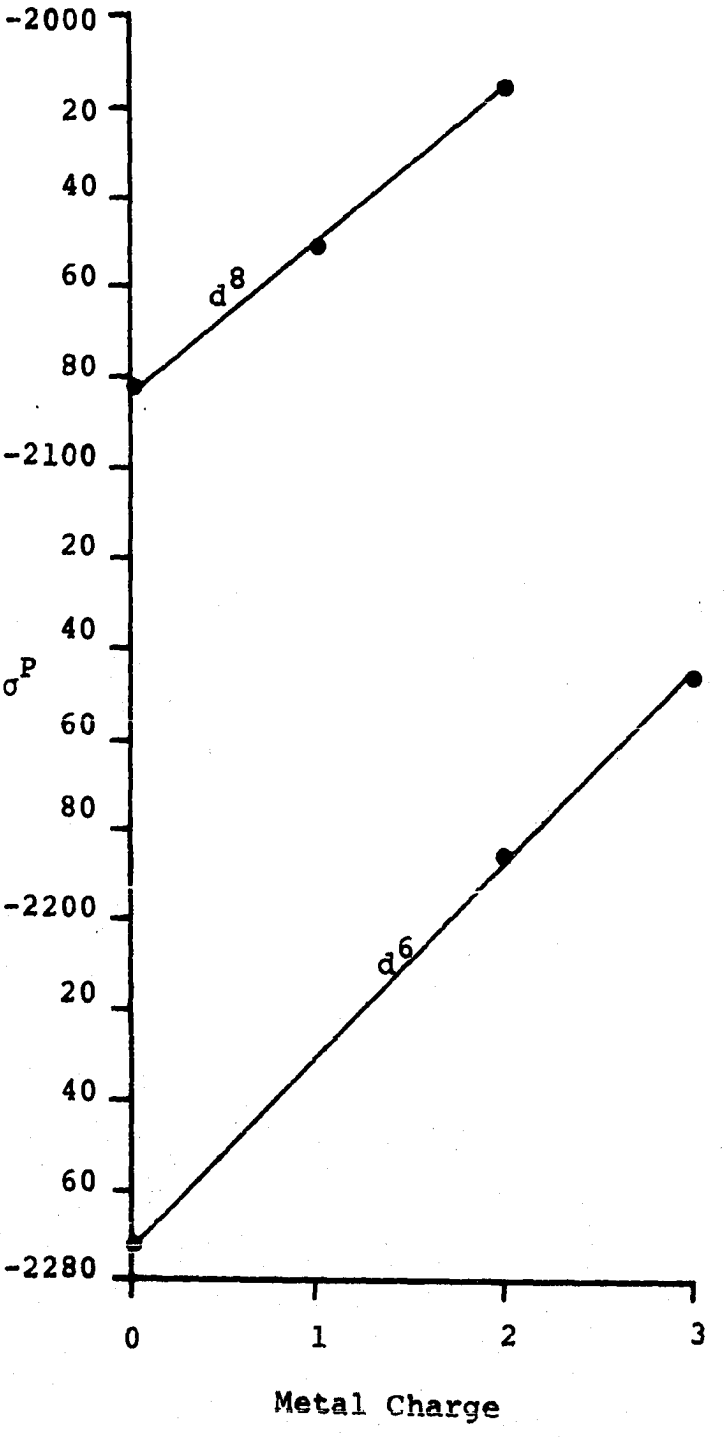
-2000
20
40
60
80
-2100
20
40
60
80
-2200
20
40
60
-2280
σ^P
d^8
d^6
0
1
2
3
Metal Charge

Substitution of the above values for the d^6 case along with the Letcher and Van Wazer values for B and f into the expression

$$Q = B[a(1) - \frac{fC(3)}{2}[\frac{a(1)}{C(2)} + M], \qquad \text{Eq. (52)}$$

gives

$$43.7357 = -7940\{-1.979 \times 10^{-3} - \frac{6.740 \times 10^{-3}(5.600)}{2} \times [\frac{-1.979 \times 10^{-3}}{7.916 \times 10^{-2}}] + M\}$$

$$= -7940[-1.979 \times 10^{-3} + 4.7180 \times 10^{-4} - 1.8872 \times 10^{-2}M]$$

$$= 11.967 + 1.4984 \times 10^{2}M$$

$$M = 2.120 \times 10^{-1} = \frac{\alpha}{\ell^3}$$

$$\alpha = 2.120 \times 10^{-1}\ell^3$$

Substituting the values for the M-P bond lengths used earlier produces

$$\alpha(Cr) = 2.613 \times 10^{-24}$$

$$\alpha(Fe) = 2.513 \times 10^{-24}$$

$$\alpha(Co) = 2.447 \times 10^{-24}$$

which average to

$$\alpha(d^6) = 2.524 \times 10^{-24}$$

An analogous calculation for the d^8 complexes yields

$$33.30 = -7940[-2.000 \times 10^{-3} - \frac{6.740 \times 10^{-3}(5.600)}{2} \times$$

$$\{\frac{-2.000 \times 10^{-3}}{7.916 \times 10^{-2}} + M\}],$$

from which is obtained

$$\alpha = 1.415 \times 10^{-1} \ell^3$$

Again substituting the M-P bond lengths produces

$$\alpha(Fe) = 1.4124 \times 10^{-24}$$

$$\alpha(Co) = 1.4362 \times 10^{-24}$$

$$\alpha(Ni) = 1.4561 \times 10^{-24}$$

which average to

$$\alpha(d^8) = 1.435 \times 10^{-24}$$

The agreement between the calculated and observed value (3.409×10^{-24} (74)) is quite good in view of the crudity of the calculation. The lower value calculated may reflect the expectation that the three highly electronegative methoxy groups induce a higher positive charge on the

bonded phosphorus (relative to elemental phosphorus) and thus reduce its polarizability.

It should be pointed out that the value of Q obtained from Fig. 9 would differ very little from the value obtained from Figs. 4-6. However, the small variations in σ^{TD} have been removed in the value of Q derived from the σ^{P} vs. charge plot.

2. Additional discussion

a. 4-α and 4-β Complexes It was hoped that easily rationalized relationships between the basicities of ligands 4-α and 4-β and the spectral parameters of their complexes could be shown to exist. However, the uv/vis and ^{31}P nmr data reveal that no simple pattern develops, and this raises the question of whether the configuration about phosphorus upon coordination had been retained. It was this question which prompted the glc work reported earlier. The failure of both the Co(I) complexes to form solids may be due to the weakening of crystal packing forces caused by a mixture of ligand orientations on the central metal. Some evidence for this contention is seen in the observation that both of the Ni(II) complexes were solid.

It appears from the ^{31}P nmr and uv/vis data that the difference in ligating ability of the α and β isomers is too small to be reliably detected. In the Ni(II) compounds

where the phosphorus configuration is maintained, there is a small difference in the ^{31}P chemical shifts ($\Delta^{31}P_{\alpha\beta}$ = 1.4 ppm) and in the energy of the lowest d-d transition ($\Delta\lambda_{max\alpha\beta}$ = 0.9 nm). In the analogous Co(I) compounds a difference in the chemical shift is observed even though the ratio of 4-β to 4-α detected by glc as the isomeric phosphates is approximately the same (∿9:1; see Section III.B.) for both complexes. Although the difference in the chemical shifts of the two complexes is small (∿0.8 ppm) it is reproducible when identical solvents, concentrations and temperatures are employed. This observation does not appear to be caused by instrumental imprecision since spectra retaken several months apart of samples obtained from a single preparation of another complex did not differ by more than ± 0.05 ppm.

It is possible that the difference in the preliminary glc results (showing 16% α and 84% β from $Co(4\text{-}\alpha)_5BF_4$ and 11% α and 89% β from $Co(4\text{-}\beta)_5BF_4$) is real. If this is so, then the slightly different δ ^{31}P values for the complexes could be accounted for by the presence of CoL_5^+ cations containing an overall 16/84 ratio of 4-α to 4-β in one case and an overall 11/89 ratio in the other. This presupposes that at least one of the samples does not have an equilibrium ratio of ligands and that the cations rapidly exchange ligands inter and intramolecularly on the nmr time scale.

The full retention of configuration in the case of the NiL_5^{+2} analogues may arise from the expected smaller tendency of this dipositive cation to dissociate and thus permit ligand isomerization. It is possible that isomerization also occurs during the disproportionation of Co(II) to form CoL_6^{+3} and CoL_6^{+1}.

Because the FeL_5 complexes of 4-α and β were oils contaminated with substantial amounts of ligand, no N_2O_4 oxidation studies were attempted. If retention of the phosphorus configuration on complexation does occur, it is odd that the ^{31}P chemical shifts are identical within experimental error for both complexes.

b. $CoL_6(BF_4)_3$ Complexes This is the first report of the ^{31}P nmr spectrum of this type of compound even though members of this class have been known for almost twenty years. Many attempts were made to observe the spectrum in the more common organic solvents (acetone, CH_3CN, CH_2Cl_2 etc.) under a wide variety of concentrations ranging from saturated (>1 g/ml) to 0.01M. Moreover, spectra recorded with varying amounts of added ligand showed the ligand spectrum to be unaffected by the complex. No resonance due to the complex could be observed at a variety of temperatures (-20 to 80°C in toluene and down to -100°C in a mixture of $CH_3CO_2CH_3$, CD_2Cl_2 and CH_2CH_2CN).

Finally, water was chosen as a solvent because of the following reasoning. The Co quadrupolar moment of 7/2 (22, page E-65) is broadening the signal very greatly. A broadened absorbance would have the signal to noise ratio further reduced by the Co-P coupling which would split peak into an octet. A highly symmetrical environment affords the best opportunity to observe coupling from a quadrupolar nucleus. The octahedral symmetry of the CoL_6^{+3} complex could be destroyed by a close association between the highly charged cation and one or more anions in solvents of relatively low polarity compared to water. The stability of the compounds in water was questionable but recovery of the materials after 24 hr in this solvent produced white powders having identical ^1H nmr spectra as before dissolving in water. It is interesting to note that even though the imprecision in J_{CoP} for the 1, 2-Me and 3 complexes is large, the magnitude of the coupling constant appears to be larger for 1 than for the cages.

A problem which immediately arises from the above arguments is the lack of observable quadrupolar coupling in ^{31}P spectra of the Co(I) compounds and in the ^1H nmr spectra of the Co(III) complexes. The asymmetry of the trigonal bipyramidal Co(I) complexes is associated with rapid relaxation of its quadrupole moment and hence the ^{31}P signal (a somewhat broadened singlet) is essentially decoupled from the

^{59}Co nucleus. The relaxation time in the symmetrical Co(III) complexes is shorter and so the ^{31}P signal, though still quite broad, is resolved into the expected eight peaks. The protons in the latter complexes are sufficiently remote from the cobalt, being four bonds distant, that no coupling is observed in the proton spectrum.

G. Summary

The following points are emphasized in summarizing the present work.

1. Phosphorus d orbital importance

The uv/vis spectral data support the Letcher and Van Wazer approach to the analysis of the ^{31}P chemical shift in that d orbital participation in the M-P bond is an important consideration. Their method is further supported by the agreement between the calculated and observed values of the polarizability of phosphorus.

2. Paramagnetic and diamagnetic effects

The contentions of Letcher and Van Wazer that the ^{31}P chemical shift is dominated by paramagnetic effects is also supported. As can be seen from consideration of the Flygare-Goodisman equation, the variations in σ^{TD} are small compared to those in σ^{P}, for series of complexes involving first-row

transition metals. However, diamagnetic effects are very important when comparing complexes within a periodic family. Without inclusion of the large diamagnetic corrections on descending a triad it was seen that the Letcher and Van Wazer approach led to questionable results for n_π. However the values of n_π' which include this correction are more in line with metal electronegativity trends. Failure of the n_π' trend to exactly parallel χ_M values may be due to erroneous M-P bond lengths.

Diamagnetic effects also clarify the comparisons of 1, 2-Me and 3 d^8 complexes. Without the inclusion of diamagnetism, the series of complexes did not follow basicity trends. However use of σ^P resolved most of this difficulty.

3. Synthesis of new compounds

A number of new compounds were prepared and nmr and uv visible spectral data taken. Metal evaporation was shown to be a low yield synthetic method for zerovalent ML_x complexes but in the case of some of these compounds it was the only method available prior to the development of Na/Hg reductions.

H. Suggestions for Further Research

The advantages of series of isoelectronic and instructural complexes discussed earlier can be applied to other examples. Although Ti(0), V(I), Cr(II), Mn(III) and Fe(IV) complexes

are known, synthetic techniques have not yet been developed for making a d^4 series with phosphorus ligands. A d^{10} series could be formed from Co(-I), Ni(0) and Cu(I) but very few Co(-I) compounds are known. Another possibility may be the extension of the present series with Mn(I) and Mn(-I) complexes. Attempts to prepare the Mn(I) complexes of 1, 2-Me and 3 thus far have been unsuccessful, however.

In addition to the phosphites studied here, PX_3 and PR_3 complexes could be prepared and studied. Extensions of the comparisons of the d^8 complexes of 1, 2-Me and 3 could be made with a view toward correlating the nmr and electronic spectral data with ligand basicity and the role of M-P π bonding.

Comparisons within periodic groups could be extended with the study of the Cu(I) and Ni(0) triads. Comparison of ^{31}P chemical shifts as a function of oxidation state changes, e.g. Co(III and I) and Fe(II and 0) could then also be made. This point is exemplified by noting that $|\Delta\sigma^P|$ for the Fe(0)/Fe(II) pair of $P(OMe)_3$ complexes is 99.3 ppm and for the Co(I)/Co(III) pair it is 92.1 ppm. These values can be compared with $|\Delta\chi_m|$ for the same two pairs, namely, 0.19 and 0.17, respectively. Further studies may reveal a consistent relationship in these parameters.

The synthetic work also suggests additional studies. Jesson et al. (30) has used $Co(C_7H_8)(C_7H_7)$ to prepare

$Co(\underline{1})_5B(Ph)_4$. This same precursor could be used to prepare the $\underline{4}$-α and $\underline{4}$-β complexes. This approach has the advantage of low temperature reaction conditions and use of an intermediate in the final oxidation state. These advantages eliminate some of the possible sources of isomerization mentioned earlier and may allow the synthesis of complexes with retention of P configurations.

The synthetic studies of the Rh(III) and Ir(III) complexes suggest that parallel syntheses with the caged ligands may be more successful. These phosphites are known (51) to react with alkyl halides in the Michaelis-Arbuzov reaction much more slowly than the open chain phosphites. If, as was suggested earlier, this side reaction is preventing preparation of pure samples of the ML_6^{3+} complexes, then the caged ligands may react more cleanly.

IV. X-RAY CRYSTALLOGRAPHIC STUDY OF $Fe(\underline{1})_6(BF_4)_2$ AND $Co(\underline{1})_6(BF_4)_3$

A. Experimental Procedures

These compounds were prepared by the methods discussed earlier. Crystals of the complexes were obtained by allowing Et_2O to diffuse by vapor transport into a CH_2Cl_2 solution of the Fe(II) and a CH_3CN solution of the Co(III) compounds. These crystal growing experiments were carried out in sealed containers placed in an inert atmosphere box. Single crystals were chosen and mounted in sealed capillaries. Further selection was made on the basis of polarizing microscope examination. Precession photographs were taken which indicated a very high degree of symmetry in both compounds, as did the Patterson and electron density maps. The density determined by flotation (Fe = 1.573g/cc, Co = 1.584g/cc) agree well with the values obtained from the reduced cell parameters and Patterson maps.

Fe: $a = b = 11.135 \pm 0.003\text{Å}$ $\quad \alpha = \beta = 90.00°$

$c = 19.281 \pm 0.004\text{Å}$ $\quad \gamma = 120.00°$

$d = 1.562\text{g/cc}$ $\quad V = 2070 \pm 2\text{Å}^3$

2 molecules/unit cell

Co: $a = b = c$ $\alpha = \beta = \gamma$

$= 16.448 \pm .002\text{Å}$ $= 90.00°$

$d = 1.590\text{g/cc}$ $V = 4450 \pm 2\text{Å}^3$

4 molecules/unit cell

Neither crystal had a well-defined physical structure and both were approximately 0.3 x 0.3 x 0.3 mm. Mo Kα radiation was used, in both cases, on a locally built diffractometer (Fe) and on a Hilger-Watts (Co) four circle diffractometer. The computer programs used were from the Oak Ridge program set (75) and others written and/or modified by the x-ray group of Professor R. A. Jacobsen, in this department.

B. Refinement of Structures

Patterson maps for both compounds were made from sharpened data. Metal-metal vectors were observed but multiple images were indicated. In both cases metal positions were at facial centers, apices, edge quarters and half positions and in the center of the unit cell. Phosphorus atom locations were found in octahedral arrangements for each of the metal atoms. The multiple images were not resolved by superposition techniques. Electron density maps also had multiple images and perfect O_h symmetry of what appeared to be P atoms was observed in each complex. The data indicated the following possible space groups for each

metal-Fe: $P_{6/mmm}$, $P_{\bar{6}2m}$, P_{6mm}, P_{6_322}; Co: $F_{\bar{4}3m}$, F_{m3m}, F_{432}. The very high degree of symmetry of the complex and anion prevented a decrease in this number of possibilities. Although the M-P bond length was determined from the Patterson and electron density maps, the positions of the atoms in the three methoxy groups could not be solved. It was felt that the main difficulty was the apparent imposition of a three-fold axis [$P(OMe)_3$] onto a four-fold [$M(P)_4$] axis. The electron density maps showed a torus of density with an extension of the M-P bond being the axis. An isotropic least-squares refinement of the MP_6 systems allowed the following M-P bond lengths and discrepancy factors:

Co-P = 2.26 $\pm$ 0.4Å (27%)

Fe-P = 2.28 $\pm$ 0.5Å (41%)

No other data were obtainable from the crystals.

It is suggested that use of a less symmetric anion (p-toluene sulfonate) may allow the location of other atoms within these systems and thus give more locations upon which to refine. This technique may then allow the location of the methoxy groups and phosphorus positions by introducing less symmetry into the unit cell.

V. APPENDIX. SAMPLE CALCULATION OF FLYGARE AND GOODISON EQUATION

Scale drawings of 1, 2-Me and 3 are shown in Figs. 12, 13, and 14, respectively. These drawings were made from the coordinates used in the Flygare and Goodisman equation calculations. In each case the bisection of the O_2PO_3 angle by a plane containing the P-O_1 bond defines the xz plane. This reference plane can be used to describe the symmetry relations in the d^6 (octahedral) and d^8 (trigonal bipyramidal) systems as shown in Figs. 15 and 16. In all cases, the local -z axis of each ligand are along the M-P bonds, and the MPO_1 plane of the equatoral ligands (P_2, P_4, P_5 and P_6 in Fig. 15; P_2, P_4 and P_5 in Fig. 16) contains the z axis in the two figures. The MPO_1 planes of the axial ligands (P_1 and P_3 in Fig. 15; P_1 and P_3 in Fig. 16) are coplanar and contain the y axis.

This system allows the following relationships (exemplified by these P to P symmetry interactions) to exist between all equivalent atoms in the ligands.

Fig. 15: P_1 to P_3 by C_2 on y axis
P_2 to P_6 to P_4 to P_5 by C_4 on z axis

Fig. 16: P_1 to P_3 by C_2 on y axis
P_2 to P_4 to P_5 by C_3 on z axis.

Fig. 12. Scale Drawing of 1

a. xy Plane: C_3 Axis

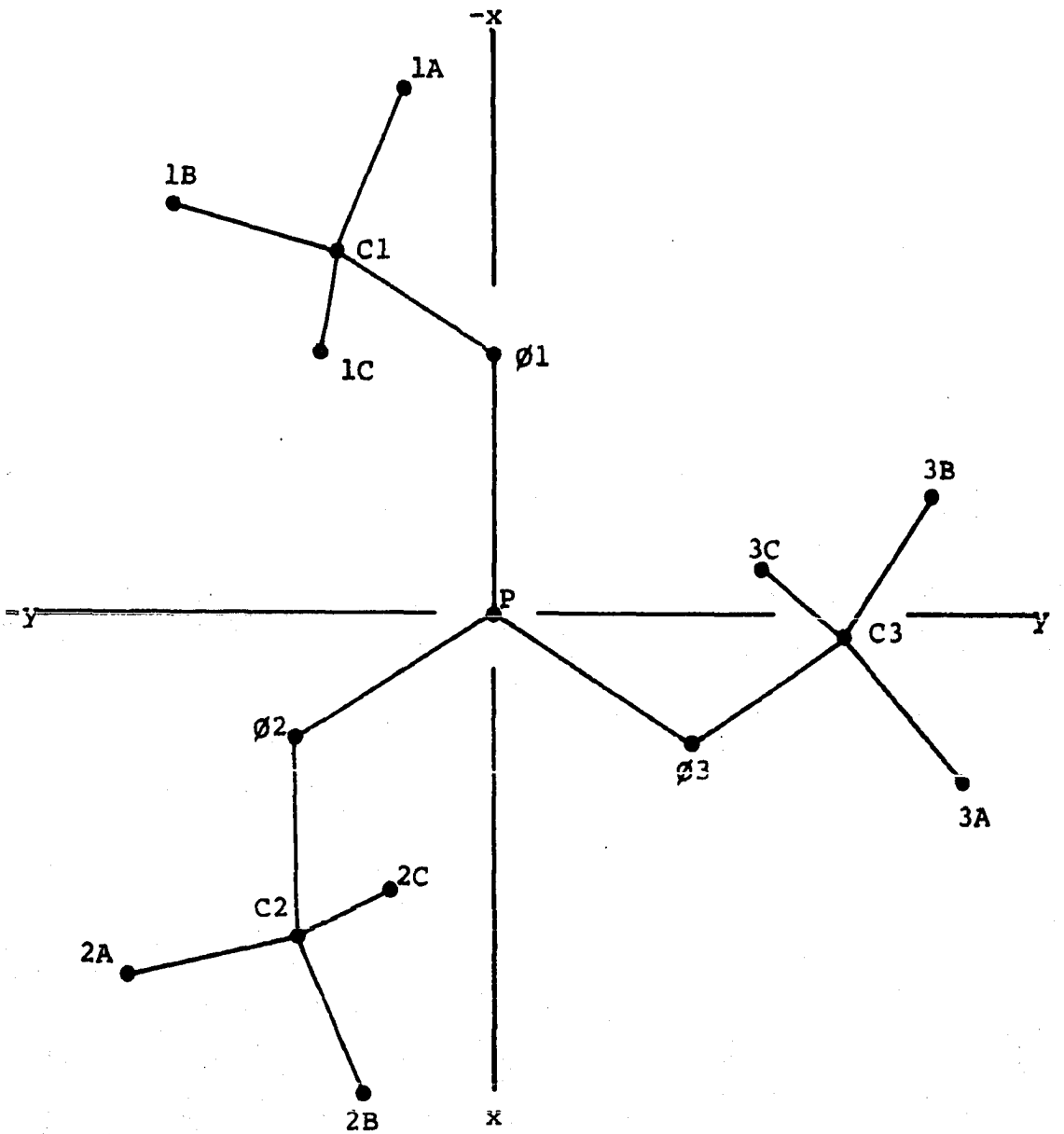
-x
1A
1B
C1
1C
Ø1
3B
3C
-y
P
C3
y
Ø2
Ø3
3A
2C
C2
2A
2B
x

Fig. 12. (Continued)

b. xz Plane

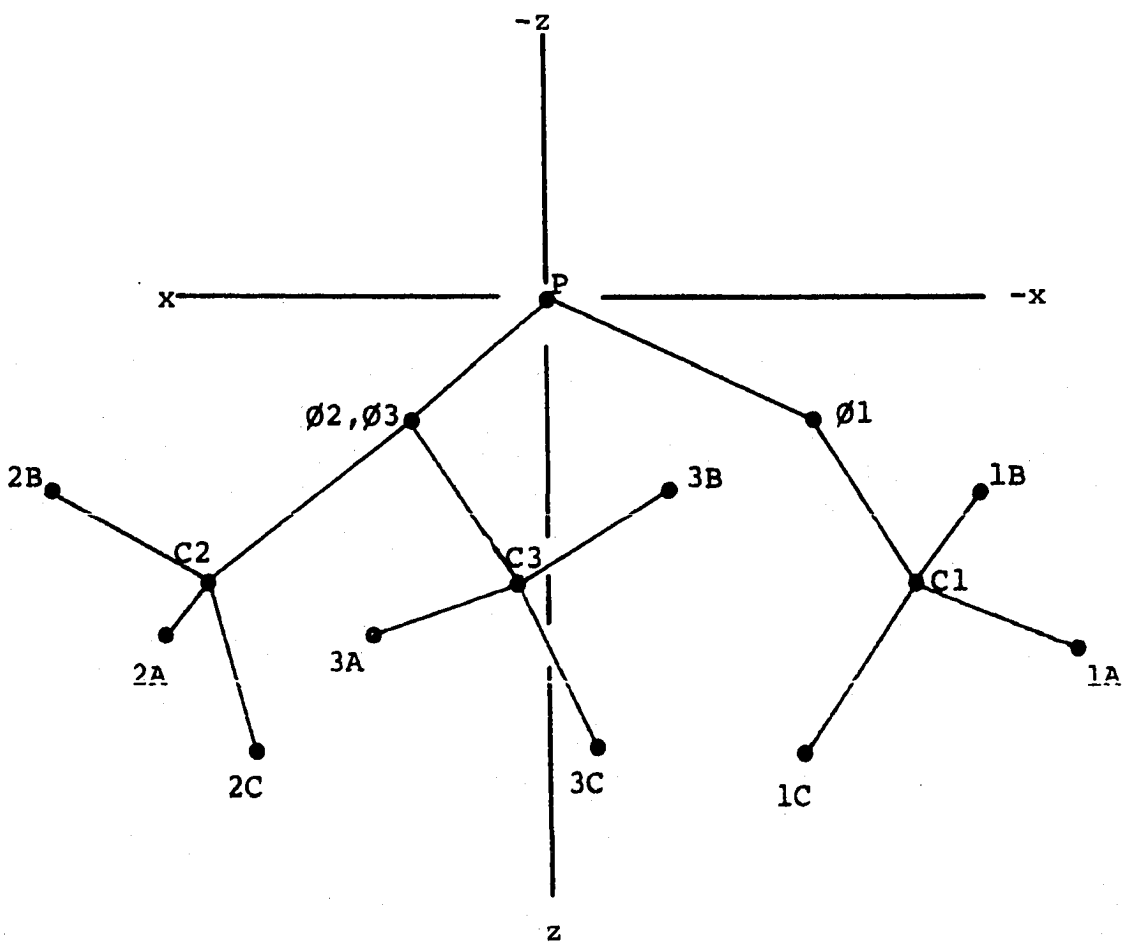
-z
x
P
-x
Ø2,Ø3
Ø1
2B
3B
1B
C2
C3
C1
2A
3A
1A
2C
3C
1C
z

Fig. 13. Scale Drawing of 2-Me

a. xy Plane: C_{3v} Axis

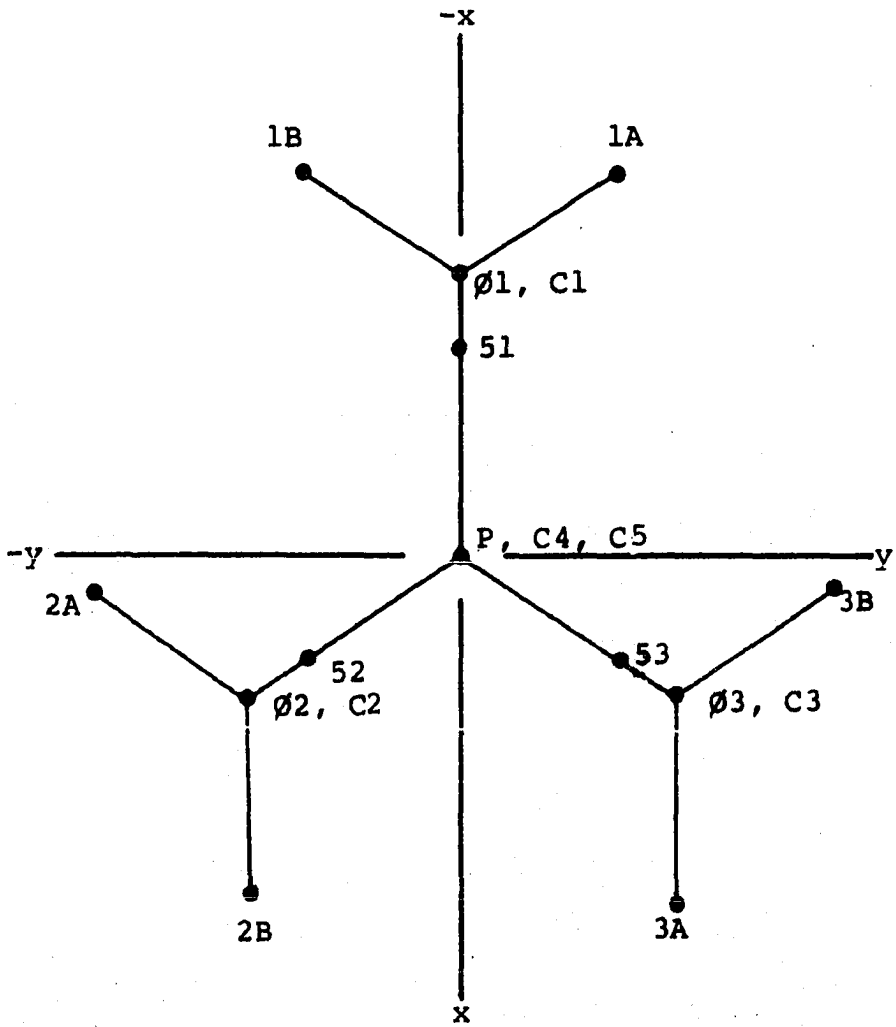
-x
1B
1A
Ø1, C1
51
-y
P, C4, C5
y
2A
3B
52
Ø2, C2
53
Ø3, C3
2B
3A
x

Fig. 13. (Continued)

b. xz Plane

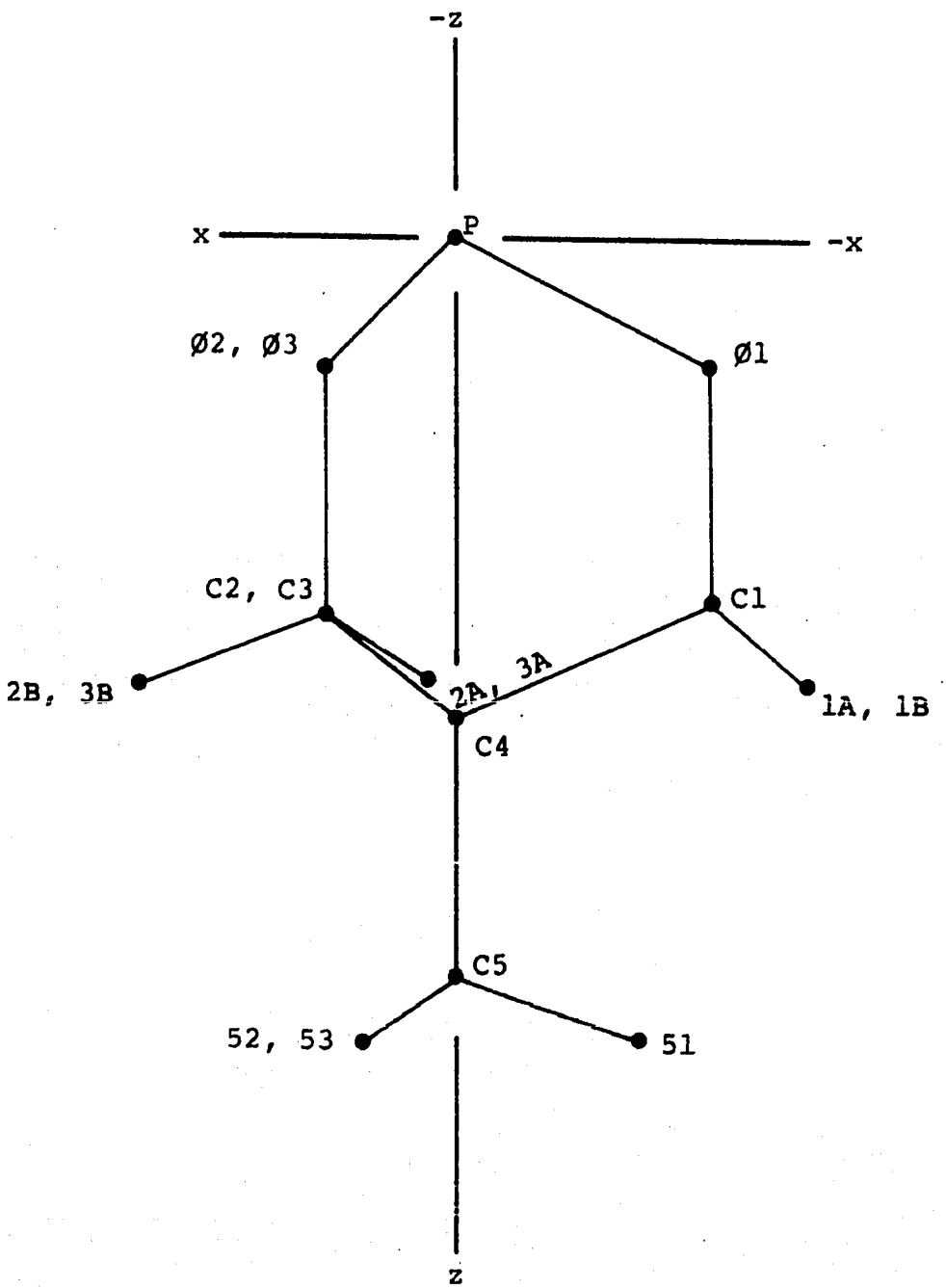
-z
x
P
-x
Ø2, Ø3
Ø1
C2, C3
C1
2B, 3B
2A, 3A
1A, 1B
C4
C5
52, 53
51
z

Fig. 14. Scale Drawing of 3

a. xy Plane: C_{3v} Axis

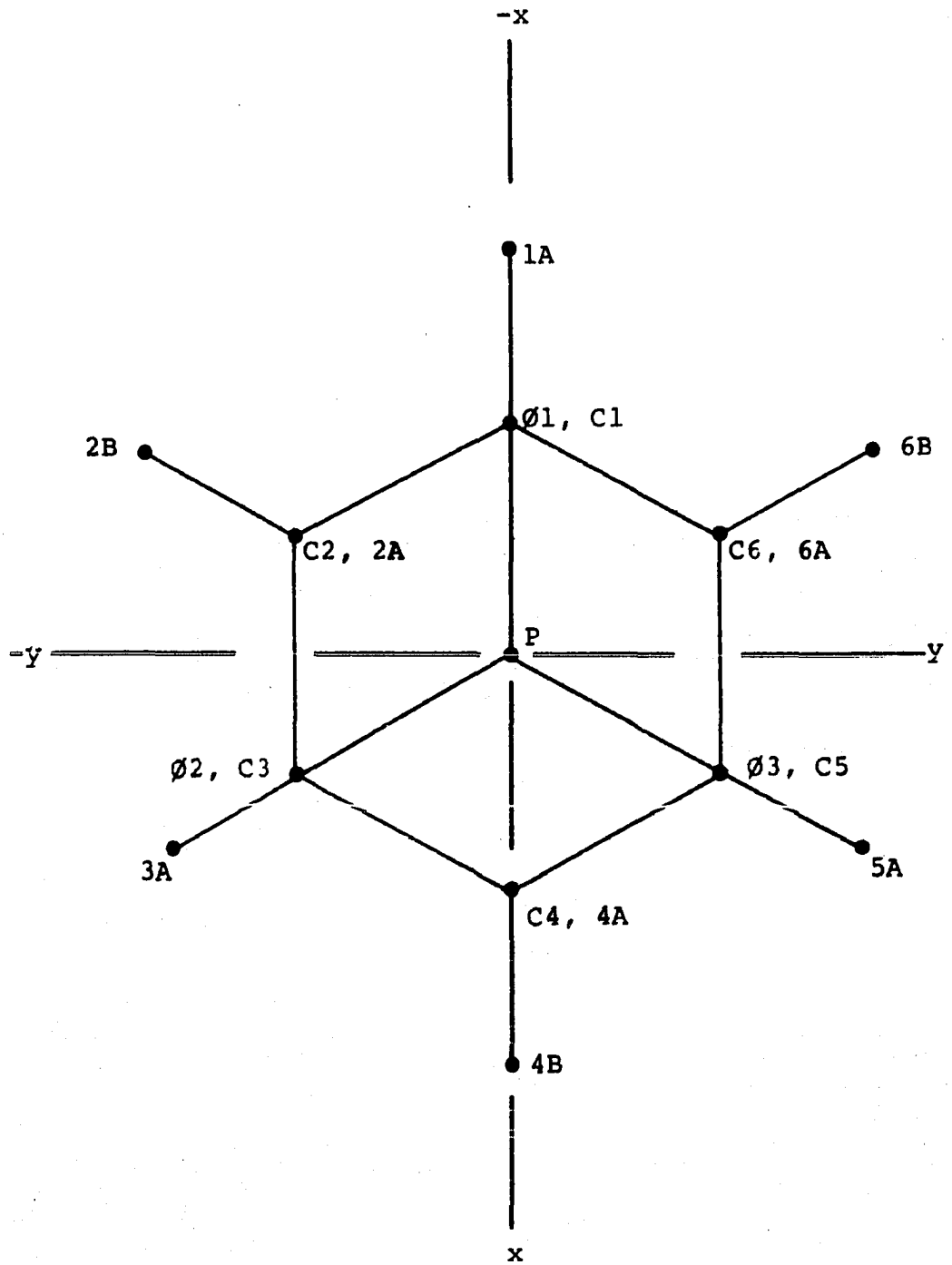
-x
1A
Ø1, C1
2B
6B
C2, 2A
C6, 6A
-y
P
y
Ø2, C3
Ø3, C5
3A
5A
C4, 4A
4B
x

Fig. 14. (Continued)

b. xy Plane

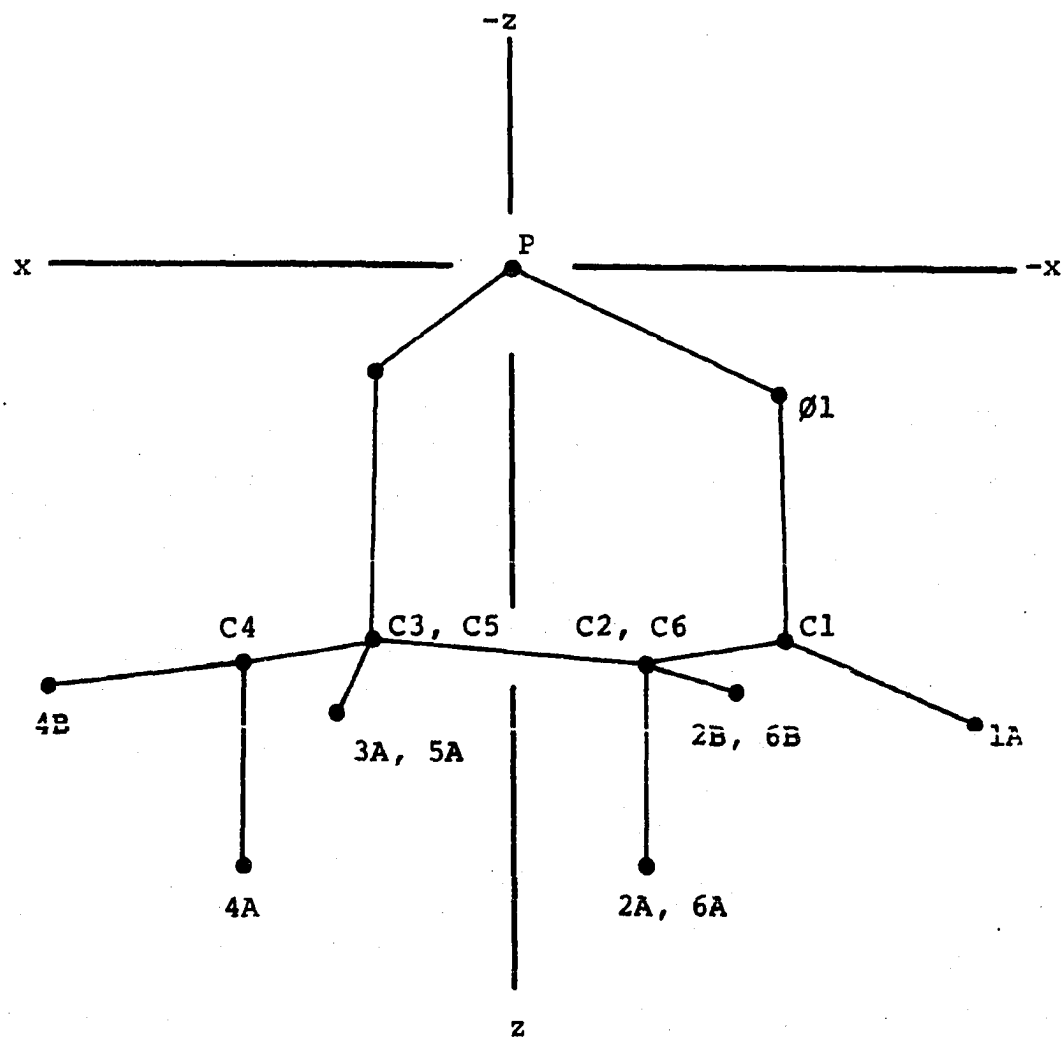
-z
x
P
-x
Ø1
C4
C3, C5
C2, C6
C1
4B
3A, 5A
2B, 6B
1A
4A
2A, 6A
z

Fig. 15. Coordinate System for d^6 Complexes

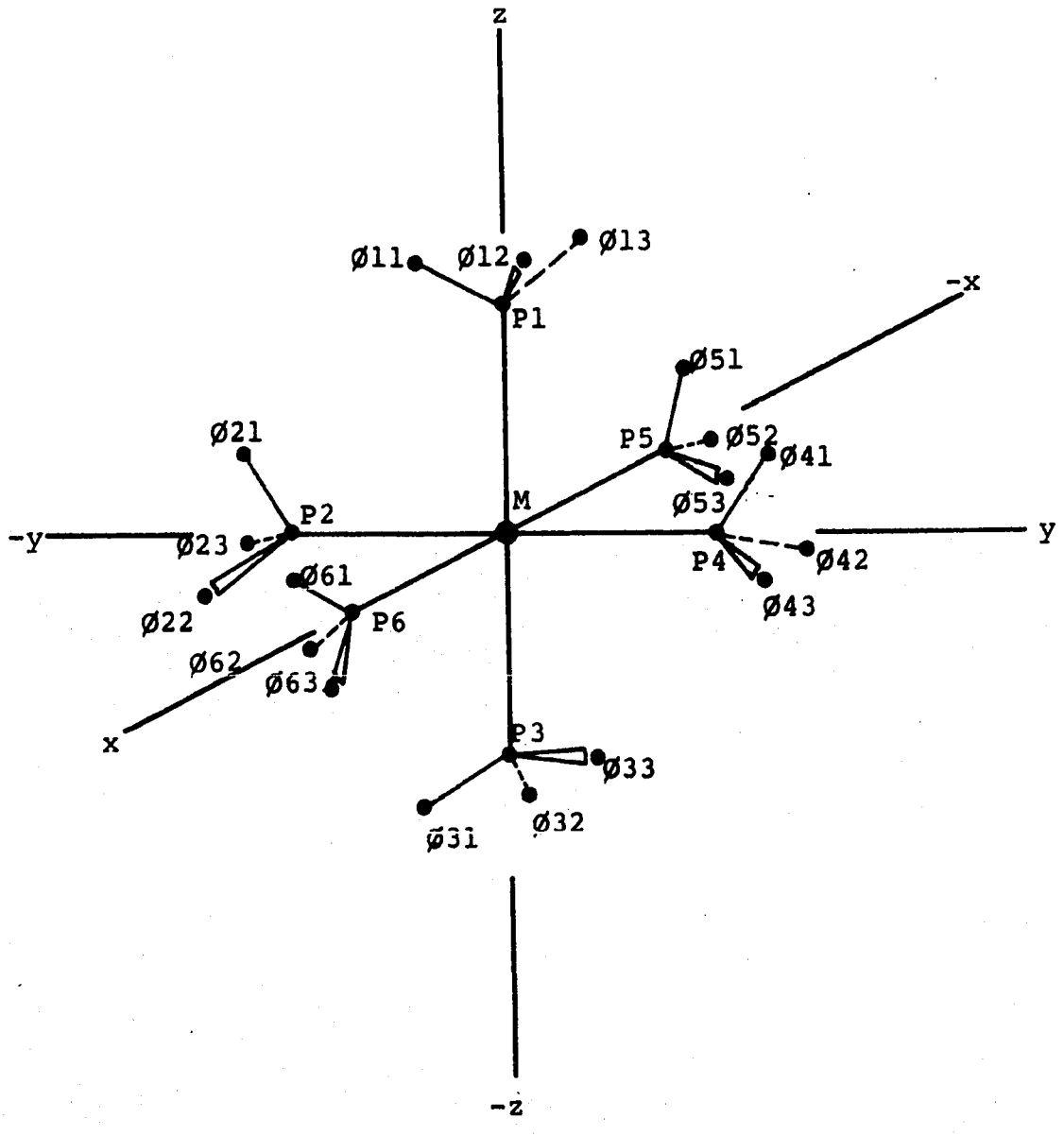
z
Ø11
Ø12
Ø13
P1
-x
Ø51
Ø21
P5
Ø52
Ø41
M
Ø53
P2
-y
y
Ø23
P4
Ø42
Ø61
Ø43
Ø22
P6
Ø62
Ø63
x
P3
Ø33
Ø31
Ø32
-z

Fig. 16. Coordinate System for d^8 Complexes

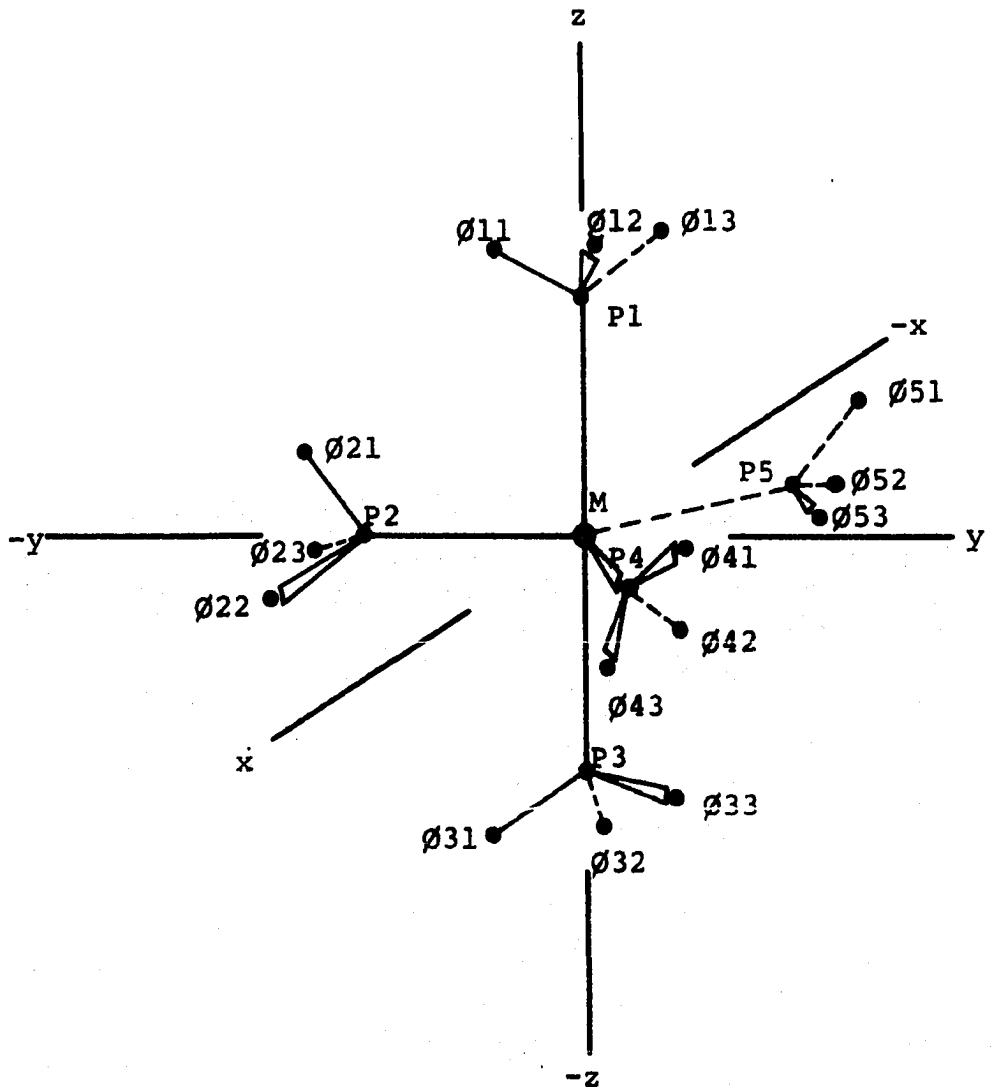
z
Ø11
Ø12
Ø13
P1
-x
Ø51
Ø21
P5
Ø52
P2
M
Ø53
-y
Ø23
P4
Ø41
y
Ø22
Ø42
Ø43
x
P3
Ø33
Ø31
Ø32
-z

Thus, we see that the P_1 to O_{21}, P_1 to O_{41}, P_1 to O_{51} and (for the O_h system) P_1 to O_{61} distances are all equivalent as are the P_1 to O_{22}, O_{23}, O_{42}, O_{43}, O_{52}, O_{53} and (for O_h) O_{62}, O_{63} distances. The data are collected in Table 11 for $Fe[P(OCH_3)_3]_5$ and the numbering system refers to Fig. 17.

The Table is divided into three main sections: interactions of P_1 with three methoxy groups making up ligand position 1 (Ligand subheading); interactions of P_1 with the three equatorial ligands (P_2, P_4 and P_5) and with the other axial ligand (P_3) (Axial subheading), and interactions of P_2 with the two axial ligands (P_1 and P_3) and the two other equatorial position (P_4 and P_5) (Equatorial subheading). Under each of these subheadings are listed the specific distances, an example of the interactions based upon the numbering scheme in Fig. 16, the number of these interactions which are symmetry equivalent and finally the value of this interaction ($\Sigma_i Z/\mathring{A}$). The summations of the subheadings are the values found in Table 9.

Table 11. Sample Flygare and Goodisman equation calculation for $Fe(\underline{1})_5$

Subheading	Example of Interaction	Distance (Å)	No. (i) of Equivalent Interactions	$\Sigma Z/Å_i$
Ligand	P_1-O_{11}	1.5740	3	15.2478
	P_1-C_{11}	2.6954	3	6.6780
	P_1-H_{11A}	3.5718	3	0.8399
	P_1-H_{11B}	2.9959	6	2.0027
		Subtotal		24.7684
Axial	P_1-P_2	3.0448	3	14.7793
	P_1-O_{21}	2.9454	3	8.1483
	P_1-O_{22}	4.2177	6	11.3806
	P_1-C_{21}	3.8577	3	4.6660
	P_1-C_{22}	5.5780	3	3.2270
	P_1-C_{23}	4.9037	3	3.6707
	P_1-H_{21A}	4.1599	3	0.7212
	P_1-H_{21B}	4.8114	3	0.6235
	P_1-H_{21C}	3.7708	3	0.7956
	P_1-H_{22A}	6.2340	3	0.4812
	P_1-H_{22B}	5.9686	3	0.5026
	P_1-H_{22C}	5.8701	3	0.5111
	P_1-H_{23A}	5.8441	3	0.5133
	P_1-H_{23B}	5.2860	3	0.5675
	P_1-H_{23C}	4.4842	3	0.6690

Table 11. (Continued)

Subheading	Example of Interaction	Distance (Å)	No. (i) of Equivalent Interactions	$\Sigma Z/\text{Å}^{\circ}_{i}$
	P_1-P_3	4.3060	1	3.4835
	P_1-O_{31}	5.1986	3	4.6166
	P_1-C_{31}	6.2793	3	2.8666
	P_1-H_{31A}	6.8889	3	0.4355
	P_1-H_{31B}	6.0730	6	0.9880
		Subtotal		63.5501
Equatorial	P_2-P_1	3.0448	2	9.8529
	P_2-O_{11}	2.9454	2	5.4322
	P_2-O_{12}	4.2177	4	7.5871
	P_2-C_{11}	3.8577	2	3.1107
	P_2-C_{12}	5.5780	2	2.1513
	P_2-C_{13}	4.9037	2	2.4471
	P_2-H_{11A}	4.1599	2	0.4808
	P_2-H_{11B}	4.8114	2	0.4157
	P_2-H_{11C}	3.7708	2	0.5304
	P_2-H_{12A}	6.2340	2	0.3208
	P_2-H_{12B}	5.9686	2	0.3351
	P_2-H_{12C}	5.8701	2	0.3407
	P_2-H_{13A}	5.8441	2	0.3422
	P_2-H_{13B}	5.2660	2	0.3784
	P_2-H_{13C}	4.4842	2	0.4460

Table 11. (Continued)

Subheading	Example of Interaction	Distance (Å)	No. (i) of Equivalent Interactions	$\Sigma Z_i/A^\circ$
	P_2-P_4	3.7291	2	8.0448
	P_2-O_{41}	3.9530	2	4.0476
	P_2-O_{42}	4.8496	4	6.5985
	P_2-C_{41}	4.9048	2	2.4466
	P_2-C_{42}	6.1737	2	1.9437
	P_2-C_{43}	5.6563	2	2.1215
	P_2-H_{41A}	5.2626	2	0.3800
	P_2-H_{41B}	5.8212	2	0.3436
	P_2-H_{41C}	4.7289	2	0.4229
	P_2-H_{42A}	6.8091	2	0.2937
	P_2-H_{42B}	6.6850	2	0.2992
	P_2-H_{42C}	6.3158	2	0.3167
	P_2-H_{43A}	6.5028	2	0.3076
	P_2-H_{43B}	6.1673	2	0.3022
	P_2-H_{43C}	5.2404	2	0.3817
		Subtotal		62.4443

Fig. 17. Coordinate and Numbering System for $Fe(\underline{1})_5$

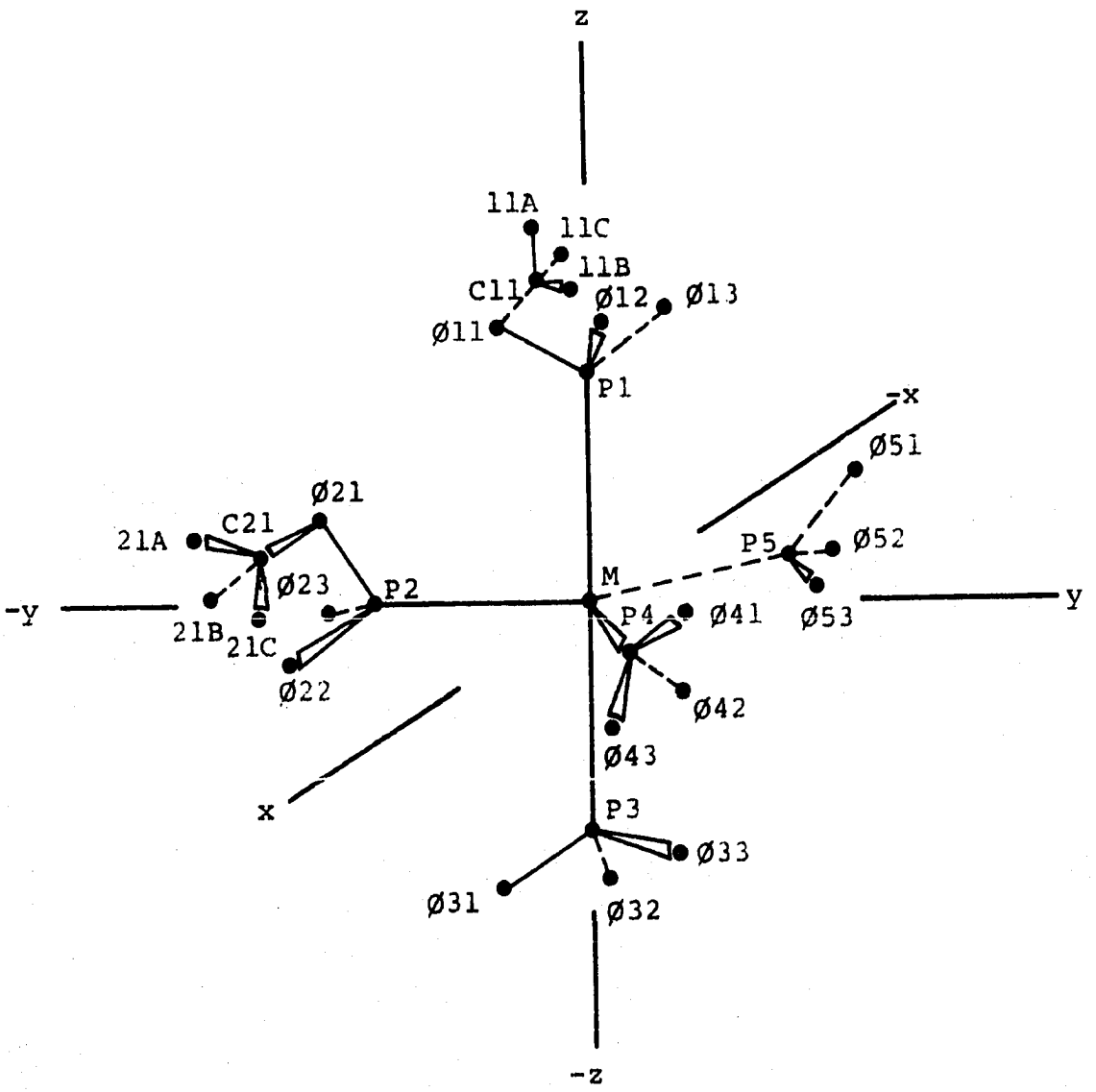
z
11A
11C
11B
C11
Ø12
Ø13
Ø11
P1
-x
Ø51
Ø21
C21
21A
P5
Ø52
M
-y
Ø23
P2
y
P4
Ø41
Ø53
21B
21C
Ø22
Ø42
Ø43
x
P3
Ø33
Ø31
Ø32
-z

VI. REFERENCES

1. G. M. Bodner and L. J. Todd, Inorg. Chem., 13, 1335 (1974).

2. G. M. Bodner, Inorg. Chem., 13, 2563 (1974).

3. G. M. Bodner, Inorg. Chem., 14, 1932 (1975).

4. G. M. Bodner, Inorg. Chem., 14, 2694 (1975).

5. G. M. Bodner and Margaretmary Gaul, J. Organometallic Chem., 101, 63 (1975).

6. H. B. Gray and N. A. Beach, J. Amer. Chem. Soc., 85, 2922 (1963).

7. N. A. Beach and H. B. Gray, J. Amer. Chem. Soc., 90, 5713 (1968).

8. A. P. Hong, J. -B. Lee and J. G. Verkade, J. Amer. Chem. Soc., 98, 6547 (1976).

9. R. Mackenzie and P. L. Timms, J.C.S. Chem. Comm., 650 (1974).

10. F.W.S. Benfield, M.L.H. Green, J. S. Ogden and D. Young, J.C.S. Chem. Comm., 866 (1973).

11. P. L. Timms, J. Chem. Soc. (A), 2526 (1970).

12. J. G. Verkade, T. J. Hutteman, M. K. Fung and R. W. King, Inorg. Chem., 4, 83 (1965).

13. J. G. Verkade, T. J. Hutteman, B. M. Foxman and G. R. Sperati, Inorg. Chem., 4, 950 (1965).

14. D. W. White, R. D. Bertrand, G. K. McEwen and J. G. Verkade, J. Amer. Chem. Soc., 92, 7125 (1970).

15. J. A. Mosbo and J. G. Verkade, J. Amer. Chem., 95, 4569 (1973).

16. A. E. Arbuzov and V. M. Zoroastrova, Bull. Acad. Sci., USSR, Cl. Sci. Chim., 705 (1952); Chem. Abstr., 47, 9901h (1953).

17. R. D. Bertrand, J. G. Verkade and D. W. White, J. Mag. Res., 3, 494 (1970).

18. D. B. Denney and S. L. Varga, Tetrahed. Lett., 4935 (1966).

19. E. L. Muetterties and J. W. Rathke, J.C.S. Chem. Comm., 850 (1974).

20. P. Meakin, A. D. English, S. D. Ittel and J. P. Jesson, J. Amer. Chem. Soc., 97, 1254 (1975).

21. K. J. Coskran, T. J. Hutteman and J. G. Verkade, Advances in Chem. Series, A.C.S. Publication, 62, 590 (1966).

22. R. C. Weast, Editor in Chief, Handbook of Chemistry and Physics, (The Chemical Rubber Publishing Co., Cleveland, 1968), 49th Edition, p. B-192.

23. R. Mathieu and R. Poilblanc, Inorg. Chem., 11, 1858 (1972).

24. R. E. McCarley, Dept. of Chem., Iowa St. Univ., private communication.

25. D. A. Couch and S. D. Robinson, Inorg. Chim. Acta, 9, 39 (1974).

26. E. W. Abel, M. A. Bennet and G. Wilkinson, J. Chem. Soc. London, 3178 (1959).

27. D. A. Couch and S. D. Robinson, Inorg. Nucl. Chem. Lett., 9, 1079 (1973).

28. L. Vaska, Chem. Ind. (London), 1402 (1961).

29. A. Oudeman, F. Van Rankwijk and H. Van Bekkum, J. Coord. Chem., 4, 1 (1974).

30. J. P. Jesson, M. A. Cushing and S. D. Ittel, Inorg. Synth., accepted for publication.

31. C. A. Tolman, L. W. Yarbrough, II and J. G. Verkade, Inorg. Chem., 16, 479 (1977).

32. P. L. Timms, J.C.S. Chem. Comm., 1033 (1969).

33. L. O. Olsen, C. S. Smith and E. C. Crittendon, Jr., J. Applied Phys., 16, 425 (1945).

34. P. L. Timms, Adv. Inorg. Nucl. Chem., 14, 121 (1972).

35. P. L. Timms, J. Chem. Soc. (A), 2526 (1970).

36. P. L. Timms, J.C.S. Dalton, 830 (1972).

37. M. J. Piper and P. L. Timms, J.C.S. Chem. Comm., 50 (1972).

38. P. S. Skell and J. J. Havel, J. Amer. Chem. Soc., 93, 6687 (1971).

39. R. Middleton, J. R. Hull, S. R. Simpson, C. H. Tomlinson and P. L. Timms, J.C.S. Dalton, 120 (1973).

40. R. D. Rieke, K. Ofele and E. O. Fischer, J. Organometallic Chem., 76, C19 (1974).

41. W. Herwig and H. H. Zeiss, J. Org. Chem., 23, 1404 (1958).

41a. G. M. Bancroft and E. T. Libbey, Proc. IV Int. Conf. on Coord. Chem., Toronto, 1972, p. 305.

42. D. G. Hendricker, R. E. McCarley, R. W. King and J. G. Verkade, Inorg. Chem., 5, 639 (1966).

43. J. G. Verkade, R. E. McCarley, D. G. Hendricker and R. W. King, Inorg. Chem., 4, 228 (1965).

44. K. Dimroth and A. Nurrenbach, Angew. Chem., 70, 26 (1958).

45. K. Dimroth and A. Nurrenbach, Chem. Ber., 93, 1649 (1960).

46. P. Beck, "Quartenary Phosphonium Compounds" in Organic Phosphorus Compounds, Edited by G. M. Kosolapoff and L. Maier, Vol. 2, Chap. 4 (John Wiley and Sons, Inc., New York, 1972) pp. 189-508.

47. Unpublished results of C. A. Tolman who privately communicated that the preparation followed the one for the $P(OCH_2)_3CCH_3$ analogue from W. G. Peet and D. H. Gerlock, Inorg. Synth., 15, 40 (1974).

48. R. Cramer, Inorg. Synth., 15, 14 (1974).

49. L. Haines, Inorg. Chem., 10, 1685 (1971).

50. J. L. Herde, J. C. Lambert and C. V. Senhoff, Inorg. Synth., 15, 18 (1974).

51. K. J. Coskran, Ph.D. thesis, Iowa State University, 1967.

52. J. P. Jesson and P. Meakin, J. Amer. Chem. Soc., 96, 5760 (1974).

53. N. F. Ramsey, Phys. Review, 77, 567 (1950); ibid, 78, 699 (1950); ibid, 83, 540 (1951); ibid, 86, 243 (1952).

54. A. Saika and C. P. Slichter, J. Chem. Phys., 22, 26 (1954).

55. W. E. Lamb, Phys. Review, 60, 817 (1941).

56. N. Muller, P. C. Lauterbur and J. Goldenson, J. Amer. Chem. Soc., 78, 3557 (1956).

57. M. Karplus and T. P. Das, J. Chem. Phys., 34, 1683 (1961).

58. J. H. Letcher and J. R. Van Wazer, J. Chem. Phys., 44, 815 (1966); ibid, 45, 2916 (1966); ibid, 45, 2926 (1966).

59. J. H. Letcher and J. R. Van Wazer, "Quantum Mechanical Theory of ^{31}P NMR Chemical Shifts" in Topics in Phosphorus Chemistry, Vol. 5 (Interscience Publ., New York, 1967), pp. 75-168.

60. C.J. Jameson and H. S. Gutowsky, J. Chem. Phys., 40, 1714 (1964).

61. J. G. Verkade, Coord. Chem. Review, 9, 1 (1972).

62. E. F. Riedel and R. A. Jacobson, Inorg. Chem. Acta, 4, 409 (1970).

63. J. O. Albright, J. C. Clardy and J. G. Verkade, Inorg. Chem., 16, 1575 (1977).

64. C. A. Coulson, Valence, 2nd edition (Oxford Univ. Press, London, 1963), p. 141.

65. E. J. Little and M. M. Jones, J. Chem. Ed., 37, 231 (1960).

66. A. L. Allred and E. G. Rochow, J. Inorg. Nucl. Chem., 5, 264 (1958).

67. A. L. Allred, J. Inorg. Nucl. Chem., 17, 215 (1964).

68. W. H. Flygare and J. Goodisman, J. Chem. Phys., 49, 3122 (1968).

69. L. VandeGriend, J. C. Clardy and J. G. Verkade, Inorg. Chem., 14, 710 (1975).

69a. M. B. Hall and R. F. Fenske, Inorg. Chem., 11, 768 (1972).

70. J. C. Clardy, D. A. Allison and J. G. Verkade, Inorg. Chem., 11, 2804 (1972).

71. J. E. Huheey, Inorganic Chemistry (Harper and Row, Publ., New York, 1972), p. 74.

72. H. J. Plastas, J. M. Stewart and S. O. Grim, J. Amer. Chem. Soc., 91, 4326 (1969).

73. R. H. Bonham and T. G. Strand, J. Chem. Phys., 40, 3447 (1964).

74. R. Rich, "Periodic Correlations" in The Physical Inorganic Chemistry Series, edited by R. A. Plane and M. J. Sienko (W. A. Benjamin, Inc., New York, 1965), p. 60.

75. W. R. Busing, K. O. Martin and A. A. Levy, "ORFFE, A Fortran Crystallographic Function and Error Program", ORNL-TM-306 (1964).

VII. ACKNOWLEDGMENT

I wish to acknowledge my wife's love, patience and biscuits.